UNIVERSITY OF CALIFORNIA,
IRVINE

Novel Strategies for Identification and Isolation of Murine Adult HSCs and Embryonic Pre-HSCs

DISSERTATION

submitted in partial satisfaction of the requirements

for the degree of

DOCTOR OF PHILOSOPHY

in Biological Sciences

by

Alborz Karimzadeh

Dissertation Committee:
Professor Matthew Inlay, Chair
Professor Matthew Blurton-Jones
Professor David Fruman

2018

DEDICATION

To my loved ones,

Violet, Javad, Rouzbeh,

and Martina

TABLE OF CONTENTS

LIST OF FIGURES AND TABLES

LIST OF SUPPLEMENTAL FIGURES AND TABLES

ACKNOWLEDGMENTS

My journey through graduate school has been influenced by the positive impact of many individuals who helped me in various ways. I have the deepest appreciation for Dr. Melissa Lodoen who gave me the opportunity to experience a research lab for the first time. This experience was immensely positive and made me realize that I wanted to do research as a profession. Melissa's excellent management style, excellent mentoship, and supportive attitude was translated into the lab environment where I learned a great deal from my graduate student mentor, Lanny Gov. Both of these individuals helped me gain the confidence to apply to graduate school, and the lessons learned from them greatly improved my experience as a graduate student.

I had an amazing experience in the Inlay lab. Thank you to all my labmates who made this possible: Tannaz Faal, Ankita Shukla, Yasamine Ghorbanian, Erika Varady, Connie Inlay, and Karin Grathwohl were all friendly, kind, and helpful during my time in the Inlay lab. Thank you all for = your helpful suggestions about my project throughout the years, and thank you for not being only great colleagues but also great friends.

I would like to thank Vanessa Scarfone who was influential in the projects I was working on. Her skill and knowledge in FACS was a great asset to all the members of the Inlay. Vanessa is not only a FACS wizard but also a great scientist and I greatly appreciate her helpful input on my projects throughout the years.

My PhD committee members, Drs. David Fruman and Matthew Blurton-Jones, provided me with great advice during my graduate school years and improved my projects with their helpful suggestions. Thank you both for being patient and supportive at all times, and for being instrumental in my growth as a scientist.

I would like to express my deep appreciation for everything that Dr. Matthew Inlay did for me as my PhD advisor. I learned a lot from Matt during these years and feel blessed to have such a helpful, supportive, and knowledgeable mentor who pushed me to think independently and take charge of my projects. Matt was not only an amazing scientific mentor but also a role model in life. I learned a lot about handling difficult situations from Matt's impeccably positive attitude throughout the years.

My parents, Javad and Violet, and my brother, Rouzbeh, provided me with the support I needed to do the best I could in graduate school. Their continuous love and support helped to calm me and to think positively during stressful times. My parents made the sacrifice of being away from my brother and I so that we would have the choice to pursue what we enjoy in life.

Finally, I have been lucky to share my life with my amazing wife, Martina. I could not have done this without her unconditional love and support. Besides her sacrifice and hard work to provide me with everything I needed in my personal life, Martina also

contributed to my growth as a scientist through our discussions about my projects. Thank you for everything that you do and for making everything more beautiful.

CURRICULUM VITAE

Alborz Karimzadeh

Professional Summary

- Doctorates degree in Biological Sciences from University of California, Irvine
- Bachelor's degree in Biological Sciences from University of California, Irvine
- Junior specialist in Dr. Melissa Lodoen's laboratory at University of California, Irvine
- Skills include FACS, mouse models (tissue harvest, colony maintenance, transplantation, transplantation conditioning), cell culture, ELISA, Western blotting, microscopy

Education

Qualification	Institution	Year	GPA
Ph.D. Biol. Sci.	University of California, Irvine	2013-2018	3.99
B.S. Biol. Sci.	University of California, Irvine	2011	3.18

Research Experience

University of California, Irvine **2013-2018**
Department of Molecular Biology & Biochemistry
Graduate Researcher; Advisor: Matthew Inlay, Ph.D.

Research focus:
Utilization of surface markers for identification, purification, and characterization of embryonic precursors to hematopoietic stem cells as well as adult hematopoietic stem cells.

- Establishing a novel two-marker strategy for FACS-purification of adult hematopoietic stem cells
- Utilization of a novel flow cytometry strategy for identification of hematopoietic stem cells in conditions of bone marrow stress when conventional approaches fail
- Conducting transplantation assays of embryonic cells in a neonatal transplant system to determine *in vivo* activity of embryonic precursors to hematopoietic stem cells from various embryonic tissues
- FACS-purification of embryonic precursors to hematopoietic stem cells using novel markers to improve characterization of these understudied cells
- Identification of surface molecules involved in bone marrow homing of transplanted cells, and over-expression of identified molecules to improve engraftment efficiency of hematopoietic cells
- Tissue harvest for donor chimerism analysis
- Maintaining mouse colonies, and utilizing useful genotypes for competitive transplantation assays
- Determining suitable culturing conditions for mouse adult and embryonic hematopoietic stem cells
- Microscopic analysis of recipient tissues for cell fate analysis of transplanted embryonic progenitors

University of California, Irvine **2011-2013**
Department of Microbiology and Molecular Genetics
Junior specialist; Advisor: Melissa Lodoen, Ph.D.

Research focus:
Mechanisms of inflammasome activation and IL-1β processing/secretion from human trophoblast, monocyte, and macrophage cell lines during *Toxoplasma gondii* infection

- Performed *T. gondii* infection of human cell lines to determine the innate immune response to the parasitic infection
- Characterized the mechanism of IL-1β processing/secretion using flow cytometry, Western blotting, and ELISA
- Cell culture

Teaching Experience

- 2015-Persent: Mentor of Karin Grathwohl, undergraduate student (recipient of UCI's Undergraduate Research Opportunities Program award)
- 2016: Teaching assistant, Biochemistry lecture (BIO98), Immunology with Hematology (M121), Advanced Immunology lab (M121L)
- 2015: Teaching assistant, Biochemistry lecture (BIO98), Molecular Biology lecture (BIO99), Advanced Immunology lab (M121L), Experimental Microbiology lab (M116L)

Publications

Karimzadeh, A., Scarfone, V., Varady, E., Grathwohl, K., Inlay, MA. CD11a identifies precursors to hematopoietic stem cells in the mouse embryo via neonatal transplantation. Manuscript in preparation (2018).

Karimzadeh, A., Scarfone, V., Varady, E., Chao, C., Grathwohl, K., Fathman J.W., Fruman, D., Serwold, T., Inlay, MA. The CD11a and EPCR marker combination simplifies and improves the purification of mouse hematopoietic stem cells. 2018: *Stem Cell Trans Med (in press)*.

Catalan-Dibene J., Vazquez M., Luu V., Nuccio S., **Karimzadeh A**., Kastenschmidt J., Villalta S., Ushach I., Pone E., Casali P., Raffatellu M., Burkhardt A., Hernandez-Ruiz M., Heller G., Hevezi P., Zlotnik A. Identification of IL-40, a novel B cell-associated cytokine. 2017: *J Immol 199(9)*.

Marsh, S.E., Abud, E.M., Lakatos, A., **Karimzadeh, A.**, Yeng, S.T., Davtyan, H., Fote, G.M., Lau, L., Wienger, J.G., Lane., T.E., Inlay, M.A., Poon, W.W., Blurton-Jones, M. The adaptive immune system restrains Alzheimer's disease pathogenesis by modulating microglial function. 2016: *PNAS* 113(9).

Gov, L., **Karimzadeh, A.**, Ueno, N., Lodoen, M.B. (2013) Human innate immunity to Toxoplasma gondii is mediated by host caspase-1 and ASC and parasite GRA15. 2013: *MBio*. 4(4).

Conference Presentations

- **Poster presentation at the 2017 International Society for Stem Cell Research**

"CD11a identifies precursors to hematopoietic stem cells in the mouse embryo via neonatal transplantation"

- **Oral presentation at the 2016 UCI Stem Cell Awareness Symposium**

"CD11a and EPCR can replace all classical markers for the purification of mouse hematopoietic stem cells."

- **Poster presentation at the 2016 La Jolla Immunology Conference**

"CD11a and EPCR can replace all classical markers for the purification of mouse hematopoietic stem cells."

- **Oral presentation at the 2015 La Jolla Immunology Conference**

"CD11a and EPCR: markers for identification of mouse hematopoietic stem cells."

- **Oral and poster presentations at the 2015 SoCal Flow Summit**

"High resolution markers for characterization of hematopoietic stem cells."

Services

- Organizer of 2015-2016 Molecular Biology & Biochemistry Research-in-Progress seminar series

- Participant in 2015 Sue and Bill Gross Stem Cell Research Center open house

ABSTRACT OF THE DISSERTATION

Novel strategies for identification and isolation of murine adult HSCs and embryonic pre-HSCs

By

Alborz Karimzadeh

Doctor of Philosophy in Biological Sciences

University of California, Irvine, 2018

Professor Matthew Inlay, Chair

Billions of blood cells are produced in the body on a daily basis. At the top of the hematopoietic hierarchy are the hematopoietic stem cells (HSCs) that are able to self-renew, give rise to all downstream progenitors, and engraft long-term upon transplantation into a conditioned recipient. HSC transplantation (HSCT) can be employed to repopulate a defective blood system with a healthy one. In fact, HSCT has the potential to treat any disease that is inherent to the blood system. Yet due to the complications associated with it, HSCT is often utilized as a last-resort option. In recent years, the advent of induced pluripotent stem cells (iPSCs) has promised a definitive solution to HSCT-related complications by introducing the prospect of patient-specific iPSC-derived HSCs (iHSCs). Encouraging advancements have produced iHSCs that exhibit HSC-like properties, however, generation of iHSCs with therapeutic potential has failed due to a lack in robust BM engraftment potential.

Generated iHSCs share similar characteristics to the embryonic precursors to HSCs, pre-HSCs, which also lack BM engraftability. Understanding the natural pathways that drive maturation of pre-HSCs into BM-engraftable HSCs can shed much-needed light on the necessary signals required for the generation of therapeutic iHSCs. However, our understanding of the development of the hematopoietic system is incomplete. The ability to better isolate HSCs and pre-HSCs would allow improved characterization of these cells and highlight the molecular differences between them, and perhaps, identify the defining factors in pre-HSC maturation.

Here we report the use of CD11a as a potent marker of adult HSCs and embryonic pre-HSCs. We introduce an efficient strategy for FACS-purification of adult HSCs. This new strategy addresses the issues associated with HSC sorting in conditions where conventional HSC markers fail. Furthermore, we provide evidence for the efficacy of CD11a in combination with another HSC marker, endothelial protein C receptor (EPCR; also known as CD201), for the isolation of all BM HSCs without the need for additional HSC markers.

CD11a can also be used to identify embryonic pre-HSCs. Here we demonstrate that CD11a greatly improves the purity of pre-HSCs in a rare sorted population. Moreover, our sorting strategy with CD11a allows the isolation of all pre-HSCs from all the tissues and the timepoints that are relevant to pre-HSC biology. Furthermore, we confirm the identity of our putative pre-HSC population with the use of an entirely *in vivo* model (instead of a commonly-used *ex vivo* assay which may not reveal pre-HSC-specific activity). Based on our findings, we propose that improved characterization of cellular and molecular players in the developing liver niche can benefit our understanding of pre-HSC maturation. Altogether, we establish CD11a as an indispensable marker for adult HSC and embryonic pre-HSC identification and isolation.

CHAPTER 1: INTRODUCTION

Opening Statement

The work presented here focuses on the utility of CD11a as a marker for FACS-purification of murine adult hematopoietic stem cells (HSCs) as well as their embryonic precursors, pre-HSCs. First, this work discusses the importance of purifying HSCs and pre-HSCs, and presents the body of work leading up to the studies described in later chapters. Second, this work examines a new sorting strategy for identification of adult HSCs with the use of CD11a. Third, this work investigates the use of CD11a for isolation of a rare embryonic pre-HSC population for further characterization of this population. Fourth, this work discusses the contributions of the novel findings reported here with respect to other developments in hematopoietic research, and presents contexts in which this work can lead to further contributions to the filed.

Historical Overview of HSCs

HSCs are perhaps the best-characterized adult stem cells in the body. Interestingly, qualitative observations coupled with imaginative creativity of scientists two centuries ago predicted some of the characteristics of HSCs. Advances in microscopy in the 19th century fueled an array of theories about HSC biology. For the first time, scientists were able to directly visualize and therefore hypothesize about a host of cellular processes. Astonishingly, the BM was theorized to be the source of blood formation in adults, existence of various blood cell types was determined, and even a common progenitor of all blood cells was proposed around the turn

of the 20th century[1,2]. Yet, definite evidence of for the presence of stem cells in the blood system required another major development.

Therapeutic use of HSCs has saved many lives and the promise it carries potentiates HSCs as even a more potent therapeutic agent in the future. Ironically though, our current understanding of HSCs owes a great deal to the invention and the use of atomic weaponry during a dark time of history. As interest peaked about the negative effects of radiation on humans in the middle of the 20th century, ways to combat these negative effects were considered[3]. The bone marrow (BM) was observed to be especially sensitive to the effects of radiation, and experiments were performed to replace affected BM cells with healthy ones. Setting the stage for future generations were the first experiments in the 1950's to show that intravenous injection of BM cells from a healthy donor protects lethally-irradiated recipient mice[4,5]. The first quantitative studies of HSCs followed, where Till and McCulloch used a limiting dilution assay (LDA) to investigate the minimum number of BM cells required to rescue irradiated animals[6]. Till, McCulloch, and others then discovered that donor BM cells formed colonies in the spleens of recipient animals, with each colony containing different types of blood lineages, lending to the idea that the BM contains individual cells capable of producing colonies with more than a single lineage[7-10]. Instead of transplanting single cells, the clonality of donor-derived cells was confirmed by matching unique karyotype abnormalities between the colony-initiating donor cell and multi-lineage cells in that colony[8]. For lack of a more creative term, the cells responsible for forming these donor-derived spleen colonies were termed spleen colony-forming units (CFU-S). Hints of long-term regeneration capacity of the CFU-S was highlighted by the fact that some CFU-S were capable of forming colonies when harvested from primary recipients and injected into secondary recipients[11]. Although the vast majority of CFU-S are not HSCs as determined by

later experiments[12], these initial experiments provided the foundation for investigating the presence of HSCs and for determining the properties associated with HSCs as we know them now. Discovery and isolation of bona fide HSCs was not accomplished until a few decades later when the Weissman group reported the physical isolation of an HSC population for the first time[13] (discussed later in this chapter). Accordingly, isolation of HSCs allowed characterization of these cells.

HSC Properties

"Stemness" is generally defined by the ability of a self-renewable cell to give rise to the entirety of downstream cells of a particular lineage[14,15]. HSCs, in particular, are defined by three properties: 1) self-renewal: the ability to persist over the lifetime of an animal through asymmetric cell division; 2) multipotency: the capacity to give rise to all hematopoietic lineages; 3) engraftability: the potential to engraft a myeloablated recipient upon transplantation[16]. Thus, HSCs can divide to give rise to daughter HSCs (self-renewal) as well as downstream progenitor cells that have an increasingly more restricted lineage output upon further differentiation. HSCs rarely divide and are therefore quiescent[17], yet billions of blood cells are produced on a daily basis[18]. To meet this requirement, HSCs can differentiate into multipotent progenitors (MPPs) which are transit-amplifying (fast-dividing) cells with no self-renewal capacity but with the potential to give rise to all blood lineages[16]. MPPs are further differentiated into committed progenitors capable of producing either the myeloid/erythroid or the lymphoid lineage. Each lineage progenitor then commits to more specific downstream lineages. Therefore, differentiation of HSCs ultimately produces all hematopoietic cell types such as B and T lymphocytes, myeloid cells, erythrocytes, and so on (multipotency)[19] (Figure 1.1). As a progenitor cell differentiates

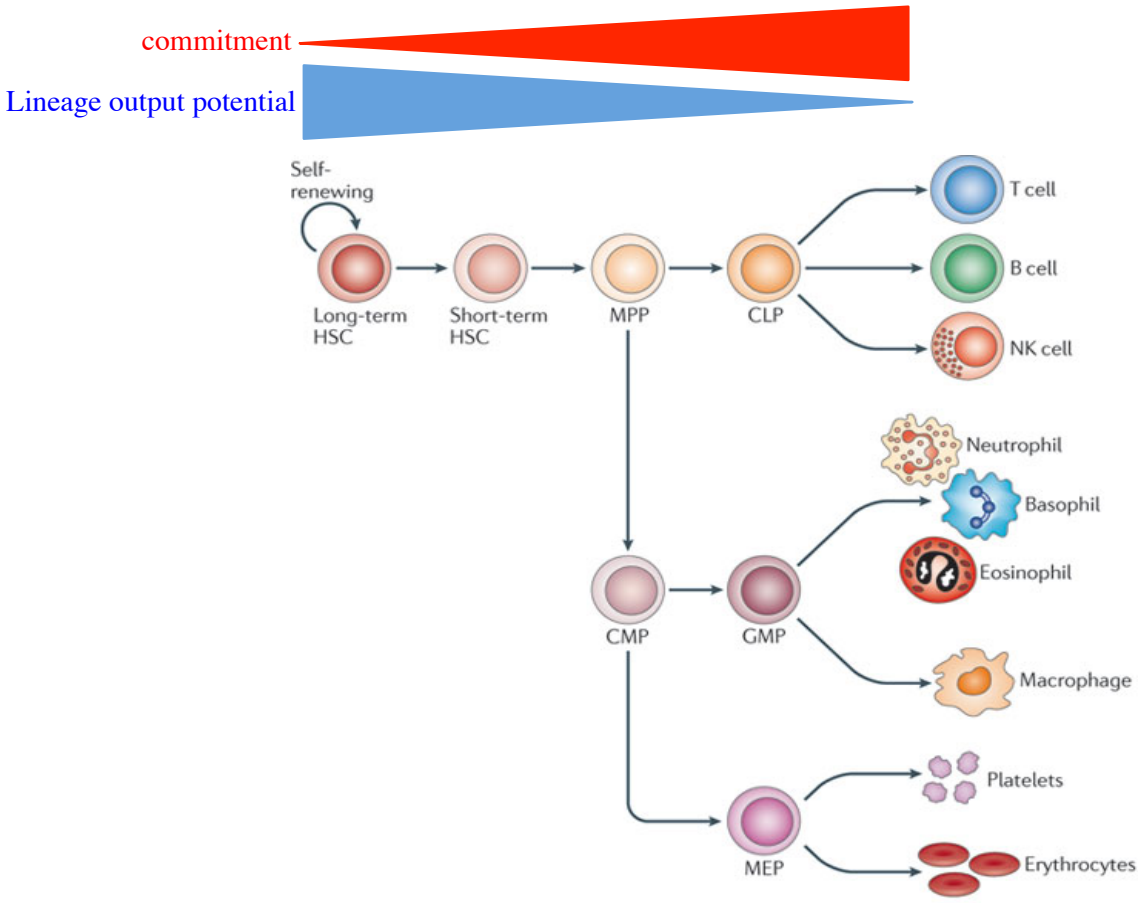

Figure 1.1. The "hematopoietic tree" and the inverse relationship between differentiation and lineage output potential. HSCs are able to self-renew and to give rise to all downstream progenitor and, ultimately, effectors cells of the blood system. With each differentiation step, a cell increases commitment to a particular lineage while losing its lineage output potential (highlighted by red and blue triangles in the figure). CLP: common lymphoid progenitor; CMP: common myeloid progenitor; GMP: granulocyte/myeloid progenitor; MEP: megakaryocyte/erythroid progenitor. *Adapted from King and Goodell, Nature reviews, 2011*[19].

down a lineage, it increases its commitment and decreases its lineage output potential[16]. Therefore, differentiation of all progenitors is unidirectional and irreversible.

Long-term engraftability as a Defining Property of HSC Identity

Self-renewal and multipotency potential can be revealed through transplantation, which is the definitive functional test to determine HSC activity. HSCs have long-term engraftment potential, therefore transplantation of HSCs results in persistent repopulation of the entire blood system of the recipient animal. To allow engraftment of transplanted cells, BM cells of the recipient are wiped with the use of radiation or mobilizing agents. Upon intravenous injection into a myeloablated recipient, HSCs circulate in blood vessels, extravasate into the BM, lodge into their niche, and engraft there for the long-term[20]. Extravasation or "homing" to the BM occurs within a few hours[21] and involves sequential steps mediated by the interaction of selectins, integrins, and adhesion molecules on HSCs and on the endothelial cells (ECs) that line the blood vessels. These interactions lead to HSCs coming to a slow roll on the EC layer, followed by firm arrest, crawling, and eventual migration of HSCs through the ECs, known as transendothelial migration (TEM)[22]. Initial interaction and the slow rolling on the EC layer requires the involvement of P-selectin glycoprotein ligand 1 (PSGL-1), very late antigen 4 (VLA-4), and CD44 on homing cells that mediate the interaction with selectins and vascular cell adhesion molecule 1 (VCAM-1) on the ECs[23-27]. VLA-4 and leukocyte function-associated antigen 1 (LFA-1) on homing cells interact with VCAM-1 and intercellular adhesion molecule 1 (ICAM-1) on ECs to mediate firm arrest and initiate TEM[28-31]. Details on the involvement of LFA-1 in this process are described later in this chapter. After TEM, expression of matrix metalloproteinases results in a highly proteolytic microenvironment leading to extracellular matrix (ECM)

remodeling, thereby facilitating the crossing of the basement membrane by the homing cell[32]. The interaction between CXCR4 on homing cells and the CXCL12 gradient produced by niche cells not only mediates the initial rolling and arrest steps but also guides HSCs to lodge to their niche, and facilitates long-term persistence of homed cells in the HSC niche[27,33,34].

CXCL12-abundant reticular (CAR) cells, perisinusoidal ECs, and leptin receptor-expressing stromal cells are all important sources of CXCL12, which maintains long-term engraftment of HSCs[34,35]. Nestin-expressing mesenchymal cells and perisinusoidal ECs express high levels of stem cell factor (SCF), which is an important factor in retaining the "stemness" of HSCs[36-41]. Wnt, thrombopoietin, N-cadherin, and osteopontin are among other important signaling molecules that regulate HSC self-renewal and differentiation in the BM niche[42]. Therefore, intricate interactions between signaling molecules allow homing of HSCs into the BM and a complex cellular network of niche cells regulate a fine balance between self-renewal and differentiation of HSCs.

Hematological Diseases and the Therapeutic Potential of HSC Transplantation

Defects in hematopoiesis can have detrimental health effects. As mentioned earlier, an intricate regulation of self-renewal and differentiation is required for preservation of a healthy blood system. Thus, defects in these regulatory mechanisms can result in unchecked proliferation or acquisition of self-renewal capacity by differentiated progenitor/effector cells, resulting in a variety of blood cancers[43-47]. Defects in a functioning immune system can result in severe combined immunodeficiency (SCID), leaving the affected susceptible to life-threatening infections[48]. Abnormal function or numbers of red blood cells can cause sickle disease and anemia, respectively[49,50]. Autoimmune diseases, such as type 1 diabetes, multiple sclerosis,

rheumatoid arthritis, and many more, can arise due to hyperactivity of the immune system[51]. Accordingly, the number of people affected with serious hematological disorders is significant.

Due to their capacity to repopulate an entire blood system upon transplantation, HSC transplantation (HSCT) has been used in the clinical setting to treat hematological diseases. In fact, successful HSCT can potentially treat *any* disorder inherent to the hematopoietic system by replacing the defective blood system with one from a healthy source[52]. However, HSCT is commonly used only as a last-sort option due to its associated complications[52,53]. These complications can arise from side-effects of the conditioning regimens of recipients and/or from unwanted immunological reactions between donor and recipient cells. Recipient blood cells are depleted by irradiation or chemotherapy to provide the resources required for donor cell engraftment. As a result of this immunodeficiency period, recipients are at high risk for deadly infections[54]. On the other hand, an important contributing factor to failed HSCT is graft-vs-host disease (GvHD), which arises when transplanted donor cells recognize recipient tissues as "non-self" and attack them[54,55]. Conversely, donor cells can be on the receiving end of unwanted immune responses, resulting in graft rejection by the immune cells of the recipient[55]. GvHD and graft rejection are concerns in allogeneic transplants, where donor and recipient sources are two different individuals. Having a genetically-matched sibling donor minimizes the risks of GvHD and graft rejection, yet the vast majority of patients in need of allogeneic transplants do not have a matched sibling donor and the threat of GvHD and graft rejection looms over a considerable fraction (30-40%)[56] of HSCT recipients[57]. On the other hand, autologous transplants, transplantation of a patient's own stem cells, are not useful when dealing with genetic defects inherent to the hematopoietic system or cancer patients due to the risk of introducing back BM-metastasized cancer cells. As HSCs cannot be maintained in culture, efficient gene-correction

manipulation of a donor source is also not attainable[58]. Insufficient numbers of transplanted HSCs can also complicate HSCT success[55,59]. Therefore, the therapeutic potential of HSCs has not been fully harnessed due to the complications originating from the lack of abundant HSC numbers, the requirement for harsh conditioning regimens, and genetic disparities between donors and recipients.

The Promise and Challenges of Pluripotent Stem Cell-Derived HSCs

To bypass the issues presented to HSCT, effort has been aimed to generate HSCs from pluripotent sources such as induced pluripotent stem cells (iPSCs). Pluripotency is defined by the ability to produce all three germ layers and, therefore, any cell type in the body. Whereas embryonic stem (ES) cells used to be the sole source of pluripotent cells, groundbreaking work by Takahashi and Yamanaka in 2006 achieved the generation of iPSCs from terminally-differentiated cells[60]. Pluripotency was achieved by the overexpression of Oct3/4, Sox2, c-Myc, and Klf4 (dubbed later as the "Yamanaka factors") in mouse fibroblasts. Follow-up studies achieved the induction of iPSCs from human fibroblasts as the starting material, signifying possible applicability of this approach in the clinic[61]. The list of iPSC sources expanded after these initial studies to include stomach and liver cells[62], pancreatic beta cells[63], B lymphocytes[64], chord blood[65], keratinocytes in hair follicles[66], and epithelial cells in the urine[67]. Thus, these developments made it possible to generate patient-specific iPSCs, capable to produce any cell type in the body, through non-invasive harvest of differentiated cells. Reprogrammed iPSCs could then be stimulated to produce the desired cell type. Therefore, production of iPSC-derived HSCs (iHSCs) would provide a patient-specific source of donor cells that can be maintained in culture, therefore circumventing genetic incompatibility (avoiding GvHD and graft rejection)

and providing an infinite number of HSCs for each patient (eliminating graft failure). In the case of genetic hematological disorders, cultured iPSCs can be gene-corrected and screened in culture, differentiated into iHSCs, and gene-corrected iHSCs can then be administered at desired numbers into patients (Figure 1.2)[68].

As iPSCs resemble an undifferentiated, embryonic-like state, these cells require temporally-defined stimuli for differentiation into the desired cell type. Although significant progress has been made, efforts aimed to generate functionally robust iHSCs from iPSCs have not been exclusively successful. iHSCs have been generated from a variety of sources and with the use of different protocols. Although self-renewable and multipotent, a common feature of generated iHSCs up do date is a lack of BM engraftment capacity[69]. Seminal work by the Rossi group has generated iPSCs from circulating lymphocytic and myeloid cells, and has derived "HSC-like" cells with multipotency potential through ectopic expression of six transcription factors (Runx1t1, Hlf, Lmo2, Prdm5, Pbx1, and Zpf37)[70]. However as noted by the authors, BM-engraftment of these iHSCs was extremely inefficient. Although more recent studies have minimally improved the engraftment of iHSCs[71-73], robust BM engraftment of iHSCs upon transplantation has not been achieved. In the most promising of these studies, Sugimura *et al*. took a two-step approach. First, iPSCs were differentiated into a hemogenic endothelial-like cell (more details on the hemogenic endothelium later in this chapter), followed by a second directed differentiation into iHSCs by enforced expression of seven transcription factors (Spi1, Lcor, Erg, HoxA5, HoxA9, HoxA10, and Runx1)[72]. These iHSCs showed multipotency potential and even, in some instances, engrafted in primary and secondary recipient mice upon transplantation, which was a significant achievement compared to previous attempts. Yet, engraftable iHSCs were rarely detected and robust engraftment potential was not achieved. The minimal overlap

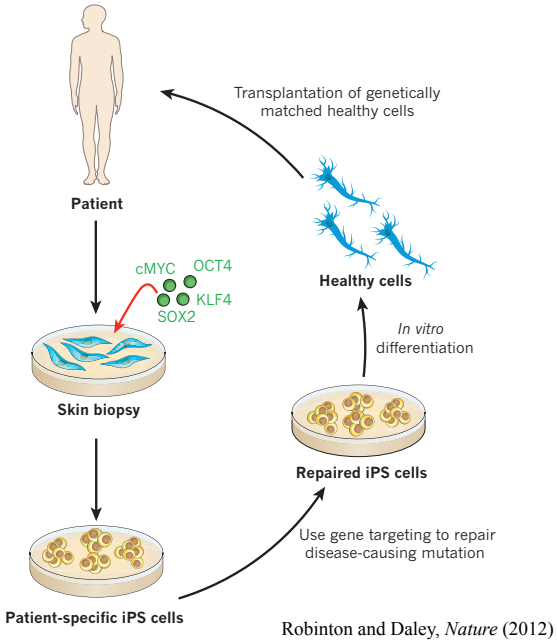

Figure 1.2. Production of patient-specific iPSC-derived HSCs for transplantation. Differentiated cells from the skin (or other sources) can be harvested using non-invasive methods. iPSCs can be generated by ectopic expression of the Yamanaka factors in cells harvested from the patient. iPSCs can then be cultured indefinitely, gene corrected, differentiated into the desired cell type, and transplanted into the patient. *Adapted from Robinton and Daley, Nature, 2012*[68].

between the transcription factors identified/used for directed differentiation in each of the two studies reported here is worth noting. On the other hand, many of these transcription factors are proto-oncogenes, potentially eliminating them as candidates in future clinical approaches[74]. Therefore, although iHSCs exhibit HSC-like properties such as multipotency, necessary cues to allow long-term BM-engraftment have not been identified. To identify factors necessary for step-wise differentiation of iHSCs from a pluripotent source, we must improve our understanding of the natural processes that give rise to HSCs during development.

Early Hematopoietic Development: Waves of Blood

Unlike the well-defined spatial and functional characteristics of HSCs in adults, embryonic hematopoietic events need further characterization. Contributing to our relative lack of understanding when it comes to embryonic hematopoiesis is the simple fact that the embryo is an ever-changing and continuously developing system. In the embryo, distinct blood-forming cells appear at different times and in different tissues, with each one exhibiting drastically different phenotypic and functional characteristics. The hematopoietic lineage is believed to arise from a specialized vascular mesodermal source, termed hemogenic endothelium (HE)[75]. First indications for the endothelial to hematopoietic transition (EHT) was provided by direct observation of blood cells forming from the vasculature in chick embryos[76]. Future studies confirmed these empirical observations by establishing, in several species, that blood cells labeled with an EC-specific dye are found when vasculature ECs are labeled prior to the initiation of embryonic hematopoiesis[77,78]. These studies were later confirmed by more advanced imaging techniques and complex genetic fate tracing strategies[79].

The first hematopoietic blood-forming cells in the mouse embryo arise around embryonic day (e) 7.5 in the blood islands on the yolk sac (YS)[80]. These primitive blood-forming cells are lineage-restricted and primarily produce primitive erythrocytes, distinguished by the presence of a nucleus (mature erythrocytes are enucleated)[81]. This primitive wave is short-lived as the numbers of primitive erythrocytes start to decrease significantly at e13.5[80]. At e8.5, establishment of a heartbeat is succeeded by the emergence of a distinct wave of hematopoietic-forming cells called erythro-myeloid progenitors (EMPs) in the YS and the placenta (PL)[82,83]. Instead of the primitive erythroid cells produced by the partially overlapping primitive wave, EMPs give rise to definitive enucleated red blood cells (RBCs) as well as megakaryocyte and myeloid progenitors[83,84]. EMP-derived macrophages persist as tissue-specific macrophages in the brain (microglia), lung (alveolar macrophages), skin (Langerhans cells), liver (Kupffer cells), and spleen (splenic macrophages) of adult animals[85]. Although the progeny produced by the EMP wave can persist into adulthood by means of local self-renewal, the EMP wave itself is transient and lineage-restricted[82,84]. Immediately preceding the emergence of mature HSCs, the first wave of multipotent and self-renewable progenitors appears. These cells are termed precursors to HSCs, "pre-HSCs" for short (Figure 1.3)[86]. Although HSCs have been detected in extremely rare instances in embryos younger than e11.5 (discussed later in this chapter), multipotential output around e9.5 until e11.5 is dominated by pre-HSCs.

The Rise of "Pre-HSCs"

Pre-HSCs emerge around e9.5 in the YS, aorta-gonad-mesonephros (AGM), and PL, and they later travel to the fetal liver (FL) where they contribute to the expansion of mature HSCs[86-88]. Pre-HSCs possess two of the three properties of HSCs (e.g. self-renewal and multipotency),

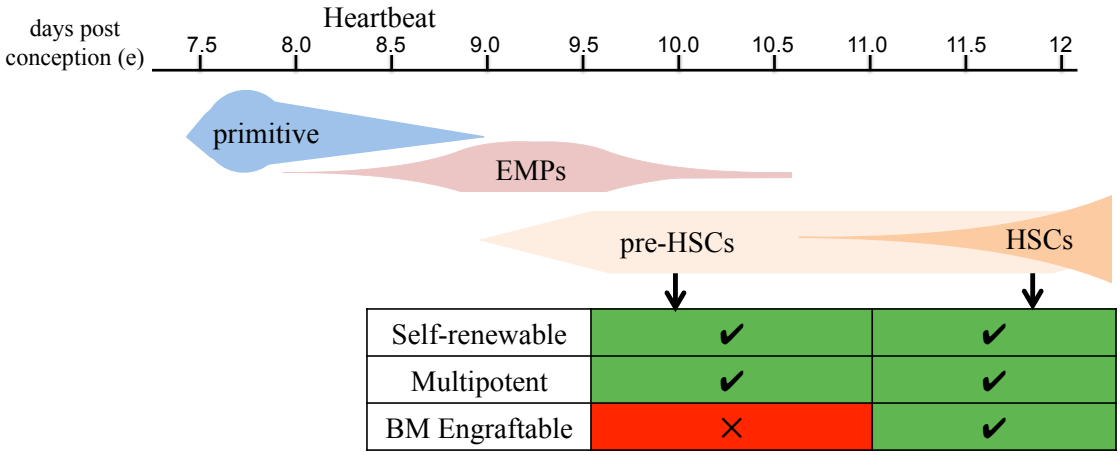

Figure 1.3. Waves of blood-forming cells during early embryonic development. Primitive blood-forming cells appear around embryonic day (e) 7.5 followed by the appearance of EMPs (erythro-myeloid progenitors) at e8.5. Pre-HSCs are the first self-renewable and multi-potent hematopoietic cells that first appear around e9.5. Pre-HSCs lack BM engraftment potential and give rise to fully-functional HSCs that persist into adulthood.

however they lack the ability to engraft the BM of an adult recipient upon transplantation[86]. Because pre-HSCs do not show conventional engraftment capacities, modifications were made to conventional transplantation assays to reveal the activity of pre-HSCs upon transplantation. Initial studies aimed to determine pre-HSC multipotency took advantage of an *in vitro* co-culture system originally developed in 1966 to reveal colony formation potential of BM cells[89]. This system consisted of co-culturing BM cells with either neonatal kidney or e17 embryo feeder cells in agar. Modification were made to the culture system, and the modified culture system was used to show *in vitro* colony formation as well as *in vivo* CFU-S activity of e8.5 (and older) YS-derived cells[80]. Later studies included further modification to the *in vitro* culture system by the addition of exogenous growth factors (such as IL-3, IL-7, SCF, Flt3l, TPO) and the use of alternative feeder stromal cells. Such studies confirmed that at around e9.5, a population of cells appears that produces colonies containing distinct lineages in *in vitro* culture systems as well as in the spleen of irradiated recipients upon transplantation after *in vitro* maturation[90-92]. Coupling of the optimized *in vitro* maturation systems with transplantation also allowed the assessment of the reconstitution capacity of what later were defined as pre-HSCs. These experiments established the presence of e9.5-11.5-derived cells that, after *in vitro* culture (aka *ex vivo* maturation), show long-term engraftment in recipient adults[93-95]. Therefore, these cells possessed self-renewal and multipotency potential and modifying conventional transplantation assays could reveal their engraftment capacity by inducing their maturation *in vitro*.

An alternative method to reveal engraftment capacity of pre-HSCs is through the use of neonatal recipients. In a series of experiments, Yoder *et al*. determined that direct transplantation of e9.5-10.5 YS and AGM cells results in the engraftment of these cells in neonatal recipients, whereas no engraftment was revealed when cells were transplanted into adult recipients[96-98]. The

exact reason for the receptivity of neonatal recipients to transplanted embryonic cells was not investigated, but it was assumed that the neonatal liver acts as an accessible site of maturation for transplanted pre-HSCs. No direct evidence has yet supported this notion. The initial studies by Yoder *et al*. therefore established a completely *in vivo* system to reveal pre-HSC engraftment potential. The neonatal transplant system, thus, eliminates the requirement of exogenous factors used in the *ex vivo* assay and promotes the maturation of the pre-HSCs in a completely natural microenvironment. Altogether, modifications made to conventional transplantation assays have revealed engraftment potential of pre-HSCs in e9.5-11.5 intra- (AGM and FL) and extra-embryonic (YS and PL) tissues[86].

Quantitative studies have determined that pre-HSCs emerge around e9.5 and increase in numbers at e10.5 with the highest frequency at e11.5[86,99,100]. Furthermore, pre-HSCs are believed to be generally rare as numbers of these cells are estimated to be, by highest estimates, approximately 30 in each AGM tissue of e11.5 embryos[101]. At e10.5-11.5, extremely rare HSC activity (defined by adult BM-engraftability upon transplantation) can be detected in the AGM, YS, and PL of embryos (i.e. about 1 HSC per e11.5 AGM)[93,102-104]. However after e11.5, fully-functional HSCs (capable of BM engraftment upon transplantation) are found in the AGM, YS, PL, and FL with robust expansion of HSCs starting at e12 in the FL[86,102,104]. After e12.5, the FL is the primary tissue for hematopoiesis tissue and it remains so until after birth when HSCs migrate to their permanent niche in the BM[93,105]. Thus, these studies defined the spatiotemporal dynamics of the emergence of pre-HSCs and HSCs as a framework for deeper characterization of events governing embryonic hematopoietic development.

HSC Markers for FACS

Molecular and functional characterization of any cell type can be achieved by purification of that cell type. Today, HSCs are the best-characterized stem cells. Though the vast body of HSC literature available to us required a major breakthrough that defined a new era in HSC research. In 1988, the Weissman group coupled the advent of fluorescent activated cell sorting (FACS) to the use of fluorophore-conjugated antibodies to achieve the very first isolation of a rare population containing mouse adult HSCs[13]. This innovation used FACS to physically isolate different BM progenitor populations (including HSCs) based on their expression of surface molecules, referred to as "markers". Transplantation of each isolated population could then reveal engraftment potential. The initial groundbreaking work by the Weissman group to isolate an HSC population determined long-term engraftment potential to be contained only within CD90^{low} Lineage (Lin)- Sca-1+ cells[13,106]. What followed was a boom in HSC research leading to our current understanding of HSCs, as these cells could be isolated to be molecularly and functionally characterized. Although the initial "HSC" population was very rare in the BM (0.05% of BM cells), follow-up experiments proved the presence of non-HSCs within it[106]. Further fractionation demonstrated the presence of three distinct progenitor populations within the CD90^{low} Lin- Sca-1+ population: long-term HSCs (LT-HSCs), short-term HSCs (ST-HSCs; HSCs with limited self-renewal capacity), and MPPs. These populations could be resolved by differential expression of additional markers, where the absence of Mac-1 and CD4 marked LT-HSCs, ST-HSCs expressed low levels of Mac-1 (Mac-1^{low} CD4-), and MPPs were Mac-1^{low} CD4^{low}[107,108]. Similar reductionist approaches that further fractionated the enriched progenitors population proved that HSCs also express Kit, establishing the "KLS" (Kit+ Lin- Sca-1+) population[109,110]. To date, the KLS is the most commonly used marker combination for the identification and isolation of hematopoietic stem/progenitor cells (HSPCs). With the addition of

each new marker to the existing panel, HSC purity of the final product was improved as the presence/absence of each additional marker noted differentiation of HSCs into downstream progenitor cells (Figure 1.4)[16]. Within the next 30 years from the first FACS-purified HSC transplantation experiment, the list of HSC markers grew to include CD34[111], CD150[38], CD48[38], EPCR[112], CD9[113], FLK2 (Flt3)[114], CD27[115], Tie2[116], and CD105[117] among others. Although no one marker has been identified for the identification of HSCs[118], various marker combinations can produce highly enriched HSC populations.

HSC Markers: Almost There…

The choice of marker combination is dictated by the goal of the study. As an example of a "tried and tested" marker combination, sorting the cells with only four markers (Lin- CD34- Kit+ Sca-1+) followed by single-cell transplantation produces multi-lineage reconstitution in 1/3rd of recipient mice[111]. Yet, the same results cannot be obtained with just any four-marker combination, as some markers show a certain amount of overlap between their expression patterns. Therefore, not all markers are equal, and marker combinations can be redundantly inefficient for isolation of a pure HSC population. Hence, a certain level of expertise is required to find the most appropriate marker combination. From a regenerative viewpoint, transplantation of the highest number of HSCs possible results in a faster reconstitution in the recipient[119]. Therefore, if shorter recovery time is desired, the choice of marker combination must be customized to strike the right balance between yield and purity. However, testing a new panel of markers can be an extremely expensive and time-consuming process. Each transplanted population should be tested for multi-lineage reconstitution potential in primary recipients

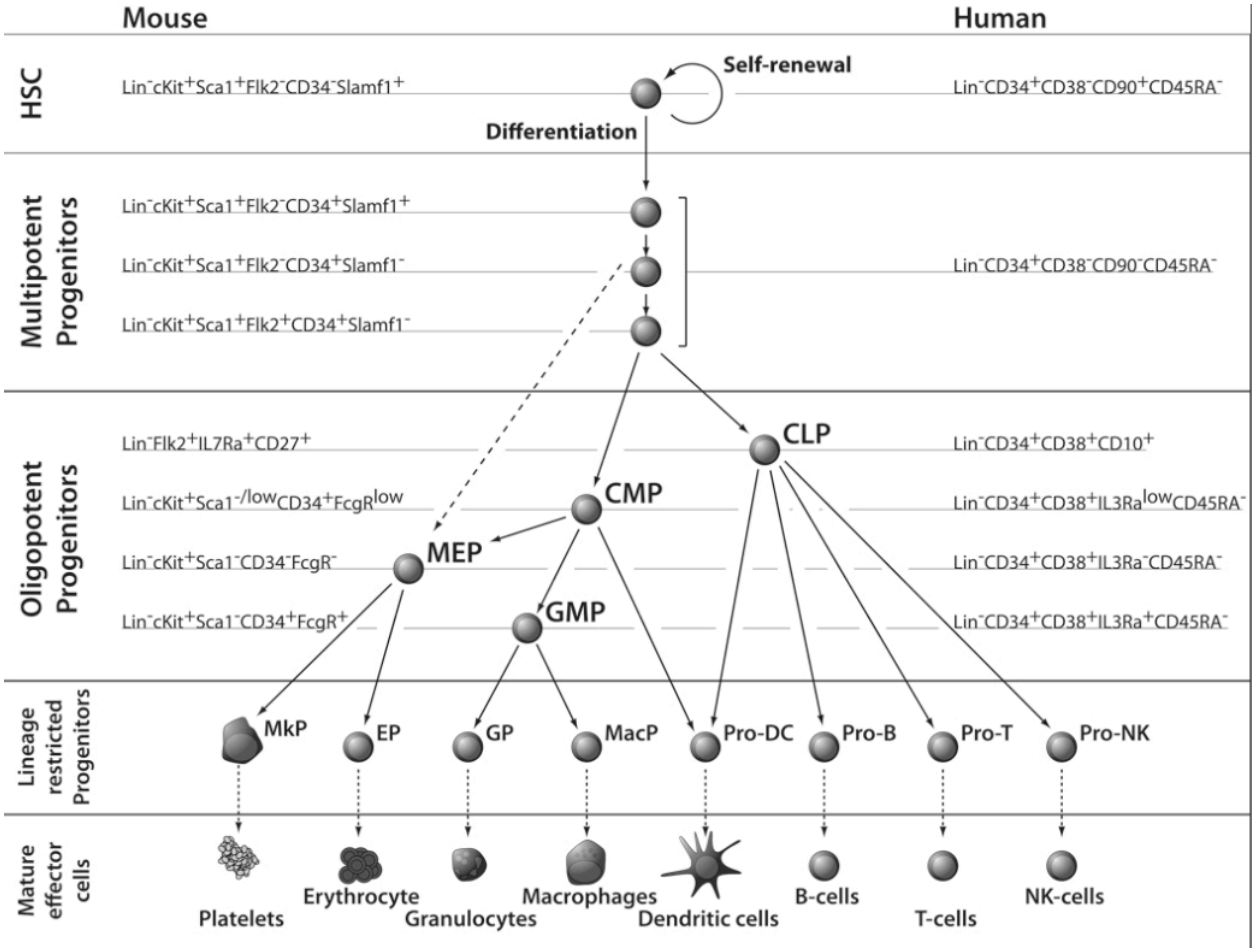

Figure 1.4. Progenitor markers up-/down-regulated with differentiation. Fractionation of progenitor populations based on marker expression allowed the identification of BM progenitor populations. *Adapted from Seita and Weissman, Wiley Interdisciplinary Reviews, 2010*[16].

(minimum of 3 months post-transplant) and further long-term engraftability potential in secondary recipients (minimum of 1-2 months). Therefore, development of sorting strategies that can be used for efficient improvement of HSC purity as well as HSC yield is of great interest.

Although established HSC sorting strategies, such as KLS, generally produce desired results in homeostatic conditions, they can fail in a number of scenarios. Conditions of BM stress as a result of inflammation or BM injury can result in changes in marker expression on HSPCs[120-124]. Induced interferon-gamma (IFN-γ) production in inflammatory conditions can result in up-regulated Sca-1 expression on hematopoietic cells, making it impossible to differentiate between normally Sca-1- downstream cells and HSPCs[125]. Accordingly, the IFN-γ-responsive elements in the flanking region of *Ly-6A/E* (gene encoding for Sca-1) have been described[126,127]. Conditions that result in IFN-γ–induced Sca-1 expression include poly (I:C)[124] and lipopolysaccharide (LPS)[123] treatment. On the other hand, Kit expression can be significantly down-regulated as a result of irradiation-induced BM stress[122] or treatment of mice with the mobilizing agent 5-fluorouracil[128]. Also, use of KLS to sort HSPCs is problematic in certain mouse models, such as NOD, BALB/cJ, C3h/HeJ, and CBA/J, that show very little Sca-1 expression on HSPCs[129,130]. Therefore, studying HSC biology in such scenarios requires alternative identification strategies. Accordingly, even though HSC markers work well in homeostatic conditions, there still is a requirement for markers that are reliable in different conditions.

Pre-HSC Markers and their Limitations

While there is a long list of markers at disposal to identify adult HSCs, reliable embryonic pre-HSC markers are scarce. A group of adult HSC markers are rendered useless for the identification of pre-HSCs as either their expression pattern is not correlated with pre-HSC

activity or because they are not yet expressed at the earlier embryonic stages. Additionally, the expression pattern can be inconsistent between embryonic timepoints and/or tissues. Because of the fast pace of development during e9.5-11.5 (when pre-HSCs are most abundantly found) and because of the structural, cellular, and microenvironmental differences of the major hematopoietic tissues in the embryo (e.g. AGM, YS, PL, FL), consistency of pre-HSC markers along different timepoints/tissues needs further investigation. For instance, the prominent adult HSC marker CD150 cannot be used in the case of embryonic pre-HSCs because it is differentially expressed in different tissues with CD150 + and – cells showing inconsistent multi-lineage potential[86]. Also, compared to adult HSCs, pre-HSCs are the more immediate divergent progeny of an endothelial source (e.g. HE). Thereby remnant expression of EC markers can be more readily detected on pre-HSCs, adding another layer of complication to the purification of these cells. The HE origin of hematopoietic cells contributes to expression of CD105[117], Tie2[116], and EPCR[112] (EC markers) on adult HSCs. Yet, EC-associated markers CD144[86] (VE-Cadherin; VC) and CD31[99] (lowly expressed on HSCs) are only expressed on pre-HSCs and absent on adult HSCs.

The choice of assay to detect pre-HSC activity is also a matter of debate. *Ex vivo* maturation assays present an artificial microenvironment and rely on the addition of potent exogenous growth factors that can potentially drive uncommitted ancestors of pre-HSCs to become mature hematopoietic progenitors[131,132]. On the other hand, many of the candidate pre-HSC markers have not been tested in the more biologically-relevant neonatal transplant system which supports *in vivo* maturation of pre-HSCs[87,96,100]. Therefore, the pre-HSC activity associated with most putative pre-HSCs can be an artifact of the *in vitro* culture system. Such markers, then, may not be accurately marking the cellular players shaping the developing blood system in the

developing embryo. So, the efficacy of such markers requires further confirmation in a more natural setting. Altogether, due to the complications discussed above, purification of a pre-HSC population with similar resolution to sorted adult HSCs has not yet been accomplished.

Embryonic Pre-HSCs and the Missing Link for Generation of iHSCs

Certain adult HSC markers efficiently identify embryonic pre-HSCs. Progenitor markers Kit and Sca-1 match their utility as adult HSPC markers in the embryo, producing an embryonic equivalent to KLS (eKLS)[86,87]. Hematopoietic lineage markers CD41, CD43, and CD45 have also been used to mark the emerging embryonic hematopoietic progenitors[86-88,99]. Although these markers have shown promise in the identification of putative pre-HSC populations, the pre-HSC purity in such populations requires further improvement. Purer pre-HSC populations are essential for prospective molecular characterization of these cells. This is especially important when we consider that embryonic pre-HSCs show an explicit resemblance to iHSCs. Similar to pre-HSCs, iHSCs represent an immature developmental stage that requires the correct conditions to move towards its fully-functional form (e.g. an engraftable HSC). Both cell types have self-renewal and multiptotency potential but show limited engraftment potential, namely a lack of BM engraftment potential[86-88]. Successful generation of functional iHSCs calls for mimicking the natural processes leading to the generation of mature HSCs *in vivo*. Yet, identification and isolation of pre-HSCs to a high resolution has not been accomplished. Also, non-pre-HSC contamination skews molecular and functional characterization of pre-HSCs. Thus, improving pre-HSC purity to highly enriched levels would allow deeper molecular characterization of these cells, and therefore contribute to the discovery of interactions between pre-HSCs and niche cells

that endow the eventual BM engraftment potential to pre-HSCs. Accordingly, introduction of reliable pre-HSC markers is essential to unlock the therapeutic potential of iHSCs.

CD11a as a Potential Marker of Murine Adult HSCs and Embryonic Pre-HSCs

CD11a (integrin αL) and CD18 (integrin β2) dimerize to form LFA-1, which is a member of the integrin superfamily that is exclusively expressed in leukocytes[133]. Integrins are transmembrane adhesion molecules that interact with ECM proteins such as laminins, collagens, and fibronectins and with cellular ligands such as selectins, cell adhesion molecules, and cadherins[134,135]. Interaction of integrins with their ligands results in attachment as well as communication between interacting cells[136-138]. As part of the integrin superfamily, LFA-1 activation plays key roles in a number of immunological processes such as activation, migration, and homing of leukocytes[139,140]. Activation of LFA-1, like other integrins, has an "inside-out" as well as an "outside-in" component[141]. LFA-1 integrins expressed on circulating leukocytes have a bent or folded conformation, and are therefore inactive. Upon sensing of stimuli such as cytokines, a signaling cascade results in initiation of the inside-out signaling. Sensing of chemokines by chemokine receptors, TCR (T cell receptor) or BCR (B cell receptor) signaling, and binding of selectins to their ligands can all initiate the inside-out activation of LFA-1[141,142]. This signaling induces conformational changes that increase the affinity of LFA-1 for its ligand, ICAM-1, by unfolding the extracellular domain of the receptor[143,144]. ICAMs -1, -2, and -3 have all been described as LFA-1 ligands. ICAM-1, which is expressed on a variety of leukocytes and on ECs, is the major binding partner of LFA-1 in most interactions[145]. Inside-out signaling also results in clustering of integrins, contributing to induced avidity of the integrin receptor. These events lead to induced adhesion mediated by the integrin[141]. Following the clustering of LFA-1

integrins, the outside-in signaling acts as a co-stimulator to enhance the inside-out-initiated responses in the cell. This sequence of events is essential in the formation of immunological synapses between T/B cells and antigen-presenting cells (APCs) expressing ICAM-1[146]. During inflammatory migration of lymphocytes, the LFA-1-ICAM-1 interaction results in firm adhesion and eventual arrest of traveling lymphocytes on ECs lining blood vessels[147]. LFA-1 also plays an essential role in TEM of leukocytes during homing to tissues[148]. Downstream signaling from LFA-1 activation can act through Erk and JNK to induce transcriptional changes, such as IL-2 production, leading to leukocyte differentiation and cell cycle progression[149].

Given its widespread involvement in trafficking and activation of leukocytes, it is not surprising that LFA-1 is highly expressed in almost all effector cells of the blood system[150]. Whereas CD18 can dimerize with other integrin α subunits to form other integrins (i.e. Mac-1), CD11a is exclusively found as part of LFA-1[151]. CD11a expression on cells is therefore synonymous with LFA-1 expression. Although regulation of the gene encoding for CD11a, *Itgal,* is unknown, previous studies have suggested possible involvement of a glucocorticoid-responsive element in the promoter region of *Itgal*[152]. Other observations have pointed to hypomethylation of *Itgal* promoter as an inhibitory mechanism to explain the cell-specific expression of CD11a[153]. CD11a-KO mice develop normally, but show defects in combating bacterial infections as a result of defective immune cell activation and trafficking[154-157].

Aside from its expression on effector blood cells, CD11a is also expressed at homogenously high levels on the majority of hematopoietic progenitors. However, when HSCs are harvested with the use of conventional markers, CD11a expression shows a bimodal pattern, revealing a CD11a- fraction of conventional HSCs (Figure 1.5A)[150]. Transplantation of each fraction revealed drastically higher engraftment potential from CD11a- fraction of an enriched

HSPC population (Figure 1.5B)[150]. Furthermore, only the CD11a- HSCs showed reconstitution capacity upon secondary transplantation. Also, compared to their CD11a+ counterparts, CD11a- HSCs were determined to be more quiescent, an attribute of adult LT-HSCs[150]. These results established that in combination with other HSC markers, CD11a could be used as a marker of LT-HSCs. Therefore these initial studies introduced an efficient marker for improving HSC purity in populations isolated with FACS. Yet, applicability of CD11a to address other shortcomings of current HSC purification methods was not addressed: as discussed earlier, there are complexities associated with optimizing multi-marker panels. Also, some commonly used strategies, such as KLS gating which was also used in this study, fail in certain scenarios (see "HSC Markers: Almost There…" for more details). Accordingly, we aimed to determine if CD11a could address some of these issues. To this end, in Chapter 2 we present our findings about a simple and efficient sorting strategy that relies on only two markers, CD11a and EPCR. We find that the CD11a/EPCR combination eliminates the need for conventional HSC markers and shows great promise in identifying HSCs in conditions where other markers fail (these finding are discussed in detail in Chapter 2). Our observations in Chapter 2 confirm the utility of CD11a as a potent HSC marker with efficacy when used with or without conventional HSC markers.

As discussed earlier, improved strategies to identify and isolate embryonic pre-HSCs are necessary for deeper characterization of these cells (see "Pre-HSC Markers and their Limitations" for more details). Our group has previously tested the utility of CD11a to mark embryonic cells that possess multi-lineage output potential *in vitro*[86]. These studies rigorously assessed the lineage output of single cells sorted from e9.5-e11.5 embryos in an *in vitro* colony

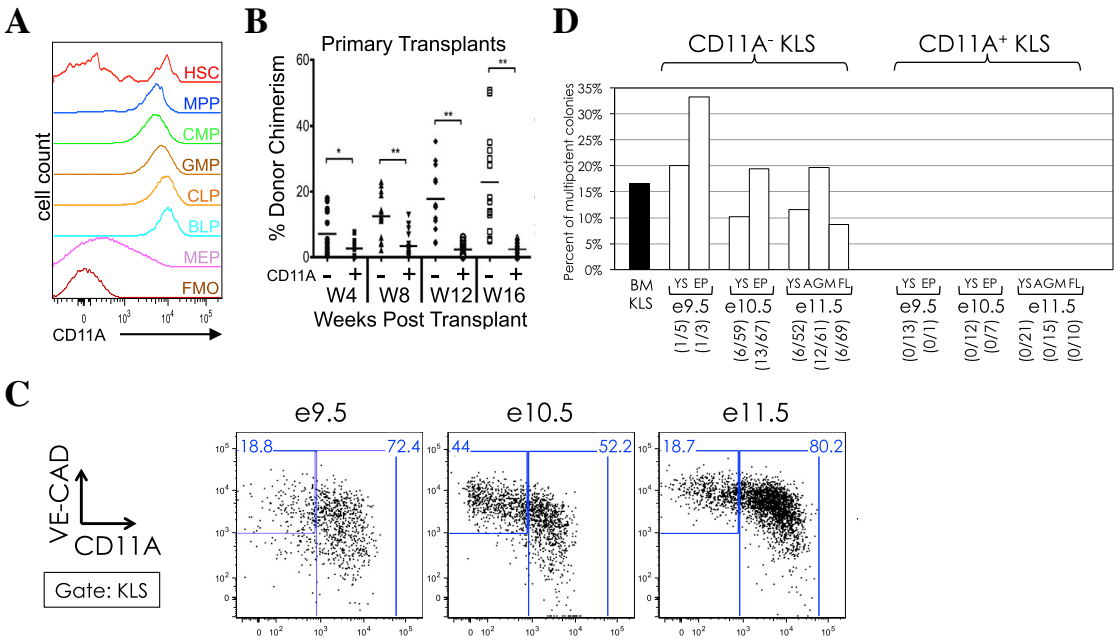

Figure 1.5. Expression and engraftment potential of CD11a on HSCs and pre-HSCs. A) Flow cytometry analysis of CD11a expression on adult hematopoietic progenitors. Adult HSCs show bimodal expression of CD11a where all other progenitors (with the exception of MEPs) show high expression of CD11a. HSCs are sorted using conventional HSC markers and defined as Lin- FcγR- IL-7Rα- Sca-1+ Kit+ CD34- CD150+. **B)** Engraftment potential of CD11a- and CD11a+ fraction of conventional HSCs in primary recipients. Total blood chimerism is shown at 4 weeks (W) intervals following transplantation. CD11a- fraction shows higher engraftment potential. **C)** Representative flow cytometry analysis showing the expression of CD11a (and VC) on cells KLS gated cells at different timepoints (e9.5-11.5) in the YS. CD11a shows bimodal expression on embryonic hematopoietic progenitors. **D)** Multipotent colony formation *in vitro* from single cells sorted from CD11a- and CD11a+ fractions of embryonic hematopoietic progenitors in different tissues and at different developmental stages. White bars represent the percentage of multi-lineage colonies (defined by the presence of B lymphocytes, T lymphocytes, myeloid, and erythroid lineages). Only CD11a- fraction shows multi-lineage output potential *in vitro*. *A-B) Adapted from Fathman et al., Stem Cell Reports, 2014*[150] *and C-D) Inlay et al., Stem Cell Reports, 2014*[86].

formation assay. Sorting single cells eliminated the possibility of falsely identifying multi-lineage output from more than one source. In these studies, single CD11a- and CD11a+ cells were sorted from an enriched embryonic progenitor population defined as Ter119- CD43+ Kit+ Sca-1+ CD144+ (Figure 1.6C)[86]. We found that only the CD11a- fraction of embryonic progenitors showed the capacity to produce all blood lineages *in vitro* (Figure 1.6D)[86], thus identifying candidate pre-HSCs to be CD11a-. However, engraftment potential and long-term self-renewal capacity of this candidate pre-HSC population was not determined. To this end, in Chapter 3 we employ a neonatal transplant system to reveal *in vivo* pre-HSC activity from e9.5-11.5 embryos. Furthermore, we provide evidence of the temporary niche environment that supports pre-HSC maturation in neonatal recipients. Using this modified transplant system, we test the utility of CD11a to sort pre-HSCs from an embryonic progenitor population and report that all pre-HSCs in both intra- and extra-embryonic tissues of e10.5 and e11.5 embryos lack CD11a expression (these findings are discussed in detail in Chapter 3). Our findings in Chapter 3 introduce a stringent sorting strategy with the use of six markers to purify a rare population enriched with pre-HSCs.

Closing Statement

Studies presented here introduce a simplified yet efficient strategy for FACS-purification of murine adult HSCs with the use of CD11a/EPCR combination. This strategy also present a solution to resolves issues that complicate multi-parameter sorting of HSCs in a variety of scenarios. Furthermore, studies presented here use CD11a in combination with other markers to introduce a rare embryonic population that contains all pre-HSCs. Together, these studies

contribute to the characterization of blood-forming stem cells at different developmental stages with the ultimate goal of contributing to the generation of patient-specific regenerative iHSCs.

CHAPTER 2: THE CD11A AND EPCR MARKER COMBINATION SIMPLIFIES AND IMPROVES THE PURIFICATION OF MOUSE HSC

Introduction

HSCs are the self-renewing, multipotent, and engraftable cells of the blood system[16]. Successful HSCT can potentially treat any disorder inherent to the hematopoietic system by ablation of the defective blood system followed by reconstitution by healthy donor HSCs[52]. However, HSCT is reserved only for high-risk patients due to the dangers of HSCT-related complications, including graft rejection, graft failure, and Graft-versus-Host Disease[52]. Transplantation of sufficient numbers of pure HSCs can bypass many of these HSCT-related complications[59,158,159]. Therefore, much effort has been invested in strategies to improve the purity of donor HSCs.

HSCs are identified by their expression of a combination of molecules on their cell surface called surface markers. In mice, the ever-growing list of surface markers whose positive or negative expression marks HSCs includes CD34, Kit, Sca-1, Lineage (a cocktail of markers of mature lineages), CD27, CD48, CD150, FLK2, CD9, EPCR and many others[38,112,113,115]. The marker combination Kit+ Lineage- Sca-1+, which defines the "KLS" population (also called "LSK" or "KSL"), contains all HSCs and multipotent progenitors in the BM. To isolate long-term HSCs within the KLS population, additional marker combinations are needed such as 1) Flk2+ CD34-, 2) CD48- CD150+, or 3) CD150+ CD34-[38,160,161]. However, the increasing number of markers needed to purify HSCs (currently around 6-8), the nuances of each of the fluorochromes and antibodies required for optimal staining and gating, and the long and expensive assays needed for gating validation have made it difficult for newcomers to properly

identify and sort HSCs. Furthermore, many of these markers can change expression during stressful conditions such as upon inflammation or after irradiation, making many of them unreliable for identifying HSCs in these contexts[120-122]. Therefore, there remains a need for simpler and more inclusive strategies for marking and identifying HSCs in healthy and challenged BM.

We previously introduced CD11a as a new marker to isolate HSCs. CD11a heterodimerizes with the β2-integrin CD18 to form LFA-1. LFA1 interacts with ICAM-1 and has roles in transendothelial migration, activation, and differentiation of lymphocytes[147,162-164]. We found that while CD11a is expressed on nearly all hematopoietic lineages, it is down-regulated on HSCs[150]. We showed that stringently-gated adult HSCs can be separated into CD11a+ and CD11a- fractions, with only the CD11a- fraction showing long-term engraftment upon transplantation. This was not due to antibody binding to the CD11a+ cells (potentially blocking LFA1-mediated migration), as the CD11a antibody itself had no effect on either BM homing or long-term engraftment of HSCs. These findings suggested that CD11a should be added to the marker panel when isolating HSCs at the highest level of purity. Here, we introduce an alternative strategy for identification and sorting of HSCs with the use of CD11a and EPCR (endothelial protein C receptor, *Procr*, CD201) as another efficient HSC marker, and compare this strategy to those using classical markers. We show that CD11a and EPCR can be used with classical HSC markers to purify HSCs, but furthermore, can be used alone as a simple two-color method to highly enrich for HSCs.

Results

CD11a and EPCR in Combination With Classical HSC Markers Reveal a Distinct Population With Enriched HSC Activity

CD11a and EPCR have each been shown independently to increase HSC purity when used with conventional HSC markers. To assess the efficiency of purifying HSCs using CD11a and EPCR together, we first examined their expression in the KLS population (Figure 2.1A). KLS is traditionally defined as Kit+ Lin- Sca-1+, but we substituted CD27 "Lin" cocktail, an expensive combination of markers (e.g. CD3, CD4, CD8, B220, Mac-1, Gr1, Ter119, NK1.1, etc.) for mature hematopoietic lineages. CD27 is expressed on HSCs and MPPs, and together with the red blood cell marker Ter119, can be used in place of Lin[122,165,166]. Because this population (CD27+ Ter119- Kit+ Sca-1+) is identical to the original KLS population (Lin- Kit+ Sca-1+), we keep the nickname "KLS" for simplicity. Within the KLS population, we identified two distinct fractions: a CD11a- EPCR+ population and a CD11a+ population (Figure 2.1A). We sorted these two populations (from CFP+ donor mice) and transplanted them into lethally-irradiated B6 adult recipients to determine which population contained long-term engraftable HSCs. We transplanted roughly 1,500 CD11a- EPCR+ KLS cells and 10,000 CD11a+ KLS cells to maintain their physiological ratios. 500,000 BM cells from Tomato+ mice were co-transplanted as "helper" BM to protect the recipients from hematopoietic failure following irradiation. Recipients were bled and analyzed for donor chimerism in different blood lineages at four-week intervals (Figure 2.1B). Donor chimerism of total blood cells (CD45+) was significantly higher from the CD11a- EPCR+ KLS population than the CD11a+ KLS population, and this difference increased over time (Figure 2.1C). Because granulocytes are short-lived, granulocyte chimerism in the peripheral blood is a more accurate indicator of HSC chimerism in

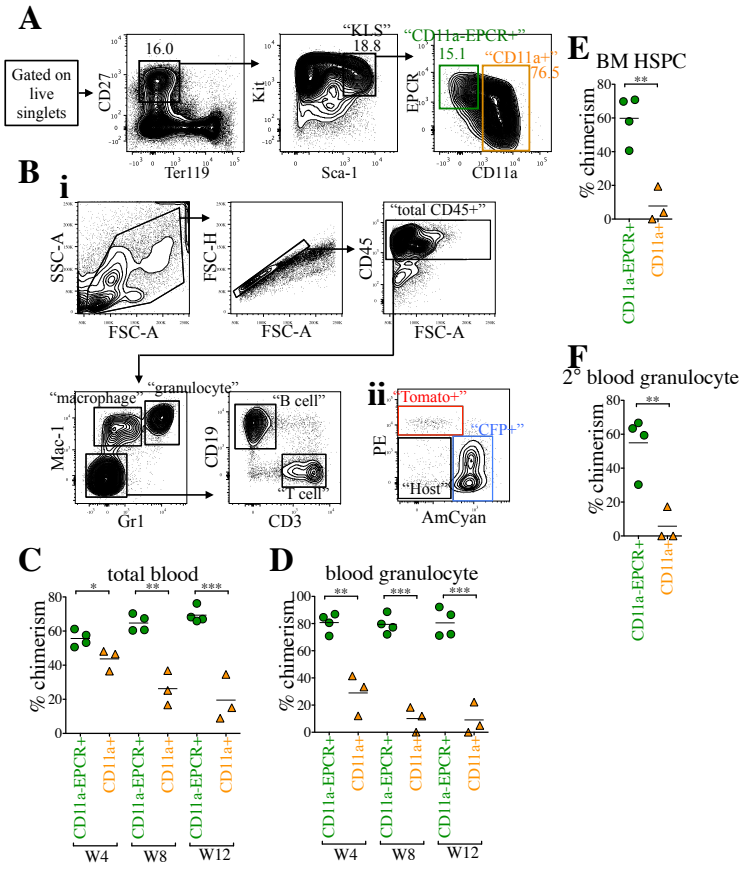

Figure 2.1. CD11a and EPCR inclusion enriches for HSCs within KLS. A) Representative sorting scheme of CD11a- EPCR+ KLS (green) and CD11a+ KLS (orange) populations from Kit-enriched CFP+ BM. Each sorted population (1,500 CD11a- EPCR+ cells or 10,000 CD11a+ cells per recipient) was transplanted into lethally-irradiated B6 recipients along with 500,000 Tomato+ WBM helper cells. **B)** Representative blood analysis of recipient mice. **i)** After gating based on size and granularity, single cells are gated on based on CD45 expression. Within CD45+ fraction, macrophages, granulocytes, T cells, and B cells can be identified as distinct populations. Macrophages are defined as CD45+ Mac-1+ Gr1-, granulocytes as CD45+ Mac-1+ Gr1+, T cells as CD45+ CD3+, and B cells as CD45+ CD19+. **ii)** Representative analysis of T cells for donor chimerism. CFP and Tomato expression can be detected in AmCyan and PE channels, respectively. "Host" cells are defined by the lack of CFP/Tomato expression. Donor chimerism within each cell type is analyzed similarly. **C-D)** Time-course analysis of donor chimerism in blood. Total (**C**) and granulocyte (**D**) blood chimerism from CD11a- EPCR+ KLS ("CD11a-EPCR+") and CD11a+ KLS ("CD11a+") sources in primary recipients at weeks (W) 4, 8, and 12 post-transplant. Total blood was defined as CD45+ and granulocytes as CD45+ Gr1+ Mac-1+. **E)** Donor chimerism of HSPCs in the BM of primary recipients 13 weeks post-transplant. HSPCs are defined as Ter119- CD27+ Sca-1+ Kit+. **F)** Blood granulocyte chimerism in secondary recipients 6 weeks post-secondary transplant. Secondary transplants were done using $1x10^6$ WBM harvested from primary recipients that received "CD11a-EPCR+" or "CD11a+" donor cells. *$*p \leq 0.05$, **$p \leq 0.01$, ***$p \leq 0.001$ (Student's unpaired t test).*

the BM compared to total CD45+ blood cells, which includes long-lived lymphocytes that may have come from lymphoid progenitors or multipotent progenitors. The difference in granulocyte chimerism between CD11a- EPCR+ KLS cells and CD11a+ KLS was even more pronounced than total blood chimerism (Figure 2.1D). Furthermore, when examining the BM of the recipients, the CD11a- EPCR+ KLS population had higher donor HSPCs (Figure 2.1E). As only HSCs are capable of serial transplantation, we next transplanted whole BM from the primary recipients into secondary hosts. Only the BM of recipients of CD11a- EPCR+ KLS cells gave rise to robust donor chimerism in the secondary hosts, indicating that nearly all HSCs are contained in this population (Figure 2.1F). Thus, CD11a and EPCR can be used to isolate HSCs within the KLS fraction of BM.

CD11a- EPCR+ KLS Directly Outcompetes CD11a+ KLS in a Competitive Transplantation Assay

To directly compare HSC activity between the CD11a- EPCR+ and CD11a+ subsets of KLS cells, we performed a competitive transplantation, in which both populations are co-transplanted into the same recipients. In this strategy, recipient mice receive both populations at their physiological ratios, providing a direct comparison of the engraftment efficiency of each. Also, because all KLS cells fall within one fraction or the other, all potential sources of HSCs in the BM are sorted and transplanted. To distinguish the two populations, we sorted one population from CFP-expressing BM, and the other population from Tomato-expressing BM and co-transplanted them along with 100,000 unlabeled B6 helper BM cells (Figure 2.2A). In the peripheral blood of the primary recipients, drastically higher percentages of donor total CD45+ cells and granulocytes were derived from the CD11a- EPCR+ KLS compared to the CD11a+

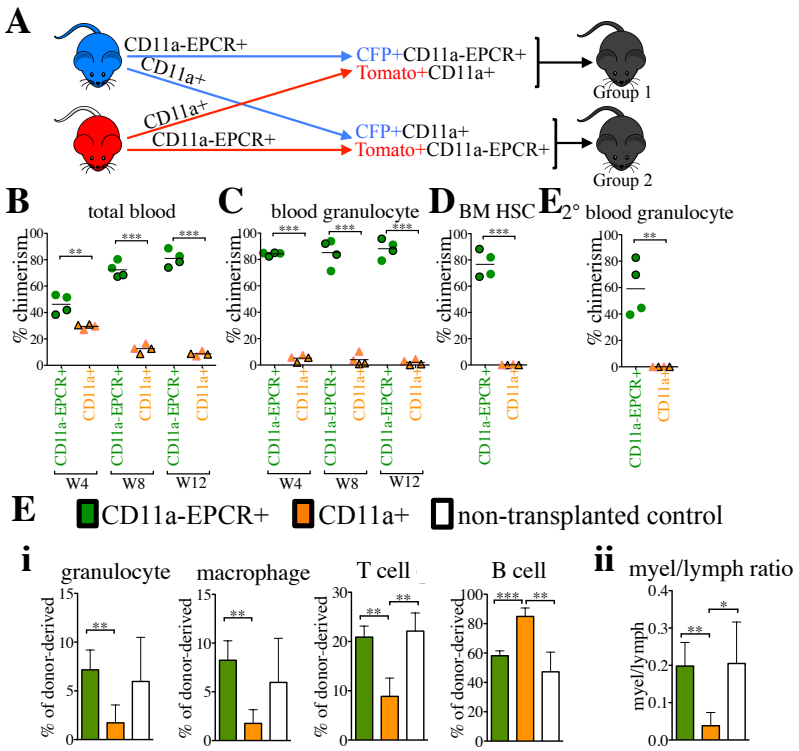

Figure 2.2. CD11a- EPCR+ KLS cells outcompete lymphoid-biased CD11a+ counterparts in competitive transplants. A) Representation of competitive transplant system. Group 1 recipients (outlined symbols in B-E) received CFP+ CD11a- EPCR+ KLS and Tomato+ CD11a+ KLS, and Group 2 (borderless symbols in B-E) received Tomato+ CD11a- EPCR+ KLS and CFP+ CD11a+ KLS. 3,000 CD11a- EPCR+ KLS and 10,000 CD11a+ KLS sorted cells (physiological ratios) along with 100,000 helper WBM (from Wt B6 mice) were co-transplanted into each lethally-irradiated B6 recipient. **B-C)** Time-course analysis of donor chimerism in blood. Total (**B**) and granulocyte (**C**) blood chimerism from CD11a- EPCR+ KLS ("CD11a-EPCR+") and CD11a+ KLS ("CD11a+") sources in primary recipients at weeks (W) 4, 8, and 12 post-transplant. **D)** Donor chimerism of HSCs in the BM of primary recipients 13 weeks post-transplant. HSCs are defined as Ter119- CD27+ Sca-1+ Kit+ CD11a- EPCR+. **E)** Blood granulocyte chimerism in secondary recipients 6 weeks post-secondary transplant. Secondary transplants were done using $1x10^6$ WBM harvested from primary recipients 13 weeks after the primary transplantation. **F)** Lineage output from CD11a- EPCR+ and CD11a+ KLS fractions. **i)** Lineage distribution of granulocytes (Mac-1+ Gr1+), Macrophages (Mac-1+ Gr1-) T cells (CD3+) and B cells (CD19+) in the peripheral blood of recipients from CD11a- EPCR+ (green) or CD11a+ (orange) KLS cells 12 weeks post-transplant, and in non-transplanted controls (n=4, error bars SD). **ii)** Ratio of myeloid to lymphoid cells. Myeloid cells are defined as CD45+, Mac-1+ or Gr1+, and lymphoid cells as CD45+, CD3+ or CD19+. CD11a- EPCR+ KLS cells show similar lineage distribution and myeloid/lymphoid ratios as the non-transplanted control, indicating they can reconstitute peripheral immune cells at physiologic ratios, indicative of HSCs. Conversely, CD11a+ KLS cells show a distinct B lineage bias and skewed myeloid/lymphoid ratios, suggesting they are more differentiated than HSCs. *$p \leq 0.05$, **$p \leq 0.01$, ***$p \leq 0.001$ (Student's unpaired t test).*

KLS source (Figure 2.2B-C). Higher donor chimerism of HSCs in the BM compartment of primary recipients as well as blood granulocyte chimerism in secondary recipients also originated only from the CD11a- EPCR+ KLS donor source, indicating that this population contained all the HSCs (Figure 2.2D-E).

We also examined the distribution of lineages derived from the two populations (Figure 2.2F). CD11a+ KLS-derived cells showed a significantly higher production of B cells than other lineages when compared to CD11a- EPCR+ KLS and non-transplanted controls. While this may suggest that CD11a+ KLS cells have a lymphoid bias, it is more likely a byproduct of the fact that lymphocytes live longer than myeloid cells. This population likely contains short-lived multipotent progenitors, which give rise to a brief outburst of myeloid and lymphoid populations. While the myeloid populations are quickly expended, the lymphocytes remain, producing the appearance of a lymphoid bias. The CD11a- EPCR+ KLS cells produced a much more balanced lineage distribution, further supporting the notion that all HSCs reside within this population.

CD11a and EPCR Alone Can Enrich HSCs Without the Need for Other HSC Markers

We next tested whether CD11a and EPCR alone were sufficient to sort HSCs in the absence of all other HSC markers. We used only these two markers for a competitive transplantation assay, and did not include any other HSC markers. We sorted CD11a- EPCR+ ("11a/EPCR") cells into one tube, and all other live cells (referred to as "Not 11a/EPCR") into another tube, then co-transplanted one population from CFP+ BM and the other population from Tomato+ BM into the same recipient mice. By sorting all cells outside of the CD11a- EPCR+ gate, we could ensure that any potential HSCs that fall outside of the CD11a- EPCR+ population would be transplanted in the "Not 11a/EPCR" fraction. Because of the rarity of the CD11a-

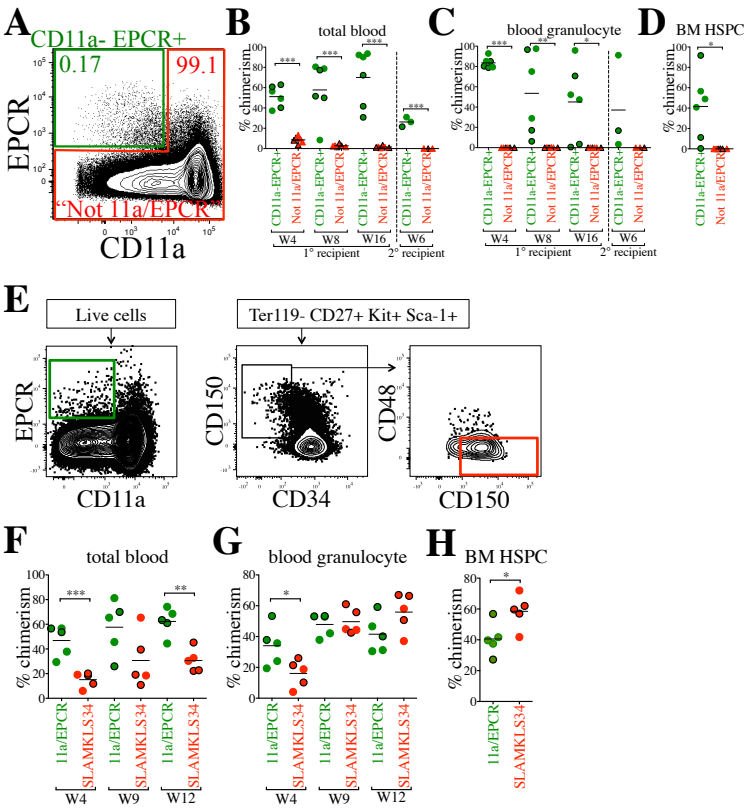

Figure 2.3. CD11a and EPCR alone are sufficient to sort a rare population enriched for HSCs. A) Sorting strategy using only CD11a and EPCR as HSC markers. CFP+ CD11a- EPCR+ and Tomato+ "Not 11a/EPCR" (not CD11a- EPCR+) cells (and vice versa) were sorted and co-transplanted in a competitive setting at physiological ratios. 850 CD11a- EPCR+ and 500,000 Not 11a/EPCR were transplanted into each recipient. Percentages of cells within each gate are shown. **B-C)** Time-course analysis of total blood **(B)** and blood granulocyte **(C)** chimerism from CD11a- EPCR+ and Not 11a/EPCR sources in primary recipients 4, 8, and 16 weeks (W) post-transplant, and in secondary recipients (separated by vertical dashed line) at W6 following secondary transplant. CFP+ donor-derived cells are represented by outlined symbols and Tomato+ donor-derived cells with borderless symbols. Not all primary recipients were selected for secondary transplantation. **D)** Donor chimerism of HSPCs in the BM of primary recipients transplanted with "CD11a- EPCR+" and "Not 11a/EPCR" sorted cells 17 weeks post-transplant. HSPCs are defined as Ter119- CD27+ Sca-1+ Kit+. CFP+ donor-derived cells are represented by outlined symbols and Tomato+ donor-derived cells with borderless symbols. **E**) Sorting strategy to compare CD11a- EPCR+ (11a/EPCR) to Ter119- CD27+ Kit+ Sca-1+ CD34- CD150+ CD48- (SLAMKLS34). 680 CFP-expressing 11a/EPCR and 60 Tomato-expressing SLAMKLS34 (and vice versa) were sorted and co-transplanted in a competitive setting. 250,000 non-labeled WBM was used as helper for each recipient. **F-H**) Time-course analysis of total blood (**F**) and blood granulocyte (**G**) chimerism from 11a/EPCR and SLAMKLS34 sources in primary recipients 4, 9, and 12 weeks (W) post-transplant and HSPC chimerism (**H**) at W13. CFP+ donor-derived cells are represented by outlined symbols and Tomato+ donor-derived cells with borderless symbols. **p ≤ 0.05, **p ≤ 0.01, ***p ≤ 0.001 (Student's unpaired t test). "Not 11a/EPCR"=not CD11a-EPCR+.*

EPCR+ fraction (~0.17% of whole BM; WBM) compared to the "Not 11a/EPCR" fraction (~99.1% of WBM), we sorted and transplanted them in such numbers as to maintain their physiological ratios. For each transplant, we sorted 500,000 total BM cells into CD11a- EPCR+ fraction and "Not 11a/EPCR" fraction. We then mixed the CD11a- EPCR+ fraction from one reporter (e.g. Tomato+) and the "Not 11a/EPCR" fraction from the other reporter (e.g. CFP) and co-transplanted them into the same recipient (Figure 2.3A). Thus, the transplanted cells are the equivalent of 500,000 WBM cells, with the CD11a- EPCR+ cells distinguishable from the rest of the BM cells by CFP or Tomato expression. In the recipient mice, we found that only the CD11a- EPCR+ donor source showed donor chimerism in primary and secondary recipients (Figure 2.3B-C). We also examined the BM and found that donor HSPCs were only derived from the CD11a- EPCR+ source (Figure 2.3D). These results indicate that all HSCs are present in the rare CD11a- EPCR+ fraction of BM, and that CD11a and EPCR together are sufficient to sort an enriched HSC population.

Because we found all HSCs were contained within the CD11a- EPCR+ (11a/EPCR) population in a two-color sorting method (Figure 2.3A-D), we next investigated the efficiency of this method in comparison to an HSC population sorted with an extremely stringent method. Cells were sorted from either 1) 11a/EPCR two-color method (CD11a- EPCR+) or 2) the "SLAMKLS34" population (defined as Ter119- CD27+ Kit+ Sca-1+ CD34- CD150+ CD48-) (Figure 2.3E). We sorted these populations at physiological ratios from a total of 500,000 WBM, and transplanted the sorted populations in a competitive setting and along with helper BM cells. Although we detected a significantly higher total blood chimerism from the 11a/EPCR source, levels of blood granulocyte chimerism were comparable after 3 months between the two methods (Figure 2.3F-G). Higher 11a/EPCR-derived total blood chimerism highlights the higher fraction

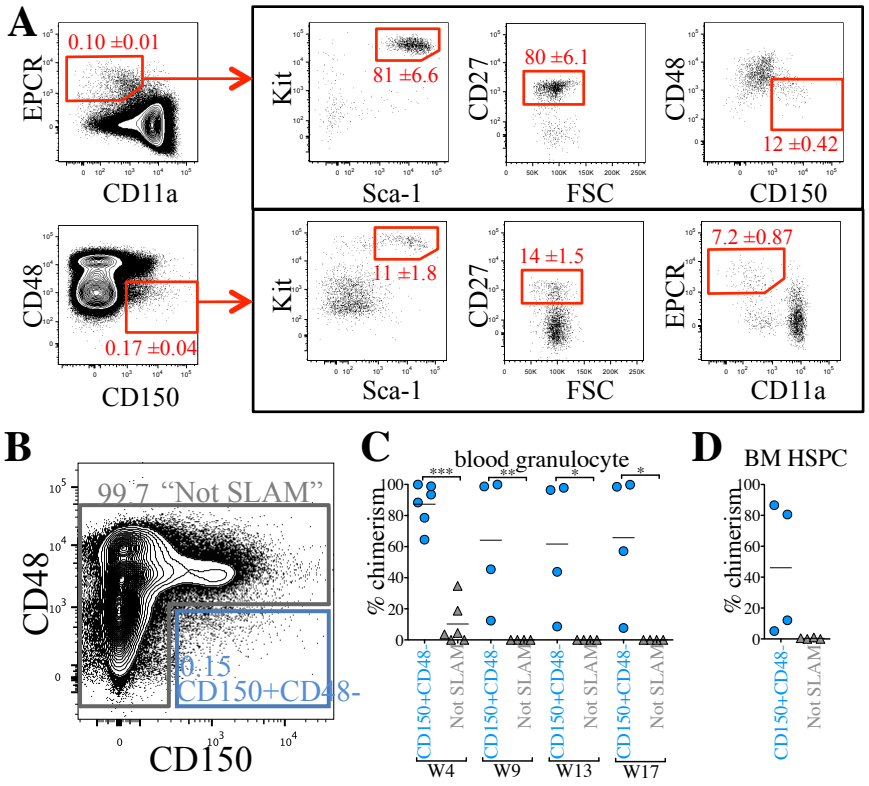

Figure 2.4. Phenotypic comparison of "11a/EPCR" versus "SLAM" 2-marker sorting methods. **A)** Analysis of HSC marker expression in CD11a- EPCR+ cells (top row) and CD150+ CD48- cells (bottom row). CD11a/EPCR and CD48/CD150 plots are gated on live, singlet, non-autofluorescent, Ter119- cells. Plots in the black boxes are gated on either CD11a- EPCR+ (top row) or CD150+ CD48- (bottom row). Percentages of cells in each gate are listed as the average of two animals ± SD. FACS plots are representative of two independent experiments. **B**) Sorting strategy using only CD150 and CD48 as HSC markers. CFP+ CD150+ CD48- and Tomato+ "Not SLAM" (not CD150+ CD48-) cells (and vice versa) were sorted and co-transplanted in a competitive setting and at the physiological ratios shown. Approximately 750 CD150+ CD48- and 500,000 "Not SLAM" were transplanted into each recipient. **C)** Time-course analysis of blood granulocyte chimerism from CD150+ CD48- and "Not SLAM" sources in primary recipients 4, 9, 13, and 17 weeks (W) post-transplant. **D)** Donor chimerism of HSPCs in the BM of primary recipients transplanted with CD150+ CD48- and "Not SLAM" sorted cells 18 weeks post-transplant. **p ≤ 0.05, **p ≤ 0.01, ***p ≤ 0.001 (Student's unpaired t test). "Not SLAM"=not CD150+CD48-.*

of non-HSC progenitors (e.g. MPP, CLP) when only these two markers are used. In the BM, we found slightly higher HSPC chimerism from the SLAMKLS34 population, though an average of ~40% of the HSPCs were derived from 11a/EPCR (Figure 2.3H). These data further demonstrate that all HSCs can be sorted using the 11a/EPCR method, although HSC purity in this population is lower than using a more stringent multi-color approach.

"11a/EPCR" Two-Color Sorting Method Produces Similar Purity of HSCs as the "SLAM" Method

While all HSCs are contained within the CD11a- EPCR+ fraction, it does not mean the population contains only HSCs. When examining BM cells gated on CD11a- EPCR+, approximately 81% are Kit+ and Sca-1+, but only 12% are CD150+ CD48- (Figure 2.4A). It was previously shown that HSCs are CD150+ CD48-, and thus there are likely non-HSCs within the CD11a- EPCR+ fraction. The SLAM markers CD150 and CD48 have also been shown to be sufficient for two-color sorting of HSCs[38]. However, when examining the SLAM fraction (CD150+ CD48-) of BM, only 11% of these cells were Kit+ Sca-1+, and only 7.2% were CD11a- EPCR+, suggesting this two-color method may also be contaminated with non-HSCs. To confirm the efficiency of the SLAM method to purify HSCs in our hands, we transplanted CD150+ CD48- (SLAM) and "Not" CD150+ CD48- (referred to as "Not SLAM") in a competitive setting, and found that only the SLAM cells were able to engraft long-term (Figure 2.4B-D).

To directly compare our "11a/EPCR" two-color sorting method with the SLAM method, CD11a- EPCR+ (11a/EPCR) and CD150+ CD48- (SLAM) cells were sorted, mixed, and co-transplanted into recipients in a competitive setting (Figure 2.5A, Group 1 recipients). Equal

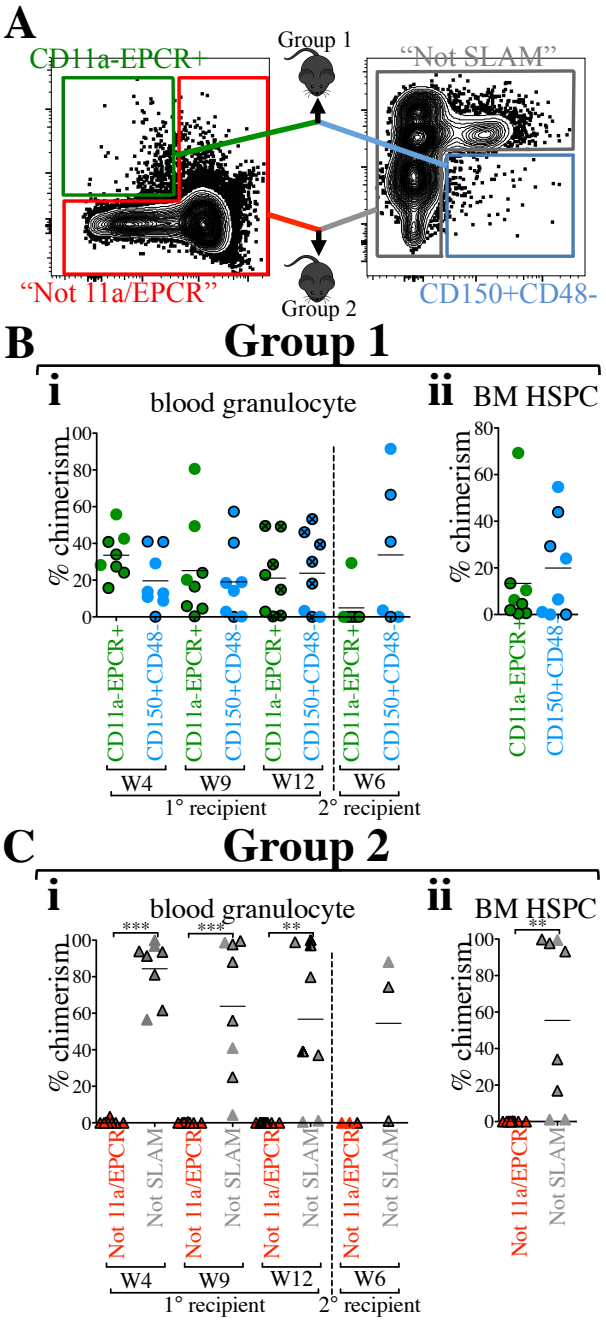

Figure 2.5. "11a/EPCR" two-color sorting is as efficient as using the "SLAM" method. A) Representation of direct comparison of two-color sorting methods. BM from CFP or Tomato mice was sorted using the combination of CD11a and EPCR only or the combination of CD150 and CD48 only. Approximately 380 cells from each of CD11a- EPCR+ and CD150+ CD48- gates were sorted, mixed, and co-transplanted with added 250,000 helper/competitor WBM (Group 1 recipients). Percentages of cells within each gate was kept consistent between the two methods. 200,000 cells from outside of the CD11a- EPCR+ gate ("Not 11a/EPCR") and outside of the CD150+ CD48- gate ("Not SLAM") were also mixed and co-transplanted (Group 2 recipients). In **B-C**, CFP+ donor-derived cells are represented by outlined symbols and Tomato+

donor-derived cells with borderless symbols. **B)** i) Time-course analysis of blood granulocyte chimerism from CD11a- EPCR+ and CD150+ CD48- sources in primary recipients 4, 9, and 12 weeks (W) post-transplant, and in secondary recipients (separated by vertical dashed line) at week 6 following secondary transplant. Primary recipients used for secondary transplants are marked with an "x" inside circles at the 12-week timepoint. ii) Donor chimerism of HSPCs in the BM of primary recipients transplanted with CD11a- EPCR+ and CD150+ CD48- sorted cells 13 weeks post-transplant. **C)** i) Time-course analysis of blood granulocyte chimerism from "Not 11a/EPCR" and "Not SLAM" sources in primary recipients 4, 9, and 12 weeks (W) post-transplant, and in secondary recipients (separated by vertical dashed line) at week 6 following secondary transplant. The primary recipients used for secondary transplant is marked (half shaded black) at the 12-week timepoint. ii) Donor chimerism of HSPCs in the BM of primary recipients transplanted with "Not 11a/EPCR" and "Not SLAM" sorted cells 13 weeks post-transplant. Number of experiments = 2. *$**p \leq 0.01$, $***p \leq 0.001$ (Student's unpaired t test). "Not 11a/EPCR"= not CD11a-EPCR+; "Not SLAM"=not CD150+CD48-.*

numbers of each population (380 cells) were transplanted, allowing us to directly compare which population contained the most HSCs. We did not detect any statistically significant difference in granulocyte chimerism between 11a/EPCR and SLAM populations in primary and secondary recipients (Figure 2.5Bi). Analysis of HSPCs in the BM also confirmed comparable engraftability between the two populations (Figure 2.5Bii). Total blood chimerism and lineage distribution were also not significantly different between the two sorting methods in primary and secondary recipients (Supplementary Figure S2.1A-B).

To determine whether any HSCs resided outside of the CD11a- EPCR+ or the CD150+ CD48- gates, we sorted each of the "Not" populations ("Not 11a/EPCR" and "Not SLAM") and co-transplanted them into recipient mice (Figure 2.5A, Group 2 recipients). We detected significantly higher "Not SLAM"-derived granulocytes and HSPCs compared to "Not 11a/EPCR" in primary recipients, as well as secondary engraftment, suggesting the presence of HSCs outside of the SLAM gate (Figure 2.5Ci-ii). We also found higher total, macrophage and lymphocyte chimerism from the Not SLAM population (Supplementary Figure S2.1C). Our data indicate that although both two-color strategies are effective at sorting HSCs, HSCs are detectable outside of the SLAM gate, but not the 11a/EPCR gate. Taken together, these experiments suggest that the SLAM two-color method is less contaminated with non-HSCs than the 11a/EPCR two-color method, but some HSCs fall outside of the SLAM gates, whereas with the 11a/EPCR method, all HSCs are sorted within the CD11a- EPCR+ gate, but also many downstream progenitors are included.

CD11a/EPCR Gating Identifies Phenotypic HSCs Following Irradiation and Poly(I:C) Treatment

Many common HSC markers change their expression when challenged, such as during an inflammatory response. Thus, the phenotypic definition of HSCs can change depending on the context. We sought to determine the expression levels of CD11a and EPCR and their ability to mark HSCs after a variety of types of challenges: irradiation, poly(I:C) treatment, and LPS treatment. First, we sub-lethally irradiated (6 Gy) B6 mice and examined their BM 48 hours post-irradiation. The percentage of CD11a+ cells appeared to increase slightly after irradiation, though EPCR expression appeared unchanged (Figure 2.6A). Other HSC markers also appeared unchanged, with the exception of CD48 which decreased after irradiation (Figure 2.6A). Consistent with previous observations, we detected a dramatic decrease in Kit expression[120,122], reducing the frequency of KLS cells (Figure 2.6B). Although CD11a expression appeared to increase overall in the irradiated BM, phenotypic HSCs were still found in the CD11a- EPCR+ fraction, suggesting these markers could still identify HSCs after irradiation (Figure 2.6C-D).

We also examined CD11a and EPCR expression after two forms of inflammation, induced by injection of either poly(I:C), a TLR3 agonist[167], or endotoxin (lipolysaccharide, LPS), a TLR4 agonist[168]. Both are known to up-regulate Sca-1 and therefore make HSC identification more difficult using standard markers[123,124,169]. After poly(I:C) injection, Sca-1 expression dramatically increased in BM cells (Supplementary Figure S2.2). However, most other HSC markers remained unchanged including CD11a and EPCR, suggesting these markers may still identify HSCs following poly(I:C) treatment. Conversely, while CD11a expression appeared unchanged in LPS-treated BM, EPCR expression changed significantly, and thus we were unable to use this marker combination to identify phenotypic HSCs in this context (Supplementary Figure S2.3). CD11a could still be combined with other HSC markers that appeared unchanged in LPS-treated mice, including CD27 and Kit. Future transplantation experiments would be

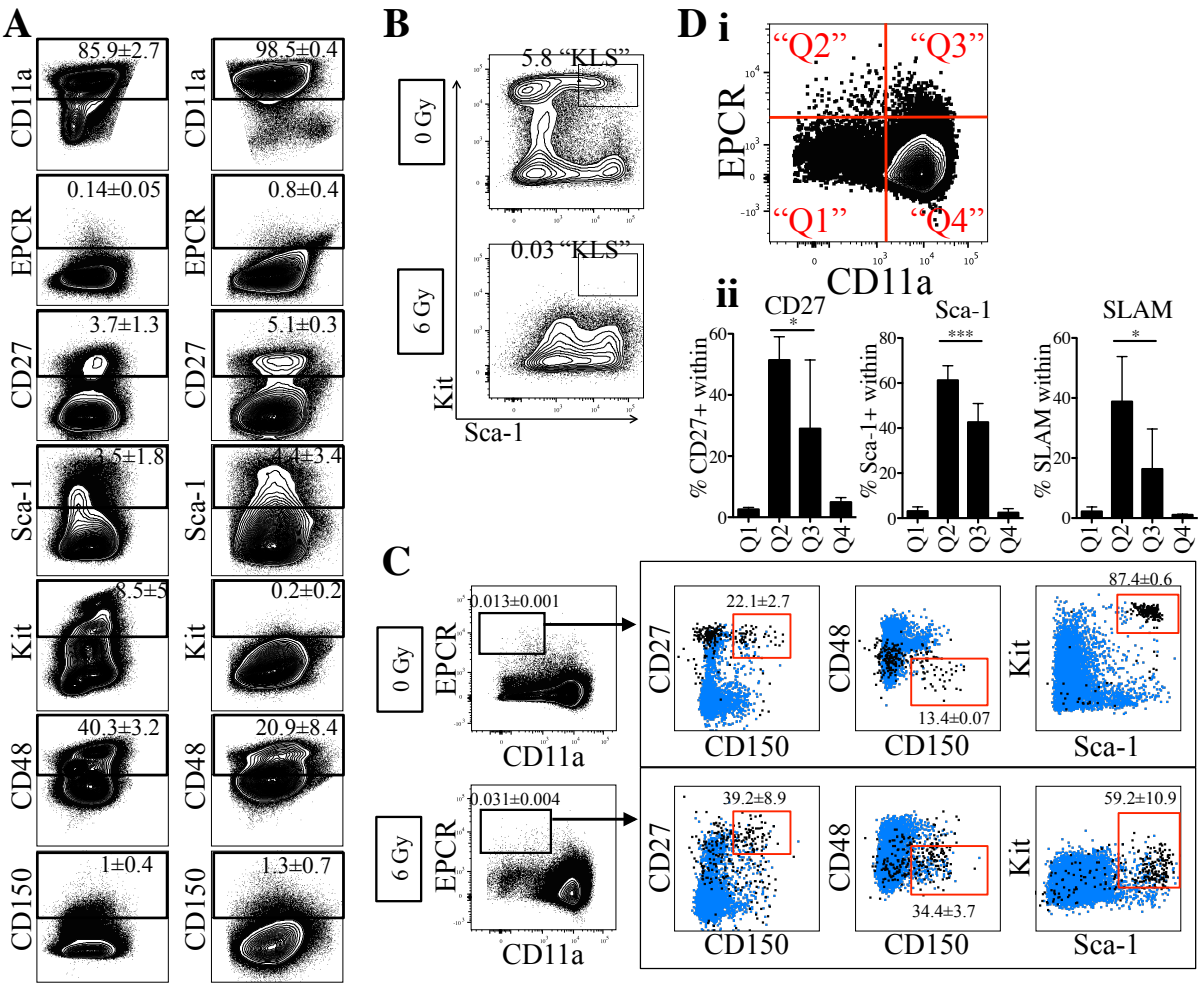

Figure 2.6. Efficacy of CD11a/EPCR combination post-irradiation injury.

A) Expression of HSC markers on BM leukocytes without irradiation (0 Gy, left FACS plots; n=3) and 48 hours post-irradiation (6 Gy, right FACS plots; n=5). FACS plots are gated on live Ter119- BM cells. Numbers are percentage of cells positive for each marker. PE/Cy5.5 (empty channel), which was not used for antibody detection, is plotted on the X-axes of FACS plots. FACS plots are representative of two independent experiments. **B)** Expression of Sca-1 and Kit on Ter119- CD27+ BM cells in non-irradiated controls (top) compared to 48 hours after 6 Gy irradiation (bottom). Percentages of KLS cells are shown. **C)** Expression of HSC markers on Ter119- CD11a- EPCR+ without (0 Gy; n=3) and with (6 Gy; n=5) irradiation-induced BM injury. Numbers shown are percentages of cells within CD11a- EPCR+ gate ± SD. Boxed plots show Ter119- CD11a- EPCR+ gated cells (black) and total Ter119- cells (blue). Gates (red) show phenotypic HSCs and what percentage of Ter119- CD11a- EPCR+ cells fall within those gates. **D) i)** Representative gating on Ter119- BM populations ("Q1"-"Q4") with differential CD11a/EPCR expression profiles. **ii)** Quantification (n=5, error bars SD) of percentages of CD27+ ("CD27"), Sca-1+ ("Sca-1"), and CD150+ CD48- ("SLAM") cells within each gate from (i). Percentages are representative of two independent experiments. *p ≤ 0.05, **p ≤ 0.01, ***p ≤ 0.001 (One-way ANOVA with Turkey's multiple comparison test).

required to confirm whether the phenotypic HSCs identified in either irradiation or inflammation are in fact functional HSCs.

Discussion

Here, we demonstrate a novel strategy for a simplified, reproducible, and efficient way for HSC sorting with the use of CD11a and EPCR. Our transplantation strategy used direct competition between the two KLS fractions as the primary method to evaluate which fraction contained the most HSCs. Methods like limit dilution assays and single cell transplantation assays can provide quantitative estimates of the number of HSCs in a population. While we did not perform those types of assay, in our system we transplanted all possible sources of HSCs at their physiologic proportions into each recipient. Thus, if more HSCs existed outside of the CD11a- EPCR+ fraction, then the "Not CD11a- EPCR+" fraction would have shown higher donor chimerism. The fact that little granulocyte chimerism was found outside of the CD11a- EPCR+ fraction indicates that this population contained all HSCs.

We found that the 11a/EPCR method was comparable to the SLAM method of two-color HSC sorting. This is despite the fact that there appeared to be very little overlap between the two populations, with only 12% of CD11a- EPCR+ cells falling within the CD150+ CD48- gate and only 7.2% of CD150+ CD48- cells falling within the CD11a- EPCR+ gate. While some HSCs were found outside of the SLAM gates (Figure 2.5C), this did not happen in every experiment (Figure 2.4) and is likely an infrequent event. Because both methods have been shown to contain nearly all HSCs, this means that likely nearly all HSCs exist within the overlapping population, which would be CD11a- EPCR+ CD150+ CD48-. This also indicates that both populations contain many non-HSCs, as expected from a two-color approach. For the CD11a- EPCR+

fraction, the contaminating cells are highly enriched for MPPs, as nearly all the cells (81%) were Kit+ Sca-1+. For the SLAM fraction, most of the contaminating cells were CD11a+ and possibly lymphoid or myeloid cells. Therefore, both strategies have their strengths and weaknesses for use as two-color method, and the user should select whether they would rather have MPPs in their sort (11a/EPCR method) or other contaminating cells which are likely not progenitors (SLAM method).

Use of CD11a and EPCR to identify HSCs after irradiation or induction of inflammation gave mixed results. The combination appeared to work after irradiation, although total levels of CD11a were up-regulated. CD11a up-regulation may be involved in HSC differentiation to progenitors, which could be necessary to replenish hematopoietic populations depleted by irradiation, and thus the true undifferentiated HSCs remain CD11a-. As part of LFA-1, CD11a up-regulation may also be involved in the migration of HSCs out of their niche and into circulation. We previously found precursors to HSCs, "pre-HSCs", to be contained within the CD11a- fraction of progenitors during early embryonic development[86]. Yet later in embryonic development and during expansion of mature HSCs in the fetal liver, a group of CD11a+ progenitors also show long-term engraftment capacity[150]. Interestingly, these CD11a+ fetal liver HSCs down-regulate CD11a after seeding the BM and remain negative for CD11a until differentiation into downstream multi-potent progenitors. These findings may suggest a role for down-regulating CD11a in HSCs during homeostasis as a means to prevent the migration of these cells out of their BM niche and into the circulation. On the other hand, EPCR has been suggested to play an active role in retention of HSCs in their niche. Whereas "pre-HSCs" are CD11a-, they express high levels of EPCR[101]. EPCR+ HSCs in the fetal liver interact with the perisinusoidal niche, and the interaction between EPCR+ HSCs and niche cells seems to persist

into the BM where EPCR shedding from HSCs has been correlated with mobilization of these cells into the circulation[170,171].

Efficient sorting of mouse HSCs allows in-depth molecular and functional characterization and contributes greatly to our understanding of the biology of these cells. CD11a and EPCR can now be added to the pantheon of available markers for stringent HSC purification, but also as an alternative method for two-color enrichment of HSCs. Lastly, while we did not address CD11a expression on human HSCs, EPCR has recently been utilized for purification of *in vitro* expanded human HSCs[172]. Whether or not CD11a can similarly be used for human HSC identification is of great translational interest, and merits further examination.

Materials and Methods

Mice

C57Bl/6 (stock no. 00664) and mT/mG (stock no. 007576 [173]) strains from Jackson Laboratory (Bar Harbor, ME, USA) were utilized as donors/recipients/helpers. CFP mice (Rosa-ECFP aka TM5) mice were generously donated by Dr. Irving Weissman. All strains were maintained at the Gross Hall and Med Sci A vivarium facilities at UCI and fed with standard chow and water. All animal procedures were approved by the International Animal Care and Use Committee (IACUC) and University Laboratory Animal Resources (ULAR) of University of California, Irvine.

Antibodies

For list of antibodies, refer to Table S2.1 ("Antibodies Table") in Supporting Information.

Cell sorting

For flow cytometry, BM was harvested from tibias and femurs by flushing with ice-cold FACS buffer (PBS + 2% fetal bovine serum) followed by red blood cell lysis by ACK lysing buffer and filtration through a 70 μ mesh. BM was harvested from donor mice by crushing leg bones in ice-cold FACS buffer followed by red blood cells lysis by ACK lysing buffer and filtration through a 70 μ mesh to remove debris. Where indicated, BM was Kit enriched using anti-Kit (anti-CD117) microbeads on an AutoMACS (Miltenyl Biotec). Cells were sorted on a BD FACS-Aria II (Becton Dickinson) into ice-cold FACS buffer for transplantation.

Transplantation, and blood and BM analysis

Defined numbers of HSCs (as indicated in each experiment) were transplanted by retro-orbital injection into lethally-irradiated isoflurane-anesthetized recipients alongside helper BM from congenically distinguishable C57BL/6 mice. Lethal doses of X-ray irradiation were 800 Rads for single dose, or 950 Rads split dose (XRAD 320, Precision X-ray). Transplanted recipients were fed an antibiotic chow of Trimethoprim Sulfa (Uniprim, Envigo) for 4 weeks post transplantation to prevent potential bacterial infections. For peripheral blood analysis, blood was obtained from the tail vein of transplanted mice at various time points, and red blood cells were depleted using ACK lysis buffer. For BM analysis, BM was harvested from tibias and femurs by flushing with ice-cold FACS buffer followed by ACK lysis and filtration. Cells were stained with lineage antibodies and analyzed on the BD FACS-Aria II. For a comprehensive list of markers used for identification of each population, refer to Table S2.2 (“Marker definitions of populations analyzed”) in Supporting Information. FlowJo software (Tree Star) was used for data analysis.

LPS-, poly(I:C)-, and irradiation-induced BM injury

For LPS and poly(I:C) treatments, 10-week-old C57BL/6 mice were injected intraperitoneally (i.p.) with 2 mg/kg of LPS (lipopolysaccharides from *Escherichia coli* 0111:B4; Sigma-Aldrich, catalog # L4391) or 5 mg/g of HMW pol(I:C) (InvivoGen; catalog # 31852-29-6) . Injected mice were sacrificed after 24 hours and bone marrow was analyzed by flow cytometry. For irradiation-induced BM stress, 10-week-old C57BL/6 mice were sublethally irradiated with 6 Gy. BM analysis was performed 48 hours post irradiation.

Statistical analysis

Statistical analysis was performed with GraphPad Prism 5 software (La Jolla, CA).

Supporting Information

Supplemental Figures

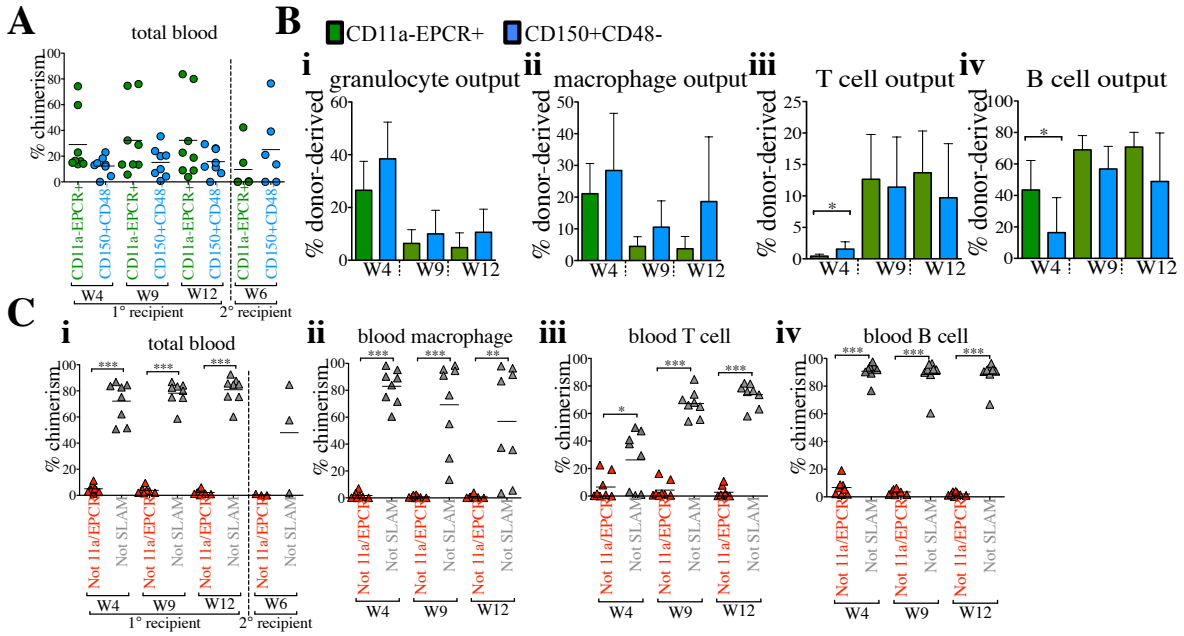

Supplementary Figure S2.1. Comparison of total blood chimerism and lineage output between two-color sorting methods. A) Time-course analysis of total blood chimerism from CD11a- EPCR+ and CD150+ CD48- sources in primary recipients 4, 9, and 12 weeks post-

transplant, and in secondary recipients (separated by dashed line) at week 6 following secondary transplant. **B)** Lineage output analysis from CD11a- EPCR+ and CD150+ CD48- sources. Granulocyte (i), macrophage (ii), T cell (iii), and B cell (iv) lineage output are shown from donor sources over time (n=8, error bars SD). **C)** Time-course analysis of total blood (i), blood macrophage (ii), T cell (iii), and B cell (iv) chimerism from "Not 11a/EPCR" and "Not SLAM" sources in primary recipients 4, 9, and 12 weeks post-transplant. *$*p \leq 0.05$, **$p \leq 0.01$, ***$p \leq 0.001$ (Student's unpaired t test). "Not 11a/EPCR"=not CD11a- EPCR+; "Not SLAM"=not CD150+ CD48-.*

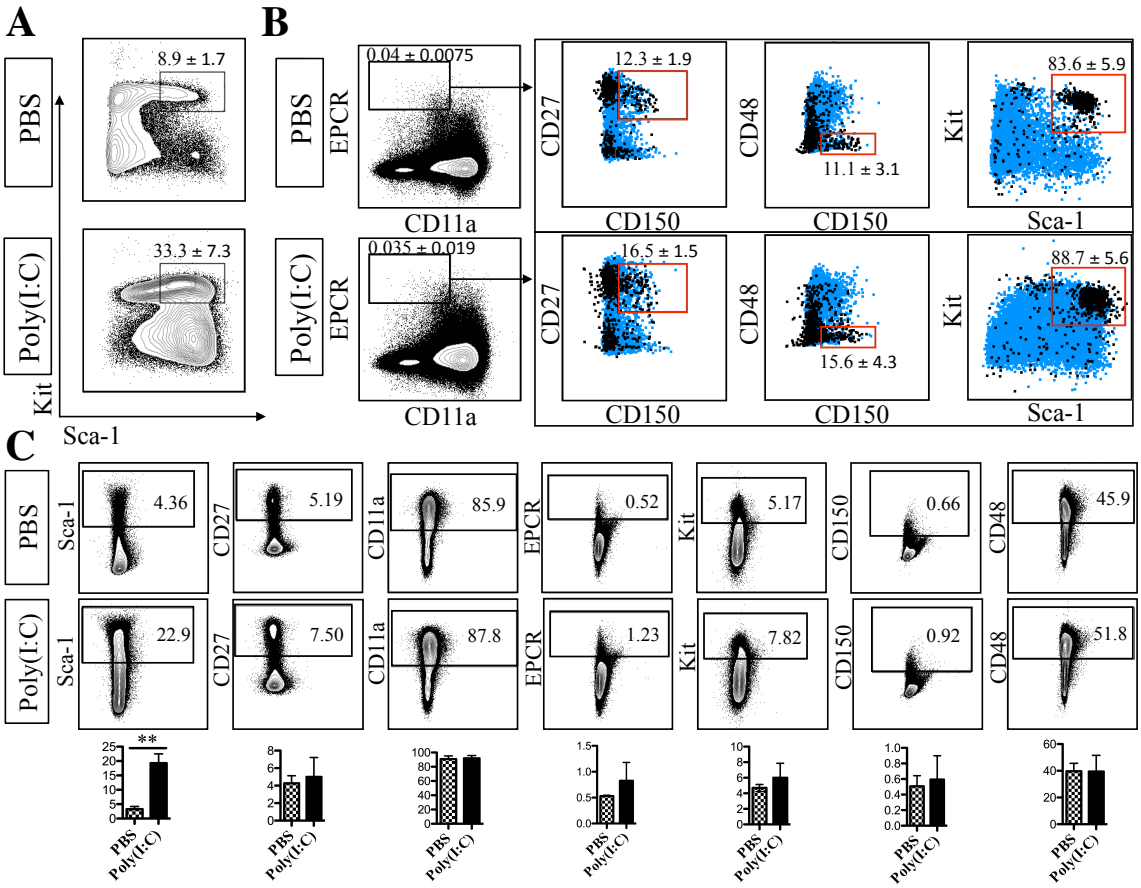

Supplementary Figure S2.2. 11a/EPCR staining identifies phenotypic HSCs during poly(I:C)-induced inflammation. A) Expression of Sca-1 and Kit on Ter119- CD27+ BM cells 24 hours after injection with PBS (top plot; n=3) or poly(I:C) (bottom plot; n=3). Numbers are percentages of KLS cells in each condition. **B)** Expression of HSC markers on Ter119- CD11a- EPCR+ in PBS (top panel) and poly(I:C) (bottom panel). Numbers are percentage of gated cells ±SD. Boxed plots show Ter119- CD11a- EPCR+ gated cells (black) and total Ter119- cells (blue). Red gates show phenotypic HSCs and the percentage of Ter119- CD11a- EPCR+ cells that fall within those gates; each condition, n=3. **C)** Expression of HSC markers on BM leukocytes of animals 24 hours after injection with PBS (top row) or poly(I:C) (bottom row), and quantification of percentages in each condition (bar graphs, error bars SD, n=3). FACS plots are gated on Ter119- BM cells. Numbers are percentages of cells positive for each marker. Empty channels AmCyan and Qdot605, which were not used for antibody detection, are the X-axes of FACS plots. Bar graphs are representative of two independent experiments. ***p* ≤ *0.01 (Student's unpaired t test).*

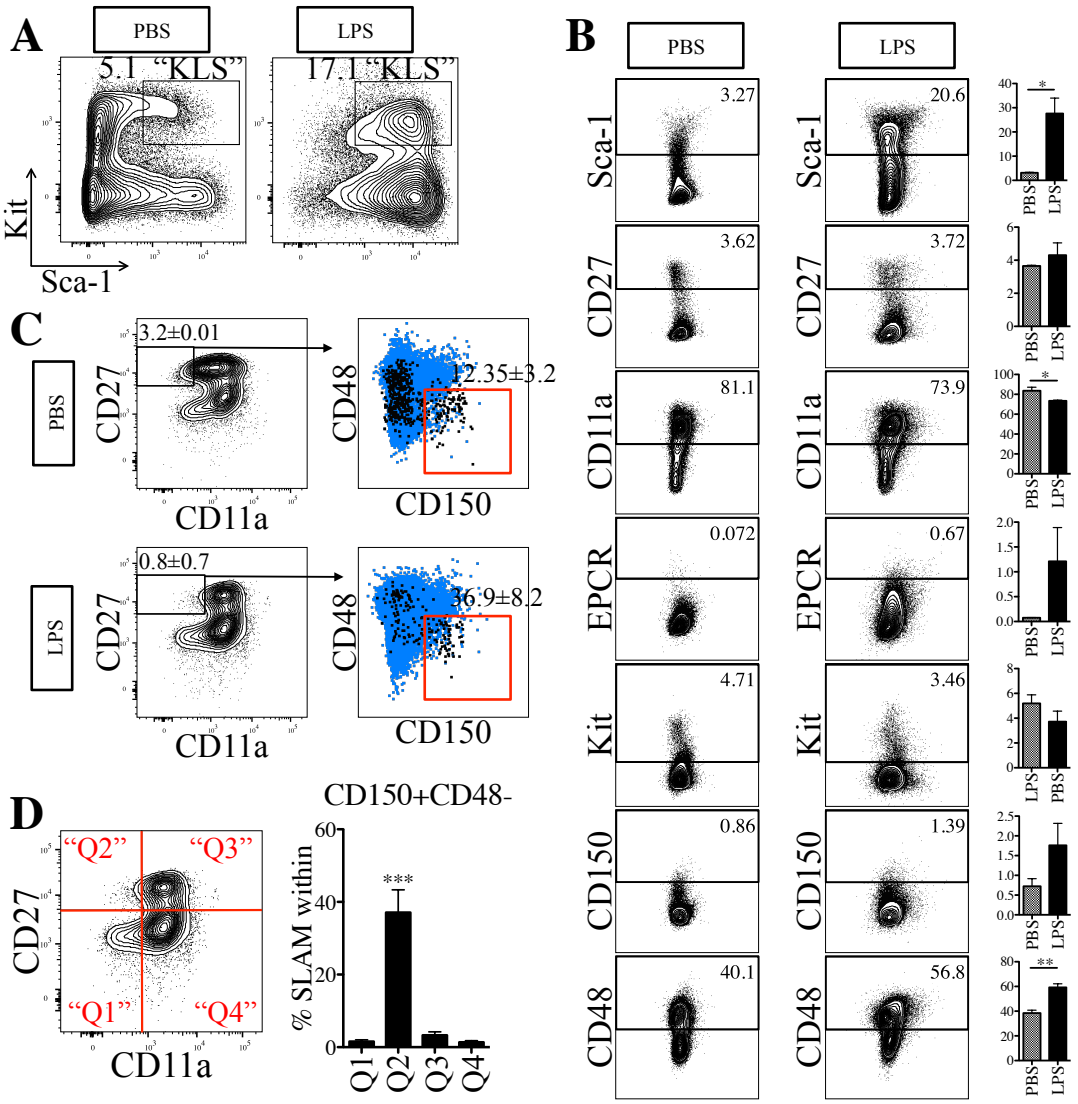

Supplementary Figure S2.3. CD11a can help identify phenotypic HSCs post LPS-induced inflammation in the BM. **A)** Expression of Sca-1 and Kit on Ter119- CD27+ BM cells 24 hours after PBS-injection (left plot) or LPS-injection (2 mg/Kg; right plot) of animals. Numbers are percentages of KLS cells in each condition. **B)** Expression of HSC markers on BM leukocytes 24 hours after injection with PBS (left FACS plots; n=2) or PBS (right FACS plots; n=3), and quantification of percentages in each condition (bar graphs, error bars SD). FACS plots are gated on Ter119- BM cells. Numbers are percentages of cells positive for each marker. Qdot605 (empty channel), which was not used for antibody detection, is plotted on the X-axes of FACS plots. Bar graphs are representative of two independent experiments. *$p \leq 0.05$, **$p \leq 0.01$ *(Student's unpaired t test)*. **C)** Expression of CD150 and CD48 ("SLAM") on Ter119- Kit+ CD27+ CD11a- BM cells from PBS-injected (top plots; n=2) and LPS-injected (bottom plots; n=3). Kit and CD27 were selected due to their unchanged expression after LPS-induced BM stress. Plots on the right show Ter119- Kit+ CD27+ CD11a- cells in black and total Ter119- cells in blue from BM of PBS- and LPS-injected animals. **D)** Representative gating on Ter119- Kit+ populations ("Q1"-"Q4") with differential CD11a/ CD27 expression profile, and quantification

(n=3, error bars SD) of percentages of CD150+ CD48- ("SLAM") cells within each gate from (i). Data are representative of two independent experiments. ***$p \leq 0.001$ *(One-way ANOVA with Turkey's multiple comparison test).*

Supplemental Tables

Table S2.1. Antibodies Table				
Antigen	**Clone**	**Conjugate**	**Source**	**Catalogue #**
TER119	TER119	PE/Cy5	Biolegend	116210
SCA1 (Ly-6A/E)	E13-161.7	FITC	Biolegend	122506
	E13-161.7	PE/Cy7	eBioscience	122514
	D7	Alexa Fluor 700	eBioscience	56-5981-82
	E13-161.7	PE	Biolegend	122507
KIT (CD117)	ACK2	APC	Biolegend	135107
	2B8	APC-eFluor 780	eBioscience	47-1171-82
	2B8	PE/Cy7	eBioscience	25-1171-81
	2B8	BV421	Biolegend	105828
CD27	LG.7F9	eFluor 780	eBioscience	47-0271-82
	LG.7F9	APC	eBioscience	17-0271-82
CD11A	M17/4	PE/Cy7	eBioscience	25-0111-30
	M17/4	Biotin	Biolegend	101103
	M17/4	APC	Biolegend	101119
	M17/4	PE	Biolegend	101107
EPCR (CD201)	eBio1560	PerCP-eFluor 710	eBioscience	46-2012-82
	eBio1560	APC	eBioscience	17-2012-82
GR1 (Ly-6G/Ly-6C)	RB6-8C5	Alexa Fluor 700	eBioscience	108422
MAC1 (CD11b)	M1/70	BV650	Biolegend	101239
	M1/70	APC	Biolegend	101212
	M1/70	FITC	Biolegend	101205
CD19	6D5	APC	Biolegend	115512
	eBio1D3	PerCP-Cy5.5	eBioscience	45-0193-82
CD45	30-F11	APC/Cy7	Biolegend	103116
CD3ε	17A2	PerCP-eFluor 710	eBioscience	46-0032-82
	17A2	PE/Cy7	Biolegend	100220
CD150 (SLAMf1)	TC15-12F12.2	PE/Cy7	Biolegend	115914
	TC15-12F12.2	BV421	Biolegend	115925
	TC15-12F12.2	BV650	Biolegend	115931
	HM48-1	FITC	eBioscience	11-04781-82
NK-1.1	PK136	APC	Biolegend	108709
MHCII	M5/114.15.2	PE/Cy7	Biolegend	107629
Secondary antibodies				
		Qdot 655-Streptavidin	Life Technologies	Q10121MP

		Qdot 605-Streptavidin	Life Technologies	Q10103MP

Table S2.2. Marker definitions of populations analyzed	
Population	*Markers used*
Total blood	CD45+
Granulocyte	CD45+ Gr1+ Mac-1+
Macrophage	CD45+ Gr1- Mac-1+
T cell	CD45+ CD3+
B cell	CD45+ CD19+
KLS/HSPC	Ter119- CD27+ Kit+ Sca-1+
HSC	Ter119- CD27+ Kit+ Sca-1+ CD11a- EPCR+ or Ter119- CD27+ Kit+ Sca-1+ CD34- CD150+ CD48-
SLAM	CD150+ CD48-

CHAPTER 3: CD11A IDENTIFIES EMBRYONIC PRE-HSCS VIA NEONATAL TRANSPLANT SYSTEM

Introduction

Hematopoietic stem cells (HSCs) in adults are the multipotent and self-renewable source of the entire blood system and hold the regenerative capacity to engraft a myeloablated recipient upon transplantation[59]. In mice, multi-parameter FACS coupled with transplantation assays have enabled the isolation of a highly purified HSC population from their niche in the BM for further molecular characterization[38,112,113,115]. Accordingly, adult HSCs are perhaps the best characterized of stem cells. However, the development origins of HSCs in the embryo remain unclear as the extensive list of adult HSC markers cannot be reliably used for identification of embryonic blood-forming cells[174]. Also, functionally distinct blood-forming progenitors emerge from various spatiotemporal origins in the embryo[175]. Therefore, the identity of the immature precursors to HSCs is not clearly determined. The ability to purify and characterize progenitor populations in early embryonic development can lead to a better understanding of how HSCs first arise during development. This information can, in turn, inform efforts aimed to generate patient-specific HSCs from undifferentiated "embryonic-like" sources such as induced pluripotent stem cells[176].

During early embryonic development and prior to the appearance of fully-functional HSCs, distinct waves of blood-forming cells overlap, with each wave functionally more mature than the last. In mice, the initial wave of hematopoiesis gives rise primarily to primitive nucleated erythrocytes and arises in the yolk sac (YS) blood islands starting from embryonic day (e) 7.5[80]. After establishment of a heartbeat, definitive hematopoiesis begins at e8.5 in the YS

and placenta (PL) with a transient wave of erythro-myeloid progenitors. These cells give rise to definitive enucleated erythroid cells and to myeloid cells that persist into adulthood as tissue-resident macrophages[82-84]. The first self-renewable and multipotent progenitors that immediately precede HSCs in the embryo are "pre-HSCs" (precursor to HSC). The functional distinction between pre-HSCs and fully mature HSCs is the inability of pre-HSCs to engraft the BM of an adult recipient upon transplantation[86-88]. As the BM cavity doesn't develop until later stage of development, it is likely that pre-HSCs do not express the necessary homing molecules required for BM engraftment potential. Pre-HSCs appear starting around e9.5 in the YS, aorta-gonad-mesonephros (AGM), and PL, with higher frequencies in e10.5 and e11.5 embryos[86,88,98-101]. Starting at e12.5, the pre-HSC wave transitions into an expanding BM-engraftable HSC pool in the fetal liver (FL)[102,104]. The FL remains the major site of hematopoiesis until perinatal seeding of the BM[93,105]. BM-engraftable FL HSCs at later embryonic stages are well-characterized. Yet, molecular characterization of events in pre-HSCs allowing them to mature into adult BM-engraftable cells remains scarce. This is in part due to the rarity of pre-HSCs[87,100,101] as well as a lack of robust experimental assays to characterize these cells.

A commonly used method to assess engraftment potential of e9.5-11.5 embryonic progenitors involves *ex vivo* co-culturing of these cells with OP9 BM stromal cells[131] or with reaggregated AGM tissue[99] prior to transplantation into adult recipients. Engraftability in adult recipients is seen only after several days of co-culturing with the addition of exogenous growth factors such as SCF, IL-4, and Flt3l. Such *ex vivo* maturation approaches have identified critical markers of multipotent populations with the potential to give rise to mature BM engraftable HSCs. These markers include hematopoietic markers CD41[88], CD43[86,88], and CD45[87,99], progenitor markers Kit[86,87] and Sca-1[86], and endothelial markers CD31[86], VE-Cadherin[86,99] (VC;

CD144), and EPCR[101] (CD201). Therefore, *ex vivo* maturation assays have provided invaluable information about pre-HSCs whilst using an artificial culture system that might drive HSC formation from progenitors more primitive than pre-HSC. An alternative approach to reveal pre-HSC activity can be achieved by direct intravenous injection of embryonic cells into irradiated *neonatal* recipients[96-98]. Although the reason for receptivity of neonatal recipients to engraftment with pre-HSCs is not determined, it has been postulated that the neonatal liver likely provides a temporary niche for maturation of pre-HSCs into BM-seeding HSCs. Although the use of the neonatal transplant system bypasses *ex vivo*-mediated maturation of embryonic cells, it has never been coupled to multi-parameter FACS for detailed investigation of pre-HSC markers[87,98,100].

Previously, we have established lack of CD11a expression as a marker of adult HSCs[150]. CD11a (integrin alpha L) forms LFA-1 (leukocyte functional-associated antigen 1; $\alpha_L\beta_2$) upon dimerization with CD18. LFA-1 interacts with ICAMs and has roles in lymphocyte activation and differentiation as well as immune cell transendothelial migration[147,162,163]. Accordingly, CD11a is highly expressed on almost all differentiated blood cells, with the exception of erythroid/megakaryocyte lineages[150]. Our previous work showed that only the CD11a- fraction of a highly enriched adult HSC population shows long-term multipotency upon transplantation[150]. In a related study, we examined the potential of CD11a as a marker of embryonic multipotent progenitors in e9.5-11.5 embryos. We hypothesized that pre-HSCs would be multipotent, and developed a single-cell multipotency assay using a modified OP9 stromal line which can inducibly express Dll1 upon treatment with doxycycline. A panel of cytokines combined with delayed Dll1 expression could generate all major hematopoietic lineages (erythrocytes, platelets, granulocytes, monocytes, NK cells, B cells, and T cells) from individual cells. To gauge clonal multi-lineage potential in different embryonic populations, CD11a- and CD11a+ single cells

were sorted from an enriched embryonic progenitor population (Ter119- CD43+ Kit+ Sca-1+ CD144+). We found that only the CD11a- fraction produced myeloid, lymphoid, and erythroid lineages, suggesting the enrichment of multipotent cells in this fraction[86]. Thus, our *in vitro* assay identified a candidate pre-HSC population based on its clonal multipotency.

In the present study, we report the successful use of CD11a coupled with an *in vivo* neonatal NSG transplant system for improved identification and characterization of pre-HSCs from e10.5 and e11.5 tissues. Our results establish that all pre-HSCs from all e10.5 and e11.5 tissues are contained within the CD11a- fraction of a rare embryonic population whereas CD11a is expressed on more differentiated embryonic progenitors. We report that the e10.5 neonatal-engraftable pre-HSCs tend to be in the G1 phase of the cell whereas CD11a+ progenitors tend to skew towards active proliferation. Furthermore, at later timepoints there is an increase in quiescent CD11a- embryonic HSCs, which coincides with a highly proliferative CD11a+ population that shows a transient long-term engraftment potential. Moreover, our short-term homing studies suggest pre-HSCs first home to the neonatal liver to mature prior to BM seeding.

Results

Establishing the NSG Neonatal Transplant System for *In Vivo* Detection of Pre-HSCs.

Studies on engraftment potential of murine pre-HSCs have been driven by *ex vivo* maturation assays and in the presence of exogenous factors to promote the development of primitive cell types into adult-engraftable cells[131]. As a more biologically relevant system for

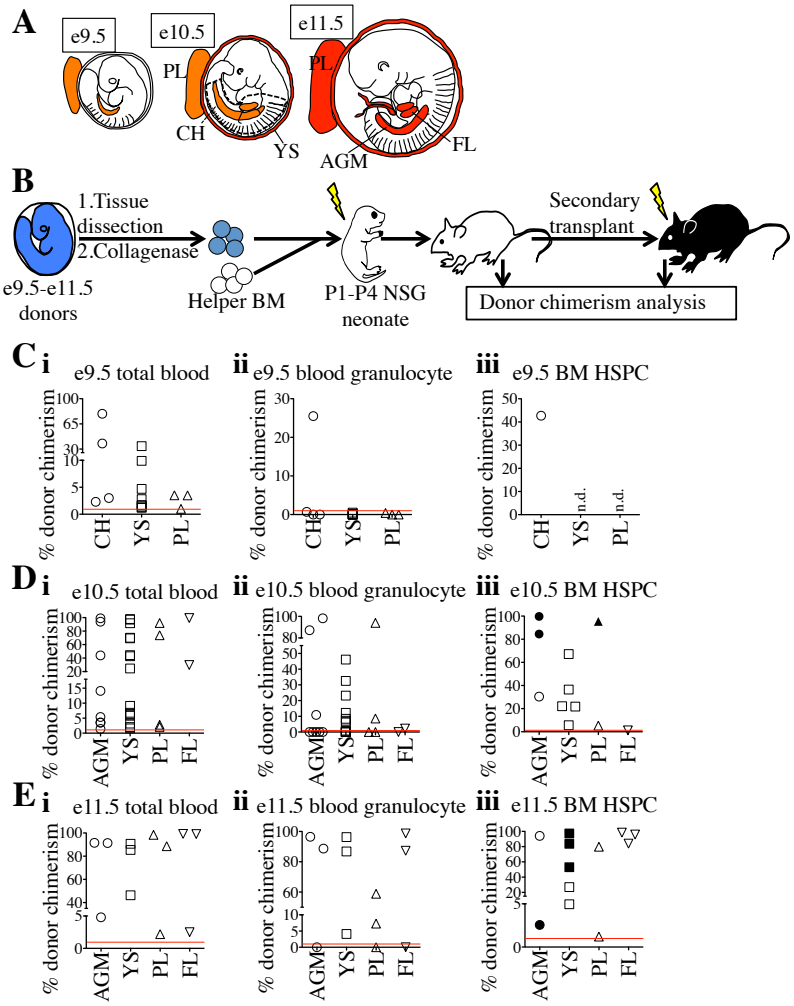

Figure 3.1. Utilization of the NSG neonatal transplant system to reveal pre-HSCs in e9.5-11.5 embryos. A) Schematic representation of hematopoietic tissues in e9.5, e10.5, and e11.5 embryos. Intra-embryonic aorta-gonad-mesonephros (AGM; depicted as orange/red stripe) and fetal liver (FL; red/orange oval in e10.5 and e11.5 embryos), and extra-embryonic yolk sac (YS; surrounding the embryo proper) and placenta (PL; depicted in orange/red) are the sites of hematopoiesis. The caudal half (CH), which contains the AGM, as well as the YS and PL are harvested from e9.5 embryos. At e10.5 and e11.5, the fetal liver (FL) is harvested separately from the AGM, YS, and PL. **B)** Schematic representation of the neonatal transplant system. Harvested tissues from e9.5-11.5 donor embryos are dissected and, after collagenase dissociation, combined with adult helper BM. Donor cells are administered intravenously (i.v.) into irradiated neonatal recipients of 1-4 days of age (P1-P4). NSG recipients are bled for donor chimerism analysis at 4 week intervals, and are then sacrificed for tissue analysis and secondary transplants. **C-E)** Percentage of total blood **(i)**, blood granulocyte **(ii)**, and BM HSPC **(iii)** chimerism from e9.5 **(C)**, e10.5 **(D)**, and e11.5 **(E)** embryo tissues in NSG neonatal recipients. Total blood and blood granulocyte graphs depict embryo-derived chimerism at the time of the last bleed. Red line marks 1% donor chimerism which was used as a threshold to define successful chimerism.

Table 3.1. Summary of unsorted embryonic transplants into NSG neonates							
dpc	**ee/recipient**	**helper BM**	**donor tissue**	**granucloyte chimerism**	**total blood chimerism**	**successful injection #**	**engraftment efficiency**
e9.5	**4-8**	**0-500K**	**CH**	**1**	**4**	**14**	**0.07**
			YS	**0**	**8**	**13**	**NA**
			PL	**0**	**3**	**9**	**NA**
e10.5	**3**	**75-200K**	**AGM**	**3**	**8**	**14**	**0.21**
			YS	**7**	**14**	**18**	**0.39**
			PL	**2**	**4**	**10**	**0.20**
			FL	**1**	**2**	**10**	**0.10**
e11.5	**1**	**100-200K**	**AGM**	**2**	**3**	**3**	**0.67**
			YS	**3**	**3**	**4**	**0.75**
			PL	**2**	**3**	**3**	**0.67**
			FL	**2**	**3**	**3**	**0.67**

Table 3.1. Compilation of whole-tissue, unsorted embryonic transplants of e9.5-11.5 embryos into NSG neonates. Number of successful tissue-specific long-term engraftment ("granulocyte chimerism") is determined by the presence of ≥1% embryo donor granulocyte chimerism at the last bleed. "Total blood chimerism" refers to the number of recipients with ≥1% embryo chimerism in total CD45+ compartment of blood. "Successful injection" is defined as engraftment of either embryo or helper adult BM donors. "Engraftment efficiency" is determined by # of successful embryo engraftment / total successful injections. dpc=days post conception; ee=embryo equivalent.

detection of pre-HSC activity *in vivo*, we employed the neonatal transplant system. Seminal studies have used neonates as recipients of early embryonic stages with success, however multi-marker sorting of putative pre-HSCs prior to transplantation has not been previously employed in this context. Due to the growing evidence for the receptivity of the NSG strain (NOD/SCID/IL2rγ$^{-/-}$) as engraftment recipients, we used this strain in our studies[177-179]. We first tested this system on non-sorted embryonic tissues from e9.5 to e11.5, the stages when pre-HSCs are thought to emerge, expand, and mature. We harvested the YS, PL, and caudal half (CH), which contains the AGM, from e9.5 embryos, and the YS, PL, AGM, and FL from e10.5 and e11.5 embryos (Figure 3.1A). We transplanted non-sorted, whole-tissues of e9.5-11.5 donors along with adult helper BM into irradiated NSG neonates followed by tissue analysis and secondary transplants (Figure 3.1B). While chimerism from e9.5 donors was detected at extremely low rates, we consistently detected engraftment from all tissues of e10.5 and e11.5 donors, with the highest engraftment efficiencies at e11.5 (Figure 3.1C; Table 3.1). As expected, granulocyte chimerism detected in the blood of neonatal recipients translated into HSPC chimerism in the BM (Figure 3.1C). To rule out the possibility that the neonatal engraftment is originating from fully-functional embryonic HSCs that heavily populate the FL at later developmental stages (e12.5 onwards), we transplanted e10.5 and e11.5 donor cells into adult recipients and confirmed the lack of embryonic-derived engraftment (Supplementary Figure S1). Therefore through a comprehensive analysis of various embryonic timepoints and tissues, we determined the NSG neonatal system fit to reveal *in vivo* pre-HSC activity from e10.5 and e11.5 donors.

Establishment of an Embryonic Competitive Transplant System.

In order to directly compare sorted embryonic populations, we developed an

experimental setup where Rosa26$^{Tomato/CFP}$ (Tomato+ CFP+) males are crossed to B6 (Rosa26$^{wt/wt}$) females so the progeny is either Tomato+ (Rosa26$^{Tomato/wt}$) or CFP+ (Rosa26$^{CFP/wt}$). Because both reporters are alleles at the same locus, only one reporter allele can be passed from the father to his offspring. This generates litters where roughly half are Tomato+ and the other half are CFP+, allowing for comparison of two colored populations within the same litter. Therefore, age-matched littermates can be distinguished by color, sorted based on marker expression, and transplanted in a head-to-head competitive setting (Figure 3.2A). Using this setup, we were also able to differentiate helper BM-derived chimerism since the helpers express the CD45.2 (Ly5.1) allelic variant whereas NSG recipients express CD45.1 (Ly5.2). Thus, this approach also serves as a control for possible differences in degrees of injection success.

All Pre-HSCs are Within the CD11a- Fraction of Progenitors in e10.5 and e11.5 Embryos.

We have previously used an *in vitro* multipotency assay to show that pre-HSCs are contained within the CD11a- fraction of e9.5-11.5 progenitors. To assess the engraftment potential of different embryonic populations in the neonatal transplant system, we sorted cells based on the expression of CD11a from within an enriched progenitor population in e10.5 and e11.5 embryos. Due to the low success rate of e9.5 whole-tissue transplants (Figure 3.1C-E; Table 3.1), we decided to eliminate this timepoint from our analyses. Moreover, as the FL showed low engraftment potential at e10.5 (1 successful embryonic engraftment in 10 successful transplants), the CH that contains both the AGM and the FL was harvested from e10.5 donors (Figure 3.1A). Ter119- CD43+ Kit+ Sca-1+ cells are defined here as "eKLS" (embryonic equivalent to adult KLS population). CD11a- VC+ eKLS (termed "11a- eKLS" hereafter) and

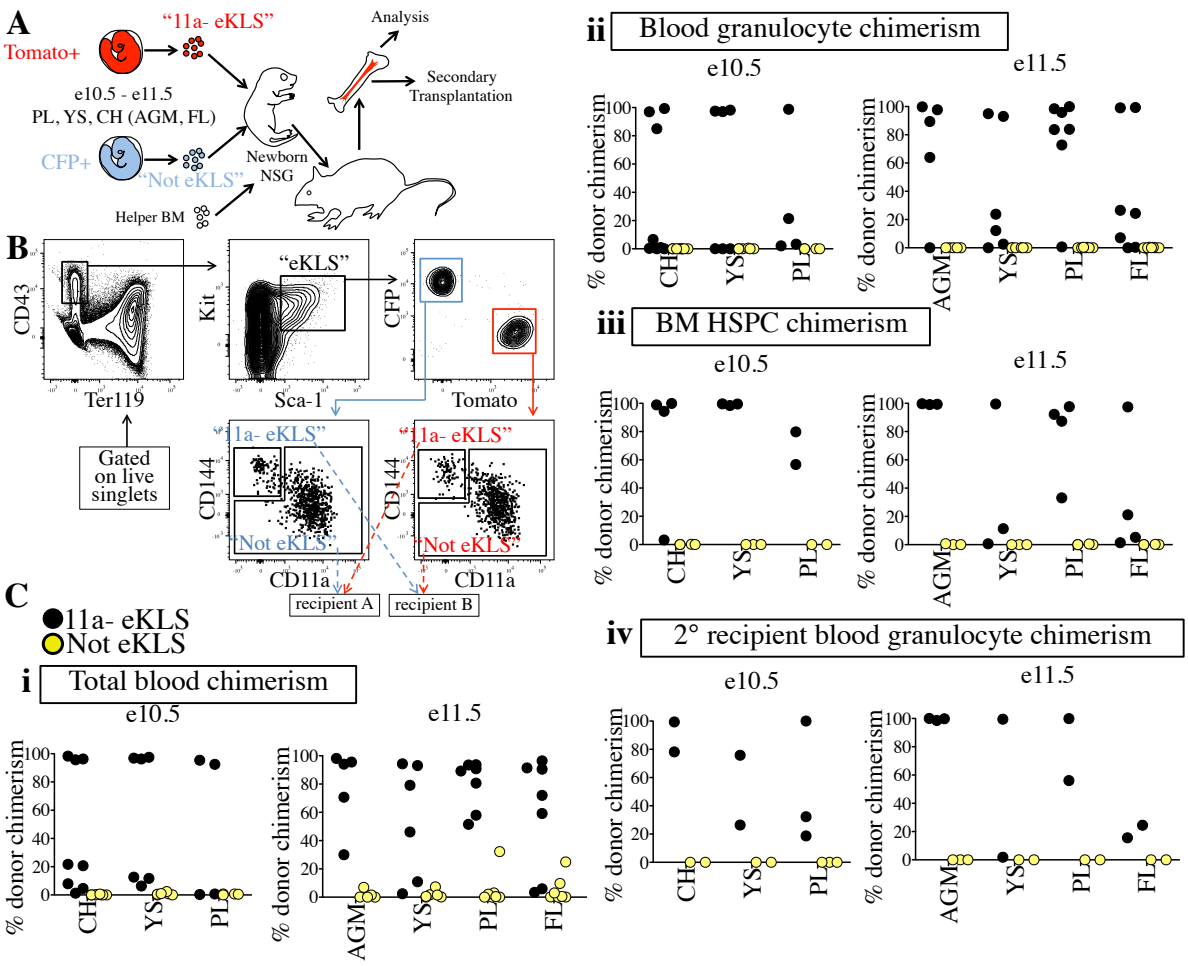

Figure 3.2. All functional pre-HSCs are contained within the CD11a- fraction of e10.5 and e11.5 embryonic progenitors. A) Schematic representation of the competitive transplant system. Sorted Tomato-expressing 11a-eKLS and CFP-expressing Not eKLS cells (and vice versa) are combined and mixed with non-fluorescent CD45.2+ adult helper BM for transplantation into newborn NSG recipients. Blood and BM analyses, and secondary transplants follow. **B)** Representative sorting strategy for the competitive transplantation of 11a-eKLS and Not eKLS populations. Live Ter119- CD43+ Kit+ Sca-1+ cells are gated on based on fluorescence. Within each color of the progenitor population, CD11a- CD144+ ("11a- eKLS") and everything else ("Not eKLS") are sorted. Opposing populations of different color are mixed post-sort and transplanted into the same recipient. **C)** Donor chimerism from 11a- eKLS and Not eKLS populations in primary and secondary recipients. Percent donor chimerism of total blood **(i)**, blood granulocyte **(ii)**, BM HSPC **(iv)** in primary recipients and blood granulocyte chimerism in secondary recipients **(iv)** from 11a- eKLS (black circles) and Not eKLS (yellow circles).

Table 3.2. Compilation of sorted e10.5 and e11.5 embryonic transplants					
dpc	**tissue**	**donor population**	**granulocyte chimerism**	**total blood chimerism**	**successful injection #**
e10.5	**CH**	**11a-eKLS**	**4**	**8**	**12**
		eNOT	**0**	**0**	
	YS	**11a-eKLS**	**3**	**6**	**12**
		eNOT	**0**	**1**	
	PL	**11a-eKLS**	**3**	**4**	**7**
		eNOT	**0**	**0**	
e11.5	**AGM**	**11a-eKLS**	**4**	**4**	**6**
		eNOT	**0**	**2**	
	YS	**11a-eKLS**	**5**	**6**	**7**
		eNOT	**0**	**3**	
	PL	**11a-eKLS**	**6**	**7**	**8**
		eNOT	**0**	**3**	
	FL	**11a-eKLS**	**5**	**7**	**8**
		eNOT	**0**	**3**	

Table 3.2. Compilation of sorted competitive embryonic transplants from e10.5 and e11.5 embryos. "Donor population" refers to the sorted population in each case. "Granulocyte chimerism" refers to number of recipients with ≥1% blood granulocyte chimerism at time of the last bleed. "Total blood chimerism" refers to the number of recipients with ≥1% embryo-derived chimerism in total CD45+ compartment of blood. "Successful injection" is defined as ≥1% chimerism from either embryo or helper adult BM donors. For a comprehensive analysis of blood chimerism over time, refer to Supplemental Figure S3.2. *dpc=days post conception*.

everything other than CD11a- VC+ cells within the eKLS population (termed "Not eKLS") were sorted from different colors, mixed together and transplanted into neonatal NSGs with the addition of differentially-labeled adult BM (Figure 3.2B). Therefore, CFP-expressing 11a- eKLS and Tomato-expressing Not eKLS (and vice versa) were transplanted in competition so that all cells within the eKLS population are accounted for (Figure 3.2A-B). Blood analysis of recipients showed higher total CD45+ leukocyte chimerism (total blood chimerism) from the 11a- eKLS population compared to the Not eKLS source at both e10.5 and e11.5 timepoints and from all embryonic tissues analyzed (Figure 3.2Ci; Table 3.2; Supplemental Figure S3.2Ai and S3.2Bi). To more accurately assess HSC chimerism, we focused on short-lived granulocyte chimerism. In all transplanted recipients of e10.5 and e11.5 tissues, granulocyte chimerism was derived only from the 11a- eKLS source with undetectable Not eKLS-derived granulocytes (Figure 3.2Cii; Table 3.2; Supplemental Figure S3.2Aii and S3.2Bii). BM analysis of recipients confirmed the presence of embryo-derived HSPCs only from the 11a- eKLS population with no contribution from the Not eKLS source (Figure 3.2Ciii). We then performed secondary transplants and confirmed long-term engraftability of 11a- eKLS-derived HSCs (Figure 3.2Civ). Also, we determined that the 11a- eKLS sorted cells showed no drastic lineage bias over time, and that 11a- eKLS-derived progeny successfully repopulated all the hematopoietic compartments we checked (Supplemental Figure S3.3). Therefore, these results establish that e10.5 and e11.5 pre-HSCs are CD11a-, and that all pre-HSCs are contained within the 11a- eKLS population.

We next aimed to better characterize CD11a- and CD11a+ embryonic progenitors by the addition of other pre-HSC markers not included in our sorts. We surveyed the expression of EPCR and CD45 on e10.5 and e11.5 CD11a- and CD11a+ progenitors, and found a higher percentage of EPCR+ cells within the 11a- eKLS in all tissues of e11.5 embryos. We also

detected a lower fraction of CD45+ cells within the CD11a- fraction (Supplemental Figure S3.4).

CD11a- Embryonic Progenitors are Slower Dividing Compared to Their CD11a+ Counterparts.

Next, we examined the absolute numbers of CD11a- and CD11a+ progenitors over time and in different tissues. Unlike AGM, YS, and PL, we found increased numbers of both CD11a- and CD11a+ progenitors in the FL over time with a relatively more pronounced expansion of CD11a+ progenitors (Figure 3.3Ai-ii). These data support the previously described migration of hematopoietic progenitors from the AGM, YS, and PL to the FL over time and confirm the FL as the primary site of hematopoiesis in mid-gestation[102]. Analysis of the frequency of each fraction of progenitors showed that the frequency of CD11a- fraction diminished over time while a higher fraction of progenitors expressed CD11a at later timepoints (Figure 3.3B), suggesting the higher expansion rate of CD11a+ progenitors.

To directly examine the proliferation status of the populations over time, we performed cell cycle analyses on early (e10.5) and late (e14.5) embryonic progenitor populations (Supplemental Figure S3.5B). In e10.5 tissues, a significantly higher proportion of the CD11a- progenitors were found in the G1 phase compared to the CD11a+ progenitors (Figure 3.3Ci). Conversely in the YS and CH, a lower fraction of CD11a- progenitors were actively proliferating (S/G2/M phase) compared to CD11a+ progenitor (Figure 3.3Ci). The slightly slower proliferation of CD11a- progenitors detected at e10.5 was more pronounced when we examined CD11a- and CD11a+ fractions in the e14.5 FL. CD11a- progenitors at e14.5 contained a higher fraction of G0 cells and a lower fraction of S/G2/M cells compared to their CD11a+ counterparts (Figure 3.3Cii). These observations suggest that slower dividing progenitors in early- to mid-

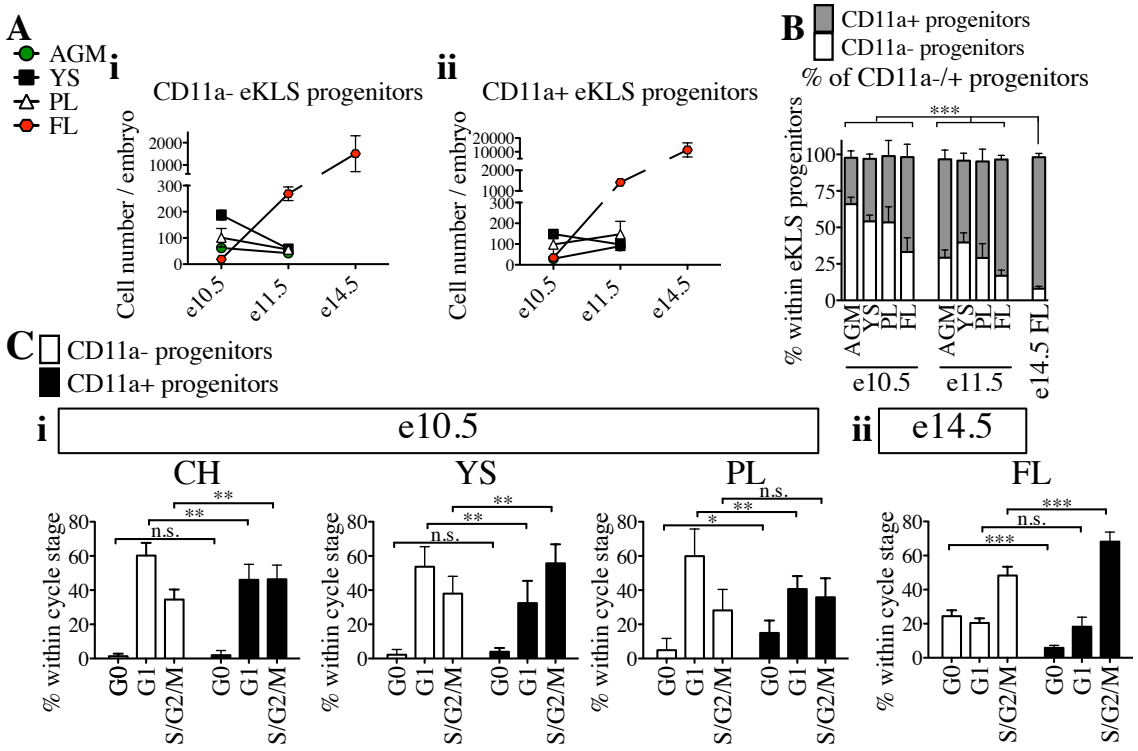

Figure 3.3. Higher proliferation rate of CD11a+ progenitors compared to CD11a- counterparts. A) Numbers of CD11a- and CD11a+ progenitors in embryos over time. Estimated number of CD11a- progenitors **(i)** and CD11a+ progenitors **(ii)** per embryo is depicted in embryonic tissues at e10.5, e11.5, and e14.5. "eKLS progenitors" are defined as Ter119- CD43+ Sca-1+ Kit+ CD144+ at e10.5 and e11.5, and as Ter119- CD43+ Sca-1+ Kit+ EPCR+ at e14.5. *e10.5, n=4 (2 independent experiments); e11.5, n=5 (3 independent experiments; e14.5, n=10 (2 independent experiments)*. **B)** Frequencies of CD11a- and CD11a+ cells within embryonic progenitors over time. "Progenitors" are defined as Ter119- CD43+ Sca-1+ Kit+ CD144+ at e10.5 and e11.5, and as Ter119- CD43+ Sca-1+ Kit+ EPCR+ at e14.5. ***$p \leq 0.001$ (Student's unpaired t test) e10.5, n=4 (2 independent experiments); e11.5, n=5 (3 independent experiments; e14.5, n=10 (2 independent experiments)*. **C)** Cell cycle analysis of CD11a- and CD11a+ progenitors at e10.5 and e14.5. Cell cycle status of each population is depicted for e10.5 tissues **(i)** and e14.5 FL **(ii)**. "Progenitors" are defined as Ter119- CD43+ Sca-1+ Kit+ CD144+ at e10.5, and as Ter119- CD43+ Sca-1+ Kit+ CD150+ at e14.5. *$p \leq 0.05$, **$p \leq 0.01$, ***$p \leq 0.001$ (Student's unpaired t test) e10.5, n=8 (2 independent experiments); e14.5=5 (2 independent experiments)*.

gestation embryos tend to be CD11a-.

Engraftment Potential Expands to CD11a+ Progenitors During FL Expansion.

We have previously shown that adult HSCs, similar to e10.5 and e11.5 pre-HSCs examined here, lack CD11a expression[150]. We aimed to investigate CD11a expression on engraftable embryonic populations during FL expansion at e13.5-14.5. At e13.5, engraftment potential was detected from CD11a- progenitors as well as from CD11a+ progenitors, albeit at lower levels (Figure 3.4Ai). This was the first instance that we detected multipotent long-term engraftable cells in the CD11a+ fraction. We next transplanted CD11a- and CD11a+ progenitors from e14.5 FL (known to contain potent adult-engraftable cells) into adult recipients. Similar to our neonatal recipient results, we found engraftment of both CD11a- and CD11a+ progenitors (Figure 3.4Aii). Flk2 (Flt-3) expression, similar to CD11a expression, marks the loss of long-term engraftment potential in adult HSCs[105,114]. However, experiments using Flk2-reporters have identified a highly proliferative and transient embryonic population of Flk2+ progenitors that can engraft adult recipients upon transplantation[105]. We therefore examined Flk2 expression on each fraction and found significantly higher percentages of Flk2+ cells within CD11a+ eKLS at e11.5 and e14.5 (Figure 3.4B). This suggests a similar pattern of CD11a and Flk2 expression with respect to engraftment potential and possibly cell cycle status[105] (Figure 3.3C). Contrary to the reported bias of Flk2+ HSCs to produce innate-like lymphocytes, we observed no lineage output bias in the production of these cells from CD11a- or CD11a+ fractions (Supplemental Figure S3.6). Therefore, although engraftment potential of CD11a- progenitors remains superior to their CD11a+ counterparts in the e13.5-14.5 FL, a transient CD11a+ progenitor population shows long-term engraftment potential in neonatal and adult recipients.

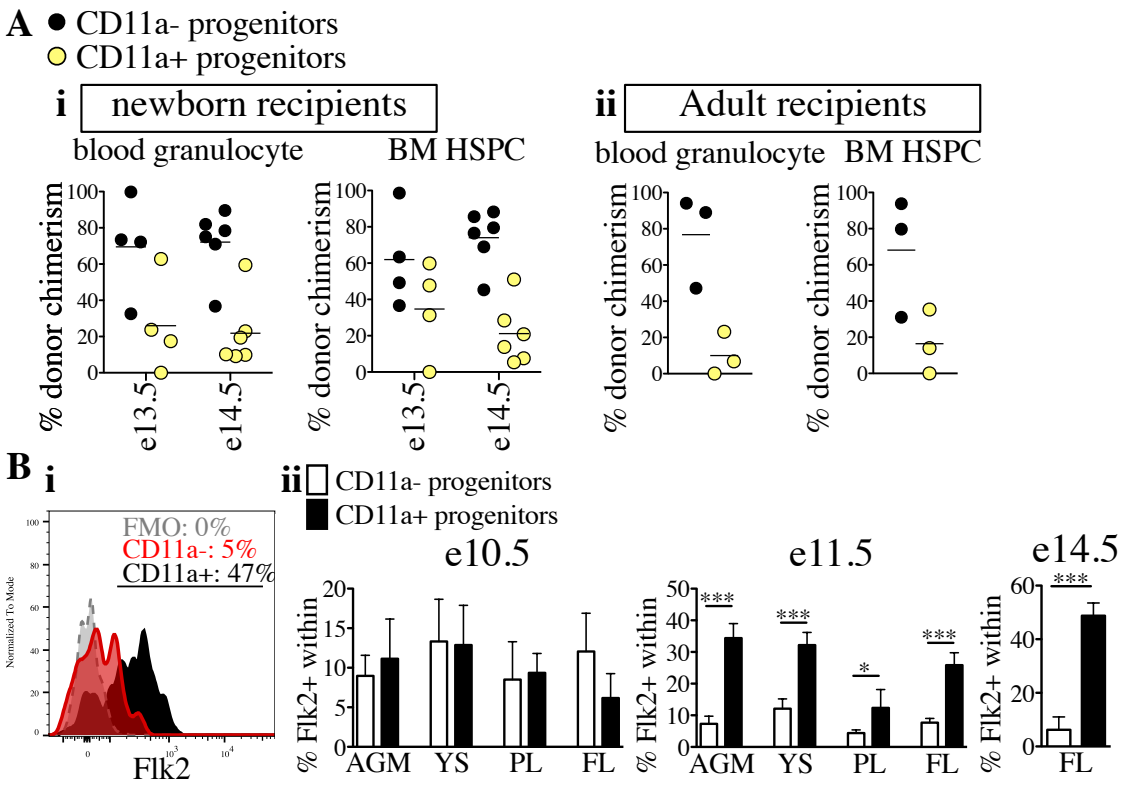

Figure 3.4. Presence of BM-engraftable CD11a+ progenitors in e14.5 FL. A) Long-term engraftment of both CD11a- and CD11a+ progenitors from e13.5-e14.5 FL in neonatal recipients **(i)** and from e14.5 FL in adult recipients **(ii)**. "Progenitors" are defined as Ter119- CD43+ Sca-1+ Kit+ EPCR+. Blood granulocyte chimerism and BM HSPC chimerism are shown for each set of recipients. **B)** Flk2 expression within CD11a- and CD11a+ progenitors. **i)** Representative FACS histogram of Flk2 expression in CD11a- and CD11a+ fractions of progenitors in e14.5 FL. Percentage of Flk2+ cells in FMO (dashed gray), CD11a- progenitors (red), and CD11a+ (black) are shown in the plot. **ii)** Percentages of Flk2+ cells within CD11a- and CD11a+ progenitors are shown in e10.5, e11.5, and e14.5 embryos. "Progenitors" are defined as Ter119- CD43+ Sca-1+ Kit+ CD144+ at e10.5 and e11.5, and as Ter119- CD43+ Sca-1+ Kit+ EPCR+ at e14.5. *$p \leq 0.05$, ***$p \leq 0.001$ *(Student's unpaired t test). e10.5, n=4 (2 independent experiments); e11.5, n=5 (2 independent experiments); e14.5, n=6.*

The Neonatal Liver Harbors Transplanted Embryonic Progenitors Shortly After Transplant.

Previous studies have suggested a role for the neonatal liver in providing a niche for the maturation of pre-HSCs prior to BM seeding, however evidence supporting this claim is lacking[100]. We transplanted fluorescent e10.5 and e11.5 sorted hematopoietic progenitors (Ter119- CD43+ Kit+) along with adult WBM into neonatal recipients, and analyzed neonatal tissues 15 hours post-transplant for the presence of transplanted cells (Figure 3.5A; Supplemental Figure S3.7A). We found that the liver contained the highest number of transplanted progenitors (Ter119- CD43+ Kit+) originating from both e10.5 and e11.5 embryonic sources as well as the adult donor source (Figure 3.5B). Similar results were found when we investigated the presence of total donor leukocytes (Ter119- CD43+) and of a more stringent progenitor population (Ter119- CD43+ Kit+ Sca-1+) (Supplemental Figure S3.7B-C). We next investigated the reason for the extremely low numbers of embryonic donor-derived cells in the limb bones. Given the involvement of CXCR4 in BM homing/retention of HSCs, we examined levels of *Cxcr4* transcript in the 11a- eKLS population and found that it is not expressed in e10.5 11a- eKLS cells (Figure 3.5C). We confirmed these results by FACS and found very low percentages of CXCR4+ 11a- eKLS cells whereas CXCR4 could be readily detected on the majority of adult HSCs (Figure 3.5D). Together, these results suggest that the neonatal liver is the most receptive environment short-term after transplant.

Discussion:

Here, we demonstrate the utility of CD11a as a marker of e10.5 and e11.5 pre-HSCs with the use of a neonatal transplant system. Other groups have reported long-term engraftment from

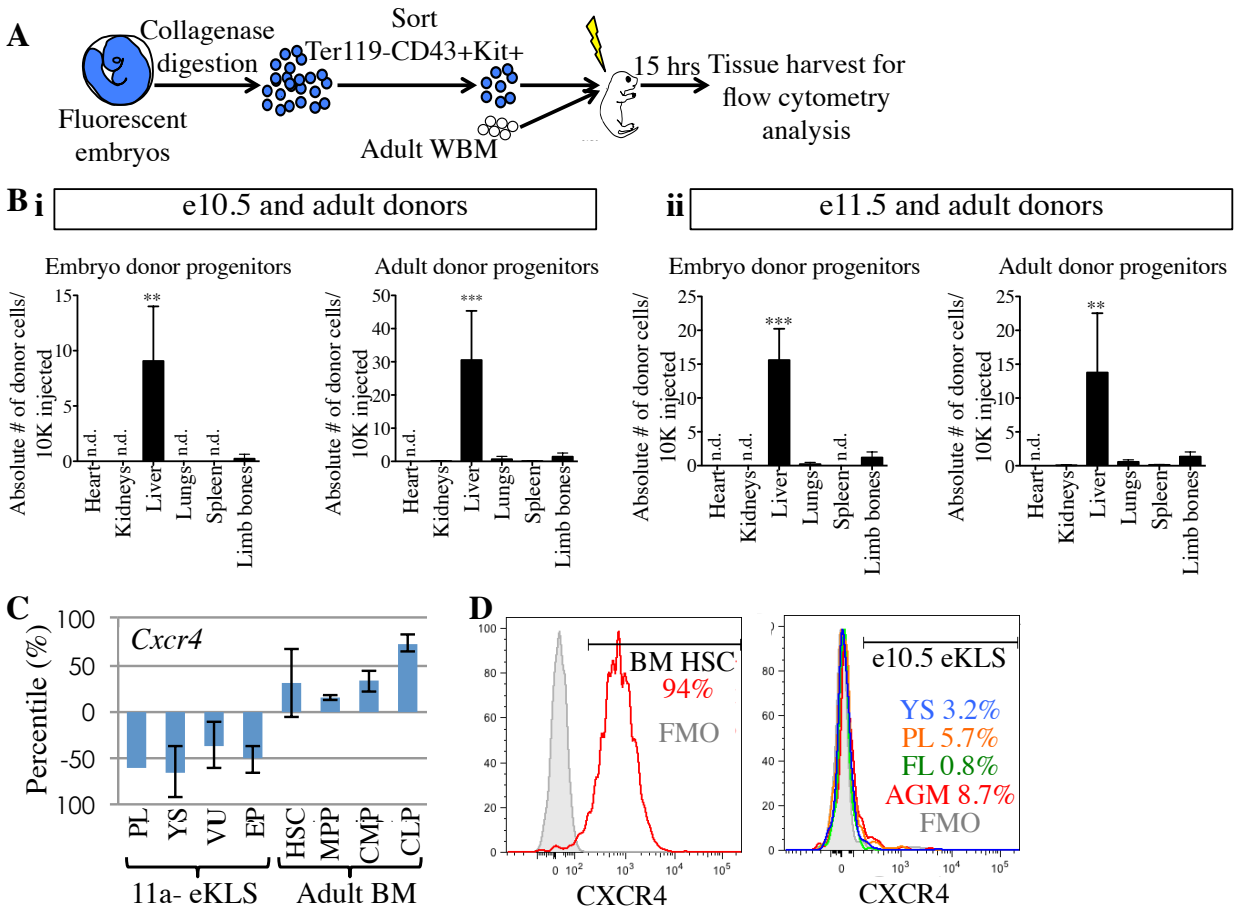

Figure 3.5. Neonatal liver harbors transplanted embryonic and adult donors in the short-term post-transplant. A) Schematic representation of short-term homing assay. Ter119- CD43+ Kit+ progenitors were sorted from whole embryos, mixed with 100,000 adult WBM and transplanted into irradiated P1-P4 neonatal recipients. 15 hours post-transplant, organs were harvested for FACS analysis. For a more detailed description of organ harvest, refer to the "Technical Discussion" in the Supplementary material. **B)** Detection of donor progenitors shortly after transplant. Absolute number of Ter119- CD43+ Kit+ progenitors originating from e10.5 **(i)** and e11.5 **(ii)** embryos and the accompanying adult source normalized to 100,000 injected cells are shown in the heart, kidneys, liver, spleen, and limb bones of the neonatal recipients. Tissues were harvested and processed in their entirety. "Limb bones" includes femurs and tibias from the hind limbs and humeri from the forelimbs. *$**p \leq 0.01$, $***p \leq 0.001$ (Student's unpaired t test). e10.5, n=3 (2 independent experiments); e11.5, n=4.* **C-D)** Expression of CXCR4 in adult and embryonic hematopoietic progenitors. *Cxcr4* mRNA levels **(C)** and CXCR4 surface expression **(D)** in different e10.5 embryonic tissues and adult BM HSCs. Percentage of CXCR4+ cells are shown in histograms. *FMO=fluorescence minus one*.

e9.5 tissues in the neonatal system[97,100]. However in line with previous reports (1 neonate-engraftable cell in 44.8 ee at e9.5 versus 1 in 2.8 ee at e10.5)[100], we found very low engraftment efficiencies from non-sorted e9.5 embryos (Table 3.1). Therefore, we decided to focus on e10.5 and e11.5 embryos in which pre-HSCs are more abundant. Transplantation of e10.5 and e11.5 cells have revealed extremely rare HSCs in the AGM, YS, PL, and FL[93,102,104]. HSCs are also able to engraft the newborn recipient, albeit at lower efficiencies compared to adult recipients[100]. Therefore, we cannot completely rule out the possibility of minimal contribution of fully functional HSCs to the chimerism in the neonatal recipients. Yet, pre-HSCs outnumber HSCs at these stages (for instance, about 30 pre-HSCs[101] versus 1 HSC in e11.5 AGM) and robust HSC activity is not detected until after e12[102]. Therefore, we believe that the great majority of long-term engrafting cells from e10.5 and e11.5 embryos are pre-HSCs. Furthermore, we confirmed the absence of detectable HSC activity in e10.5 and e11.5 embryos by transplanting these cells into lethally-irradiated adult recipients (Figure S3.1).

Our multi-parameter FACS identifies an enriched population within which all e10.5 and e11.5 pre-HSCs are contained (Figure 3.2). Due to time constraints and the technically difficult nature of the neonatal transplant system, we did not set out to determine the frequency of pre-HSCs in the 11a- eKLS population by a limiting-dilution approach. Compared to Not eKLS, 11a- eKLS shows a higher overlap with the expression of the newly established pre-HSC marker, EPCR[101] (Supplemental Figure S3.4A). Despite a high degree of overlap, 11a- eKLS can be fractionated based on EPCR expression. Therefore inclusion of EPCR can potentially improve the purity of our proposed pre-HSC population. In our previous studies, we have previously detected *in vitro* multi-lineage output from e10.5 and e11.5 EPCR- cells[86]. Thus, we believe that the inclusion of EPCR can also "miss" a minor fraction of pre-HSCs.

Pre-HSCs have been classified into "type 1" and "type 2" based on the differential expression of the pan-hematopoietic marker CD45, where expression of CD45 is thought to mark the transition from type 1 to type 2[131]. The CD11a- fraction of eKLS contains significantly lower percentages of CD45+ cells, compared to the almost homogenous CD45 expression on the CD11a+ fraction (Supplemental Figure S3.4B), suggesting that type 1 pre-HSCs are contained within the 11a- eKLS. Recent live section imaging of e11.5 AGM have suggested that type 1 pre-HSCs are more likely to be found at the base of intra-aortic hematopoietic clusters whereas CD45+ type 2 pre-HSCs tend to be on the apical (budding) side[180]. It would be interesting to characterize the possible differences in engraftment capacity of these subtypes upon neonatal transplantation.

We have previously reported that adult HSC activity is restricted to the CD11a- fraction of a highly enriched HSPC population[150]. In adults, long-term HSCs are quiescent, and up-regulation of CD11a marks downstream transit-amplifying progenitors and, therefore, cell cycle entry[150]. Although the majority of embryonic cells are in cell cycle, we found that e10.5 11a-eKLS tend to be more slowly dividing (G1) compared to 11a+ eKLS that are more likely to actively proliferate (S-G2-M) (Figure 3.3C). Recent work by Batsivari *et al*. investigated the cell cycle status of precursor populations to HSCs in the embryo and found engraftment potential of cells in both G1 and S-G2-M in the e10.5 AGM[180]. In the e11.5 AGM, this engraftment potential shifts to pre-HSCs in the G1 phase, and it is almost exclusively restricted to cells in G0-early G1 in the e14.5 FL[180]. Therefore, starting around the time of pre-HSC expansion, a group of engraftable precursors seem to be slowing down their proliferation and moving towards a resting phase, reminiscent of adult HSCs. We also found more quiescent and fewer proliferative cells among CD11a- HSCs in the e14.5 FL, relative to CD11a+ HSC counterparts (Figure 3.3C).

These observations along with the higher rate of expansion of the CD11a+ progenitors during development (Figure 3.3A-B) suggest a correlation between CD11a up-regulation and active proliferation.

Based on our findings, embryonic pre-HSCs and adult HSCs are CD11a-[150]. Yet here we also report a neonate- and BM-engraftable CD11a+ HSC population in the e14.5 FL (Figure 3.4A). Furthermore we previously detected a similar CD11a+ HSC population in the e17.5 FL and found that this population down-regulates CD11a after homing to the recipient BM[150]. Lack of Flk2 expression (similar to CD11a) is a marker of BM HSCs[114]. Interestingly, Flk2 and CD11a follow a similar pattern of expression also on engraftable cells during embryonic development. Using a "Flk2-switch" mouse model, Beaudin *et al*. report a transient and proliferative Flk2+ HSC population in the e14.5 FL that shows long-term engraftability upon transplantation[105]. Moreover, Flk2-switch HSCs are not found in the adult BM during normal development but can persist into adulthood if transplanted. Our analysis at e11.5 found a correlation between the lack of CD11a and Flk2 expression on embryonic progenitors (Figure 3.4B). Whether e14.5 FL CD11a+ HSCs persist into adulthood in normal conditions or if their reconstitution/self-renewal capacity comes about only upon transplantation (similar to the Flk2-expressing HSCs) is an interesting question. From a mechanistic stand, possible involvement of CD11a and Flk2 up-regulation in mediating cell cycle entry of HSCs during a time of FL expansion is worth investigating. Flk2+ FL HSCs were proposed to contribute to the pool of innate-like lymphocytes. Yet, our comparative analysis of CD11a- and CD11a+ FL HSCs did not reveal significant differences in B-1 B cell or γδ T cell outputs (Supplemental Figure S3.6).

Ex vivo maturation assays are potent enough to drive the development of primitive blood-forming cells, as primitive as hemogenic endothelial cells[132], into adult-engraftable multipotent

cells. Accordingly, we reasoned that utilization of the neonatal transplant system would provide a more natural environment to reveal pre-HSC activity. Yet, the reason for the receptivity of neonates to pre-HSC engraftment has not been directly investigated. We reasoned that because the liver persists as an active site of hematopoiesis until after birth (up to 3 weeks)[181], the neonatal liver may provide a temporary niche for transplanted embryonic cells. Indeed, our short-term homing analyses revealed that almost all transplanted embryonic progenitors homed to the liver of neonatal recipients shortly after transplantation (Figure 3.5). This suggests that the developing liver microenvironment provides pre-HSCs with maturation signals required for eventual BM homing/engraftment. Because robust BM-engraftable HSCs in the embryo are initially detected in the FL a day after the peak of the pre-HSC wave, we believe that detailed analysis of molecular and cellular structure of the FL niche can provide invaluable information critical for embryonic progenitor maturation. Rare studies in the past have highlighted the potent effects of the FL niche cells on HSC maintenance[182-185]. Yet more rigorous studies are required to delineate the cellular and molecular players that mediate HSC expansion and, possibly, pre-HSC maturation in the FL niche. Efforts aimed to generate HSCs from pluripotent sources, although promising and improving, have failed to display robust BM engraftment of the differentiated HSCs[70-72]. Characterization the developing liver niche could shed light on the programing necessary to turn multipotent hematopoietic cells into BM-engrafting therapeutic agents.

Materials and Methods

Mice:

In our experiments, we used embryos from a Rosa26$^{Tomato/CFP}$ male crossed to a Rosa26$^{wt/wt}$ (C57Bl/6; Jackson Laboratory; stock no. 00664) female. Rosa26$^{Tomato/CFP}$ male was generated from a cross between Rosa26$^{Tomato/Tomato}$ (mT/mG; Jackson Laboratory; stock no. 007576) and Rosa26$^{CFP/CFP}$ (TM5; generous donation by Dr. Irving Weissman). NSG (NOD-*scid* IL-2Rgamma^{null}; Jackson Laboratory; Stock no. 005557) mice were used as neonatal recipients. All strains were maintained at the Gross Hall and Med Sci A vivarium facilities at UCI and fed with standard chow and water. All animal procedures were approved by the International Animal Care and Use Committee (IACUC) and University Laboratory Animal Resources (ULAR) of University of California, Irvine.

Antibodies:

A detailed list of all antibodies used in this study is shown in Table S3.

Embryo harvest and tissue processing:

Mating cages were established and vaginal plugs were checked every morning to determine the time of pregnancy. The morning of plug detection was assigned as day 0.5. Pregnant mice were dissected and embryos harvested in PBS + 2% fetal bovine serum (FACS buffer) and kept on ice during tissue dissection. Somite pairs were counted and averaged for each experiment to determine dpc. Dpc designation is as follows: 15-29 somite pairs: e9.5; 30-39 somite pairs: e10.5; 40-50 somite pairs: e11.5. For tissue analyses and non-sorted transplants, CH, YS, and PL were harvested from e9.5 embryos. For e10.5 and e11.5 embryos, AGM and FL were harvested separately instead of together (e.g. CH). For sorted transplants, CH, YS, and PL were harvested from e10.5 donors and AGM, YS, PL, and FL from e11.5 donors. For non-sorted transplants, YS was harvested with the vitelline vessels, and PL was harvested with umbilical vessels. For sorted transplants, YS was separated without the vitelline vessels, and PL was harvested with umbilical

vessels. Separated tissues were digested with 1 mg/mL Collagenase Type IV (ThermoFisher Scientific; cat. no. 17104019) for 30-45 minutes at 37°C. Tissues were pipetted up and down at 15-minute intervals to aid with the digestion. Single cell suspension was filtered using a 40 μ mesh. We recommend using 40 μ (instead of 70 μ) mesh for donor cells to minimize clogging of blood vessels upon injection into neonatal recipients. Cells were washed twice and resuspended in FACS buffer for staining/transplantation.

Cell sorting:

Single cell suspensions of cells were typically stained for 20-30 minutes on ice. We recommend using ACK lysis buffer *after* completion of cell staining as pre-staining use can affect the VE-cadherin signal. For sorting, a BD FACS-Aria II (Becton Dickinson) with FACSDiva software was used. For sorted transplants, the "purity" mode was used for cell sorting. Since opposing populations from differentially labeled embryo cells were combined together, only embryo batches with close to 50-50% color distribution were used for the competitive sorted transplant. Therefore, physiological ratios of opposing populations were reflected in the final tube to be transplanted. For short-term homing sorts, the "yield" mode was used for cell sorting.

In vivo transplantation and analysis:

For non-sorted transplants, the embryo equivalent used for each timepoint is as follows: ≥4 ee for e9.5, ≤3 ee for e10.5, and ≤1 ee for e11.5. For all transplants, single cell suspensions were resuspended in 50-70 μL FACS buffer for injection with defined numbers of adult helper BM added. For neonatal transplants, cells were injected into the facial vein of sublethally irradiated (180-200 Rads; XRAD 320, Precision X-ray) P1-P4 NSG recipients. Nursing NSG mothers were fed an antibiotic chow of Trimethoprim Sulfa (Uniprim, Envigo) for 4 weeks post transplant to prevent bacterial infections. For secondary transplantation into adult recipients, recipient

C57BL/6 mice were conditioned with 800 Rads, anesthetized by isoflurane, and retro-orbitally injected with 1-2 million whole BM harvested from primary recipients. For peripheral blood analysis, blood was obtained from the tail vein of transplanted mice at various timepoints, and red blood cells were depleted using ACK lysis buffer. For BM analysis, BM was harvested from tibias and femurs by flushing with ice-cold FACS buffer followed by ACK lysis and filtration. Cells were stained with lineage antibodies and analyzed on the BD FACS-Aria II. FlowJo software (Tree Star) was used for data analysis.

Cell cycle analysis:

FoxP3 Intracellular staining kit (Tonbo Biosciences; cat. no. TNB-0607) was used for cell cycle analyses. Briefly, cells stained with extracellular antibodies were fixed with Tonbo Foxp3/Transcription Factor Fix/Perm buffer for 45 min at 4°C, permeabilized/stained with PE anti-ki-67 antibody (Biolegend; cat. no. 652403) diluted in Tonbo Flow Cytometry Perm Buffer for 45 min in the dark at room temperature. Cells were then washed and stained with 1 microM DAPI (Biolegend; cat. no. 422801) for 10 min prior to flow cytometric analysis. We recommend avoiding separation of e10.5 tissues into fewer than 4 ee as the fix/perm process results in loss of cells.

Short-term homing analysis:

Neonatal recipients were sacrificed 15 hours post-transplant for tissue dissection. Care was taken to harvest tissues in their entirety. All tissues except bones were harvested by crushing in between slides followed by separation using a 28-gauge needle. Limb bones were crushed using a pestle and mortar. Crushed bone particles were passed through a 28-gauge needle for further separation. All tissues were filtered through a 40 μ mesh and ACK lysed prior to staining.

Statistical analysis:

Statistical analysis was performed with GraphPad Prism 5 software (La Jolla, CA).

Supporting Information

Technical discussion

Engraftability of 11a- eKLS pre-HSCs from head, circulating blood, and vitelline vessels.

In a few non-sorted transplants, we also included the head and the circulating blood, and detected pre-HSCs in those tissues (data not shown). Also in the non-sorted transplants, we harvested the vitelline vessels (VVs) with the YS. In order to distinguish between the contributions of the YS from that originating in the VV, we harvested the YS without VV in the sorted transplants. At the same time, because we aimed to use age-matched neonatal recipients, we opted to focus on the major hematopoietic tissues (AGM, YS, PL, FL) and leave out the abovementioned tissues. Inclusion of the VV, circulating blood, and the head would have required 6 more healthy neonatal recipients, 2 for each color combination of competing sorted populations, increasing the number of recipients to 12 for e10.5 and to 14 for e11.5 sorted transplants. Accordingly, although it is a possibility that pre-HSCs are not within the 11a- eKLS population in the VV, circulating blood, and the head, it is extremely unlikely as all the major tissues and timepoints we tested point to pre-HSCs being CD11a-.

Short-term homing experiments and limb bones.

Our short-term homing experiments revealed drastically higher numbers of recently transplanted cells in the liver of neonatal recipients, compared to other tissues including limb bones. It is worth noting that not the entire bone tissue was harvested from the recipients (e.g. rib bones, skull, spine were not harvested). Therefore, the number of donor cells in all of the "bones" might be slightly higher than what is found in the entirety of limb bones. Regardless, we believe that the drastically higher numbers of donor progenitors in the neonatal liver are an indication of initial homing of transplanted cells into the liver prior to eventual BM seeding.

Supplementary Figures

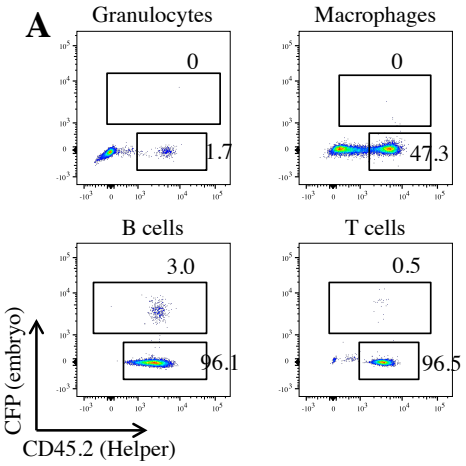

B

Embryo donor dpc	ee transplanted	Adult recipient genotype	# recipients with helper BM engraftment	# recipients with embryo donor lymphocyte engraftment	# recipients with embryo donor granulocyte engraftment	Total # transplanted recipients
e11.5	1-2	NSG	4	4	0	4
		Bl/6	5	5	0	5
e10.5	3-4	NSG	3	2	0	3

Supplementary Figure S3.1. Lack of engraftment of e10.5 and e11.5 embryonic donors in adult recipients. A-B) Blood chimerism analysis of adult recipients of embryonic donors. **A)** Representative analysis of the blood of adult recipients transplanted with 1 ee of non-sorted e11.5 embryonic tissues (extra- and intra-embryonic tissues). Plots show live single CD45+ cells. CD45.2 marks helper BM and CFP expression marks embryo-derived chimerism. **B)** Compilation of embryo donor transplants into adult recipients.

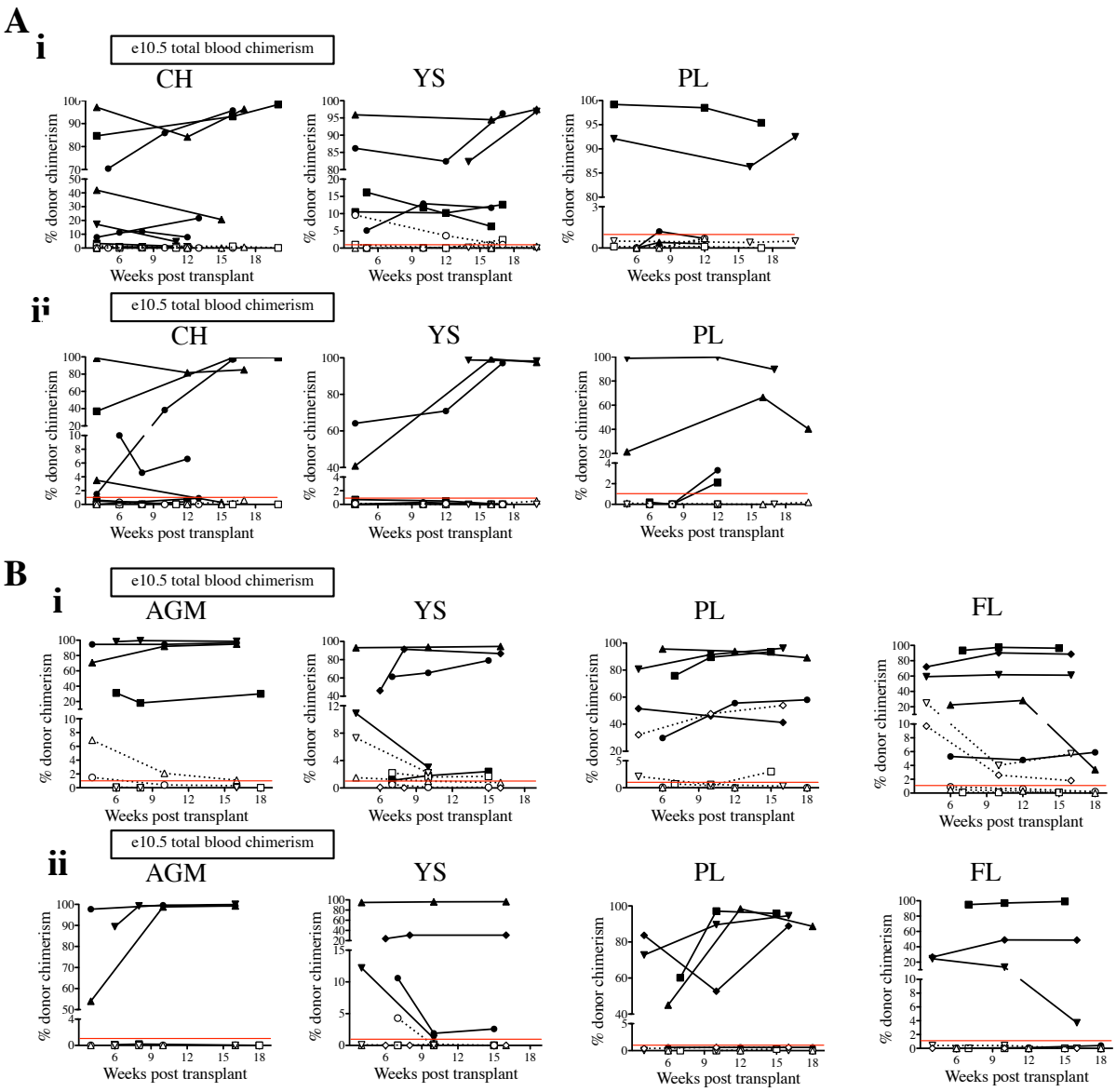

Supplemental Figure S3.2. Dynamics of chimerism from 11a-eKLS and NOT eKLS donor sources over time. A-B) Dynamics of blood chimerism in e10.5 and e11.5 recipients over time. Total blood chimerism **(i)** and blood granulocyte chimerism **(ii)** from sorted populations from e10.5 **(A)** and e11.5 **(B)** donors are shown. Black symbols and solid connecting lines represent the 11a- eKLS source while white symbols and dashed connecting lines represent the Not eKLS source. Matching symbol shapes indicate competing donors. Red lines mark 1% donor chimerism, used to set the threshold for successful engraftment.

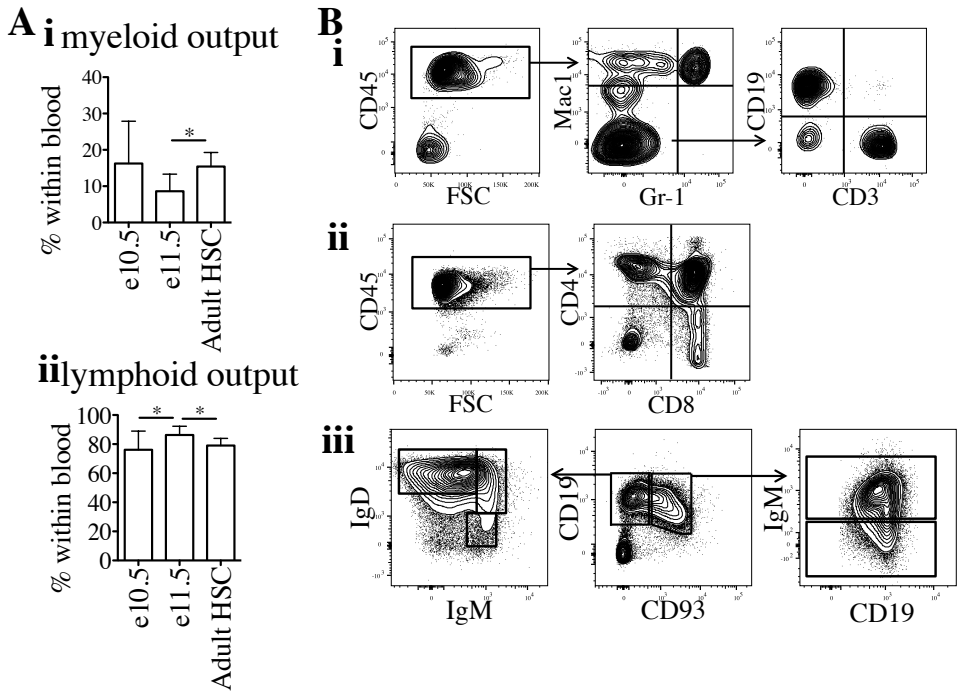

Supplemental Figure S3.3. 11a-eKLS-derived blood system shows no bias and encompasses all blood compartments. A) Myeloid **(i)** and Lymphoid **(ii)** output from 11a-eKLS donors. Myeloid is defined as CD45+ Mac1+ Gr1-/+, and lymphoid is defined as CD45+ Mac1- CD3+/CD19+. Myeloid and lymphoid output from adult HSCs transplanted into adult B6 recipients are shown as a comparison. *$p \leq 0.05$ *(Student's unpaired t test). e10.5, n=9; e11.5, n=12; adult HSC, n=4*. **B)** Representative FACS plots of blood at the last bleed **(i)**, thymus **(ii)**, and spleen **(iii)** of primary recipients transplanted with e10.5 11a- eKLS donor cells. Starting plots in **(i)** and **(ii)** (leftmost plots) are gated on live single cells. Starting plot in **(iii)** (middle plot) is gated on CD45+ live single cells.

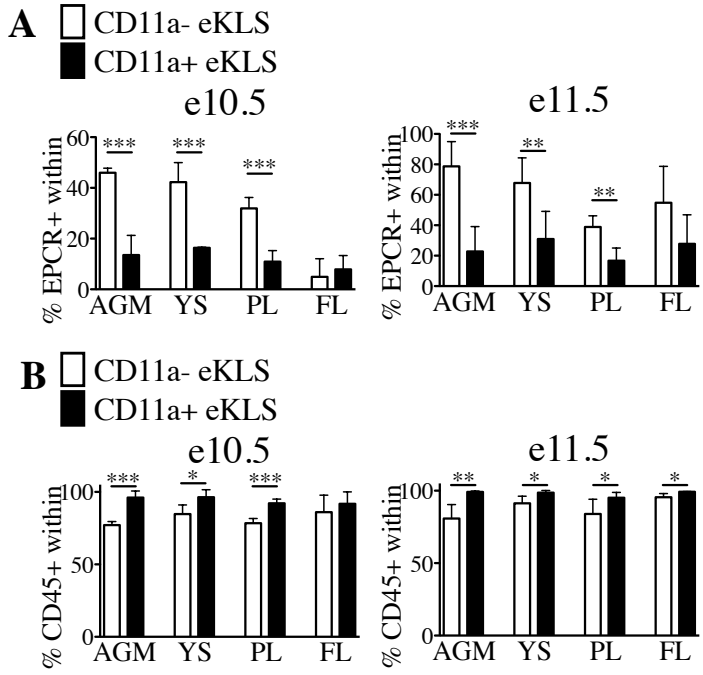

Supplemental Figure S3.4. Expression of EPCR and CD45 on CD11a- and CD11a+ embryonic progenitors. A-B) Percentages of cells expressing EPCR **(A)** and CD45 **(B)** within 11a- eKLS and 11a+ eKLS gates. **p ≤ 0.05, **p ≤ 0.01, ***p ≤ 0.001 (Student's unpaired t test). n=4 (2 independent experiments); e11.5, n=5 (2 independent experiments); e14.5, n=6.*

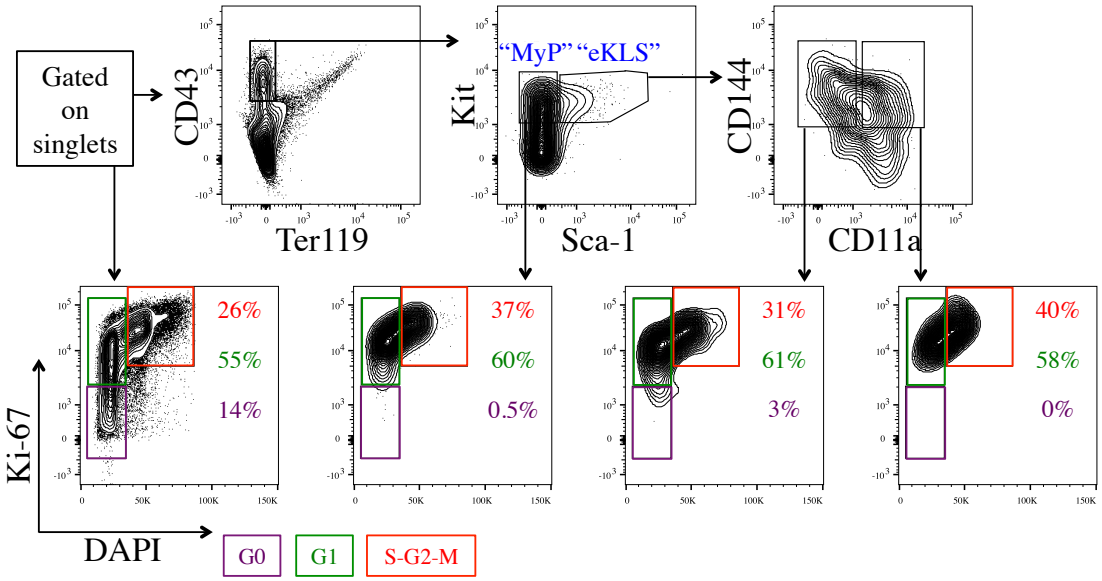

Supplemental Figure S3.5. Cell cycle analysis of embryonic cells. Representative analysis of the cell cycle status in embryonic population. Bottom plots show DAPI (x-axis) and Ki-67 (y-axis) within total single cells, myeloid progenitors (MyP), 11a- eKLS, and 11a+ eKLS from left to right. The color of percentage values inside the gates correlate with the color of each gate/cell cycle phase.

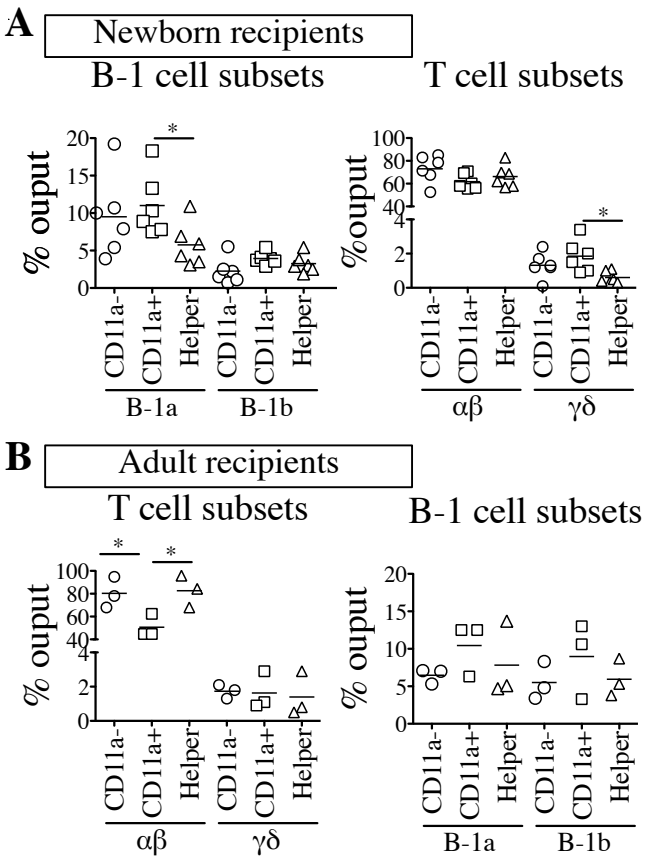

Supplemental Figure S3.6. Engraftable e14.5 FL CD11a+ progenitors do not show a bias to produce innate-like lymphocytes. A-B) Peritoneal B-1 subsets and γδ T cells derived from CD11a- and CD11a+ progenitors of e14.5 FL in neonatal (**A**) and adult (**B**) recipients. B-1 cells are defined as CD45+ CD19+ CD43+ CD23- IgD^{lo} IgM+, and B-1a cells are defined as CD5+ whereas B-1b cells are defined as CD5-. T cells are defined as CD45+ CD3- Mac-1-. *$p \leq 0.05$ *(Student's unpaired t test).*

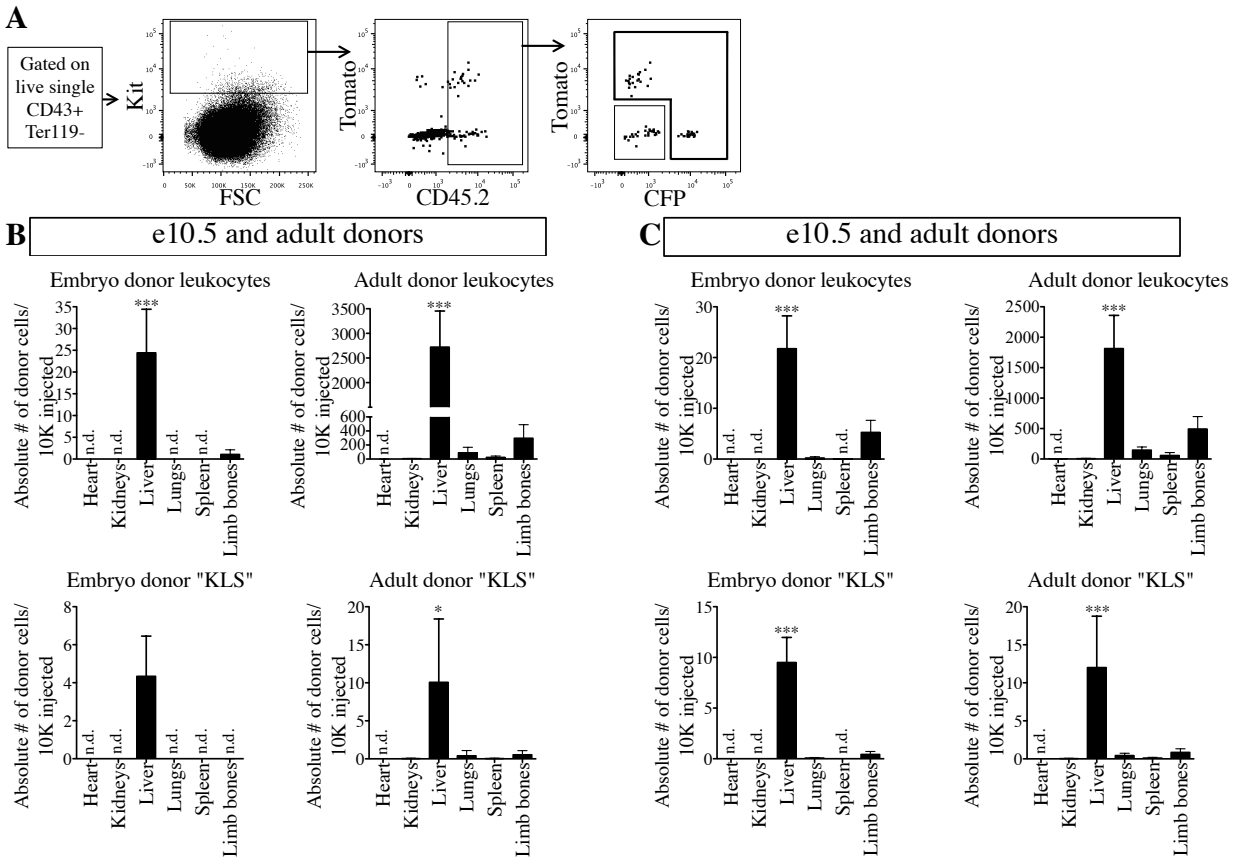

Supplemental Figure S3.7. Detection of embryo donor- and adult donor-derived populations in neonatal recipients shortly after transplantation. A) Representative analysis of recipient tissues in short-term homing recipients. Embryo donors are identified as CFP+ or Tomato+ cells expressing CD45.2+ within the population of interest (in this case, Ter119- CD43+ Kit+). Adult WBM is distinguished using the expression of CD45.2 (recipient NSGs exclusively express CD45.1) along with lack of fluorescence (fluorescent proteins are specific to embryos). **B-C)** Detection of e10.5 **(B)** and e11.5 **(C)** donor cells shortly after transplant. "Donor leukocytes" is defined as Ter119- CD43+ and "donor KLS" is defined by Ter119- CD43+ Kit+ Sca-1+. ***p ≤ 0.01, ***p ≤ 0.001 (Student's unpaired t test). e10.5, n=3 (2 independent experiments); e11.5, n=4.*

Supplementary Tables

Table S3.1. Antibodies Table				
Antigen	**Clone**	**Conjugate**	**Source**	**Catalogue #**
TER119	TER119	PE/Cy5	Biolegend	116210
	TER119	BV421	Biolegend	116233
SCA1 (Ly-6A/E)	E13-161.7	PE/Cy7	eBioscience	122514
	E13-161.7	PE	Biolegend	122507
KIT (CD117)	ACK2	APC	Biolegend	135107
	2B8	APC-eFluor 780	eBioscience	47-1171-82
	2B8	BV421	Biolegend	105828
CD27	LG.7F9	eFluor 780	eBioscience	47-0271-82
	LG.7F9	APC	eBioscience	17-0271-82
CD11A	M17/4	PE/Cy7	eBioscience	25-0111-30
	M17/4	Biotin	Biolegend	101103
	M17/4	APC	Biolegend	101119
	M17/4	PE	Biolegend	101107
	M17/4	FITC	Biolegend	101106
	M17/4	Alexa Fluor 488	Biolegend	101111
EPCR (CD201)	eBio1560	PerCP-eFluor 710	eBioscience	46-2012-82
	eBio1560	APC	eBioscience	17-2012-82
GR1 (Ly-6G/Ly-6C)	RB6-8C5	Alexa Fluor 700	eBioscience	108422
MAC1 (CD11b)	M1/70	APC	Biolegend	101212
	M1/70	FITC	Biolegend	101205
CD19	6D5	APC	Biolegend	115512
	eBio1D3	PerCP-Cy5.5	eBioscience	45-0193-82
	6D5	BV421	Biolegend	115537
CD45	30-F11	APC/Cy7	Biolegend	103116
	30-F11	Alexa Fluor 700	Biolegend	103128
CD45.2	104	FITC	Biolegend	109806
CD45.1	A20	PE/Cy7	Biolegend	110729
CD3ε	17A2	PerCP-eFluor 710	eBioscience	46-0032-82
	17A2	PE/Cy7	Biolegend	100220
NK-1.1	PK136	APC	Biolegend	108709
Flk2 (Flt3)	A2F10	PE	Biolegend	135305
CD4	RM4-5	PE/Cy7	Biolegend	100527
CD8a	53-6.7	APC/Cy7	Biolegend	100714
CD5	53-7.3	PE/Cy5	Biolegend	100609
IgD	11-26c.2a	Alexa Fluor 700	Biolegend	405729
IgM	RMM-1	APC/Cy7	Biolegend	406515
B220	RA3-6B2	BV605	Biolegend	103243
Cxcr4	L276F12	PE	Biolegend	146505
Ki-67	16A8	PE	Biolegend	652403
CD43	S7	APC	BD Biosciences	560663

VE-Cadherin	BV13	Biotin	Biolegend	138008
TCR γ/δ	GL3	PE	Biolegend	118108
TCR β	H57-597	APC	Biolegend	109211
CD23	B3B4	PE/Cy7	eBioscience	25-0232-81
CD21/CD35	eBio8D9	PE	eBioscience	12-0211-82
Secondary antibodies				
		Qdot 655-Streptavidin	Life Technologies	Q10121MP
		Qdot 605-Streptavidin	Life Technologies	Q10103MP
		eFluor710-Streptavidin	eBioscience	49-4317-80

Table S3.2. Marker definitions of populations analyzed	
Population	*Markers used*
Total blood	CD45+
Granulocyte	CD45+ Gr1+ Mac-1+
Macrophage	CD45+ Gr1- Mac-1+
T cell	CD45+ CD3+
B cell	CD45+ CD19+
KLS/HSPC	Ter119- CD27+ Kit+ Sca-1+

CHAPTER 4: DISCUSSION AND FUTURE DIRECTIONS

Opening statement: All aspects of the promise of regenerative medicine are present in the potential of patient-specific iHSCs to treat *any* hematopoietic defect inherent to the blood system. Characterization of adult HSCs and their embryonic precursors is an important step in the journey for generation of transplantable iHSCs. FACS purification of murine HSCs has been complicated by a number of issues, including reliability on markers that don't preform in all conditions. Here we report a simplified two-color method of isolating adult HSCs. Moreover, we use CD11a in combination with other markers to isolate an enriched pre-HSC population capable of long-term engraftment upon neonatal transplantation. Our sorting strategy allows for better identification and deeper molecular characterization of pre-HSCs.

HSC Sorting Made Simple

In Chapter 2, we establish a two-color method of sorting murine adult HSCs using CD11a and EPCR. The advantage of using such an approach is its simplicity and efficiency when the goal is HSC yield, as our 11a/EPCR method does not "miss" any HSCs. Yet, the 11a/EPCR gate is also contaminated with non-HSCs. We did not directly assess the identity of the contaminating cells, but these are likely comprised of ST-HSCs and some MPPs, both of which having the capacity to show temporary multi-lineage reconstitution. Accordingly, we did not detect any multi-lineage output from the Not 11a/EPCR population, even at the shortest timepoint post-transplant. These data suggest that all long- and short-term multi-lineage reconstituting cells are contained within the 11a/EPCR gate. For further technical simplicity and to save time, a CD11a/EPCR-based magnetic-activated cell sorting (MACS) approach can be

developed. Currently, kits for progenitor isolation are sub-optimal for studying HSCs. These include kits that employ Kit or Sca-1 for positive selection of progenitors or Lin for negative selection of differentiated cells. Although these approaches improve the frequency of progenitor cells to an extent, they require additional antibodies and further FACS-based purification for isolation of HSPCs. We believe that a CD11a/EPCR MACS approach (by depletion of CD11a+ cells and positive selection of EPCR+ cells) has the potential to resolve this issue and make fast and efficient isolation of HSPCs possible.

In addition to making HSC sorting more accessible, a simplified panel would facilitate HSC imaging through methods such as imaging cytometry or microscopy. Historically, microscopic imaging of the BM niche has been difficult because of structural makeup of the BM[186]. However recent developments in imaging techniques have allowed chemical clearing of tissues for efficient of visualization of cellular networks[187,188], and such techniques have been employed for improved imaging of the BM niche[160,186]. The CD11a and EPCR combination can be utilized in HSC imaging approaches. Because HSCs (like ECs) lack CD11a expression and because EPCR is expressed also on ECs, this marker combination might result in noisy backgrounds. Therefore, use of a pan-hematopoietic marker (i.e. CD45) can help to distinguish between the endothelial and hematopoietic lineages and facilitate HSC identification in imaging approaches. In the context of imaging cytometry, an enrichment step (i.e. Kit enrichment) can also minimize the background noise. On the other hand, elegant HSPC-specific mouse reporters have been developed by the identification of HSPC-specific genes (*Hoxb5*[160], *Hoxb4*[189], *α-catulin*[186], and *Fgd5*[190]). Our proposed CD11a/EPCR staining can be employed to compliment identification of HSCs in the abovementioned mouse models.

The Potential of CD11a as a Marker of Human HSCs

From a translational standpoint, follow-up studies would have to investigate the expression pattern of CD11a on human HSCs. Whereas numerous *murine* HSC markers have been established (see Chapter 1), these marker don't necessarily have applicability to identify their *human* counterparts[191]. Human HSCs (harvested from peripheral blood, BM, and umbilical cord blood or CB) are commonly enriched in the CD34+ fraction of blood cells[192-194]. Yet, this population is far from a homogenous HSC population, and HSCs make up a small fraction of CD34+ cells[195,196]. Regardless, CD34 remains the most prominent and commonly used human HSC marker[194]. Other proposed human HSC markers include CD133[197], CD90[198], KDR[199], CDCP1[200], CD38[201], CD45RA[202], and the more recently established GPI-80[203]. CD34+ CD90+ CD38- is commonly used to define human HSCs, however HSC activity within CD34-[204] and CD90-[205] fractions has also been reported. Moreover, even the most restrictive human sorts produce poor HSC purity, nowhere near what is accomplished in mice[206]. Recently, EPCR has been identified as potential marker of human CB HSCs[207]. Fares *et al*. found that EPCR expression enriches for phenotypic CB HSCs, defined as CD34+ CD90+ CD133+. As the frequency of HSCs in CB is suboptimal for transplantation therapy, expansion of CB progenitors has been employed with the use of small molecules[208]. CB HSC expansion with the self-renewal agonist UM171[209] resulted in induced expression of EPCR on phenotypic HSCs. Primary and secondary transplants into recipient mice revealed that only the EPCR+ fraction of CB HSCs showed long-term engraftability[207]. These interesting observations highlighted the potential of EPCR as a marker of human HSCs. Also, EPCR expression on both human and murine HSCs suggests a functional role of EPCR expression in HSC biology.

On the other hand, the utility of CD11a as a human HSC marker has not been investigated. CD11a is expressed on CB and BM cells in humans, as expected based on its important immunological roles. Interestingly, CD11a is expressed at low levels on CD34+ CD38- (progenitors) CB and BM cells, whereas it is highly expressed in the CD34+ CD38+ (differentiated) fraction[210]. Lower expression of CD11a in human progenitor/stem population is suggestive of a similar pattern of expression of CD11a in mouse and human hematopoietic cell hierarchy. Preliminary experiments performed with freshly-thawed CB and BM have suggested that the CD11a- fraction of HSCs (defined as Lin- CD34+ CD38- CD90+ CD45RA-) can engraft in recipient mice upon transplantation (personal communication with Matthew Inlay). Therefore, fractionation of human blood cells (from CB and/or peripheral blood samples) based on CD11a and EPCR expression is an exciting future direction. Multi-lineage output of candidate populations can be tested *in vitro* using CFU assays, and *in vivo* reconstitution potential can be examined upon transplantation into NSG recipient mice. Increasing the purity of human HSCs would greatly benefit characterization of these cells in a laboratory setting while also improving the success of therapeutic transplantations in the clinic.

Defining a Functional Significance for CD11a Expression on Hematopoietic Progenitors and Lack of it on Pre-HSCs/HSCs

During adult hematopoiesis, EPCR has been proposed to play a functional role in HSC biology by maintaining HSC interaction with niche cells and therefore retaining HSCs in that microenvironment[171]. However, no functional role has been described for the lack of CD11a expression on adult HSCs and their embryonic precursors. In Chapter 3, we report a correlation between the up-regulation of CD11a and more advanced cell cycle status in embryonic

hematopoietic progenitors, leading to higher proliferation and expansion of CD11a+ fractions. Similarly, CD11a expression differentiates quiescent adult HSCs from proliferative downstream progenitors[150]. Our BM inflammation/injury studies in Chapter 2 revealed the persistence of CD11a- HSCs (identified by marker expression and not transplantation) in conditions that are characterized by a global increased proliferation of blood cells. Assessment of the cell cycle status and engraftment potential of phenotypic HSCs that persist post-inflammation/injury can define a possible role for CD11a up-regulation in cell cycle entry. In T cells, LFA-1 signaling (through CD11a) contributes to induced IL-2 production and subsequent cell cycle entry, independent of TCR signaling[211]. TCR-stimulated CD11a-deficient T cells fail to enter cell cycle upon stimulation *in vitro,* whereas wild-type counterparts exhibit cell cycle progression when presented with exogenous ICAM-1[212]. As the culture system was devoid of APCs (and therefore antigens being presented on MHC molecules), these observations were not dependent on differential ability of CD11a-deficient or wild-type cells to form immunological synapses in the classical sense. Yet, possible involvement of LFA-1 in regulating cell cycle entry in the absence of TCR signaling has not been investigated. Based on these data, it would be interesting to investigate the possible role of CD11a in the context of regulating cell cycle entry in hematopoietic progenitors.

As part of LFA-1, CD11a plays an essential role in a variety of immunological processes. Yet, global deficiency of CD11a manifests in major defects only when mice are challenged by bacterial infections (see Chapter 1). In the absence of infection, hematopoiesis development is unperturbed until lymphoid commitment (CLPs). As a result, thymus cellularity and peripheral T and B cell numbers are affected[213]. Deficient CD18 expression, and therefore abnormal LFA-1 signaling, leads to leukocyte adhesion deficiency-1 (LAD-1) in humans. LAD-1 patients are

extremely susceptible to infections, exhibit defective wound healing, and are affected by tooth loss due to severe inflammation of the gums[214]. Yet, LAD-1 can is caused by deficiencies in all integrins which CD18 is a part of and not specific to LFA-1 deficiency only (CD18 is also a part of Mac-1, p150/95, and CD11d/CD18 integrins). Given the broad range of processes that are mediated by CD11a (as part of LFA-1), the relatively mild phenotype in $CD11a^{-/-}$ mice and the lack of gross defects in the myeloid compartment are surprising. As proposed before for germ-line deficient lines[213], this can suggest a compensatory mechanism where another integrin takes over the responsibilities normally mediated by LFA-1. To answer such questions, development of conditional and cell type-specific CD11a-deficient lines can be helpful. For instance, generation of a $CD11a^{loxP}$ mouse line and a cell type-specific CreER mouse (for example, $FLK2^{creER}$ to target MPPs and downstream cells) would allow temporally-controlled elimination of CD11a from specific cell types.

Mediation of immune cell migration and tissue homing are other major functions of CD11a in immune cells (see Chapter 1). Whether CD11a regulates cell trafficking in progenitors is unknown. In Chapter 2 and previous studies[150], we established that long-term engraftable adult HSCs are CD11a-, at both the transcript and surface expression levels. BM homing after intravenous introduction of donor cells is completed within only a few hours[21]. Therefore, it is unlikely that CD11a expression turns on and is expressed on the surface of sorted CD11a- HSCs during this short time to mediate the homing of transplanted cells into the BM. Furthermore, our previous observations[150] established that blocking CD11a interaction has no effect on BM homing of donor progenitors upon transplantation. Therefore in HSPCs, CD11a most likely does not play a role in tissue homing.

In Chapter 3, we detected a late-gestation (e14.5) population of CD11a+ progenitors capable of long-term engraftment in adult recipients. Since CD11a is not present on early embryonic pre-HSCs and adult HSCs, it would be informative to investigate this rare and transient CD11a+ HSC fraction. Our studies indicate that these CD11a+ cells down-regulate CD11a upon long-term lodging in recipient BM. However, we do not have the necessary tools to trace these cells during normal development. Does this population, similar to transient Flk2+ FL HSCs discussed in Chapter 3[105], have long-term engraftability only when transplanted? Do a fraction of FL HSCs transiently up-regulate CD11a to serve a function during FL expansion? To directly assess these questions, a genetic reporter of CD11a (for instance, $Rosa26^{mTmG}$;$CD11a^{Cre}$) can be employed to track the fate of CD11a+ HSCs, and the dynamics of CD11a turn-over on FL HSCs. Brain resident macrophages, microglia, are also CD11a- (personal communication with Ankita Shukla). Similar to other tissue-resident macrophages, microglia are believed to originate in the YS and from the EMP wave that precedes the pre-HSC wave (see Chapter 1). A CD11a-based lineage fate-mapping tool would then reveal CD11a- cells with a history of CD11a up-regulation. Accordingly, this information can inform us about the functional significance of CD11a in a variety of contexts.

11a- eKLS Sorting: Implications For Future Discoveries

A major goal in the field of embryonic hematopoiesis is identification and characterization of a purified pre-HSC population. Our findings in Chapter 3 establish the lack of CD11a expression as a maker of embryonic pre-HSCs. We used CD11a in combination with five other markers to isolate a rare neonate-engraftable pre-HSC population from e10.5 and e11.5 embryos. We believe that this efficient sorting strategy is a helpful contribution to the goal of

identifying pre-HSCs. Also using a neonatal transplant system, performing the transplants in a competitive setting, and the comprehensive nature of our study to assess all relevant tissues and timepoints are all welcome additions to previous studies. With the use of this method, pre-HSC purity is improved significantly while also allowing the capturing of *all* embryonic pre-HSCs. Although our proposed pre-HSC population is capable of repopulating all hematopoietic compartments that we checked (e.g. granulocytes, monocytes, B and T lymphocytes) upon transplantation, it will be interesting to follow-up these experiments with assays to confirm the functionality of donor-derived cells. For instance, established protocols for challenging recipients with Ovalbumin (OVA)[215] can be used to confirm a functional antigen-specific immune response. Such approaches can reveal possible differences between natural development of pre-HSCs and when they are modulated in a transplantation-associated microenvironment.

In our studies, we did not investigate the frequency of pre-HSCs within our proposed population (Chapter 3). Performing limiting dilution assays can address the abundance of pre-HSCs within the 11a- eKLS population. To further improve the purity of pre-HSCs, we can employ additional markers that have been proposed as pre-HSC markers in *ex vivo* maturation assays, such as EPCR[101] and CD47[101]. Our results indicate that 11a- eKLS can be further fractionated based on EPCR expression (Chapter 3), therefore EPCR can be a potentially useful addition to our proposed pre-HSC marker panel. Inclusion of EPCR is further encouraged due to its described function in mediating the interaction of mid-gestation and adult HSC with the niche cells in the FL[170] and the BM[171], respectively. The efficacy of EPCR and CD47 as pre-HSC markers should be confirmed upon transplantation of e10.5 and e11.5 embryonic cells into *neonates* without *ex vivo* maturation (disadvantages of the *ex vivo* maturation assay discussed in detail in Chapters 1 and 3). Inclusion of such markers can also facilitate the identification of

downstream progenitor populations (i.e. progenitors with limited self-renewal and/or multipotency potential). Our results in Chapter 3 highlighted the presence of lymphoid-restricted progenitors in the CD11a+ fraction of embryonic progenitors. Fractionation of this population with additional progenitor markers can identify lymphoid- and myeloid-primed progenitors during early embryonic development.

Early Hematopoietic Progenitors and the Gut Microbiota

Genetic determinants that shape the immune system compartments by influencing cell fate decisions have been studied in the context of development[216]. However, studies of how environmental factors contribute to the immune system development and homeostasis has been largely limited to adult hematopoiesis[217]. For instance, the gut microbiota vastly affect adult hematopoiesis, even at stem and progenitor levels[218]. Furthermore, transmission of microbial-derived components (such as microbial short-chain fatty acids) from the mother to the developing fetus has been reported[219,220]. Yet how the microbiota composition and microbial-derived products influence embryonic hematopoiesis has not been investigated, mostly due to a lack of defined embryonic populations. Accordingly, defining embryonic progenitors at a higher resolution can inform studies aimed to determine the role of the microbiota in health and disease during embryonic development and beyond. Utilization of germ-free mice or antibiotics treatment of conventional mice coupled to FACS analysis of embryonic hematopoietic progenitors can be a starting point with vast implications in a variety of diseases affected by the microbiome. Inclusion of novel markers, such as CD11a, can facilitate these efforts.

Can CXCR4 Expression Make Pre-HSCs BM-Engraftable?

Our findings in Chapter 3 introduce CD11a as a tool to improve pre-HSC purity, allowing for more accurate molecular characterization of these cells. Single-cell RNA sequencing of 11a- eKLS (possibly with the addition of markers such as EPCR and CD47 as discussed above) can reveal with a high resolution the gene expression patterns unique to pre-HSCs in comparison to embryonic as well as adult HSCs. As discussed in detail in Chapter 1, embryonic pre-HSCs share similar characteristics with iHSCs, such as the inability to home to and engraft in recipient BM. Therefore, molecular characterization of the natural development of pre-HSCs into HSCs would inform efforts aimed to generate BM-engraftable iHSCs. We have utilized a microarray database (Gene Expression Commons; https://gexc.riken.jp) to investigate transcript differences between our proposed pre-HSC population and adult HSCs. We have identified *Cxcr4* (and others) as a candidate with involvement in BM homing/engraftment[221-223] that is expressed in adult HSCs and absent/lowly expressed in pre-HSCs. We confirmed that low *Cxcr4* transcript level in pre-HSCs translates into the absence of CXCR4 on these cells, whereas majority of adult HSCs showed surface CXCR4 expression (Chapter 3). We hypothesized that

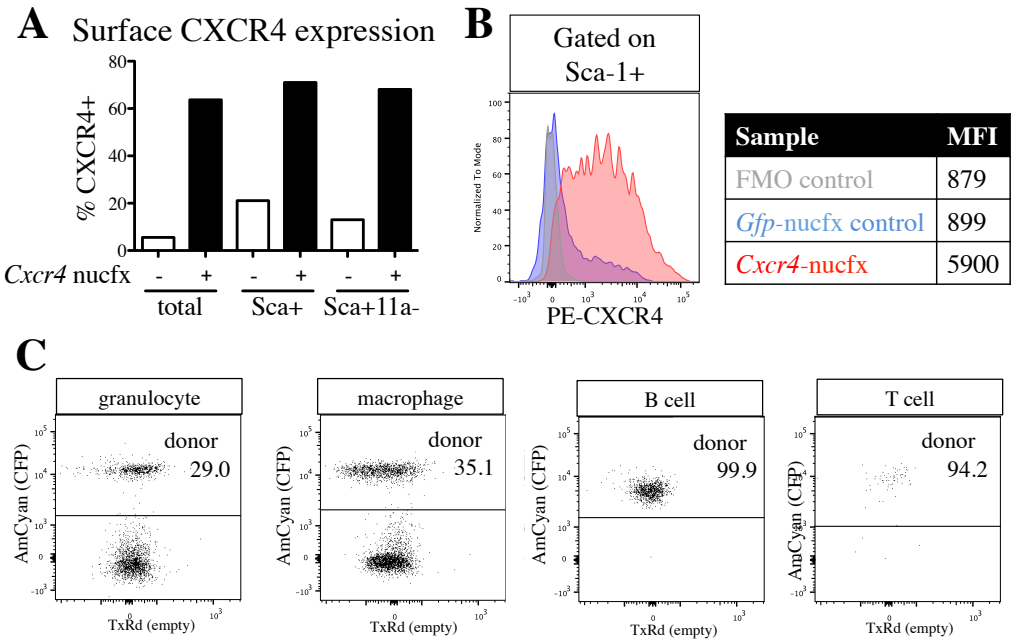

Figure 4.1. Nucleofection of embryonic progenitors to induce CXCR4 expression and preserved fitness of nucleofected cells in neonatal transplantation. A) Percentage of CXCR4+ e11.5 hematopoietic cells nucleofected with a control *Gfp* plasmid (-) or *Cxcr4* plasmid (+) 14 hours post-nucleofection. "Total" refers to total live cells. "Sca+11a-" refers to Sca-1+ CD11a- progenitors. Higher percentage of CXCR4-expressing cells are detected upon *Cxcr4* nucleofection. **B)** Shift in the intensity of CXCR4 signal in Sca-1+ progenitors upon *Cxcr4* nucleofection. Experiment conditions are the same as in (A). **C)** Blood donor chimerism analysis of neonatal recipients transplanted with e10.5 embryonic cells nucleofected with a control *Gfp* plasmid. Blood analysis was performed 4 weeks post-transplant. Donor embryonic cells are detected based on CFP expression. Note that GFP expression (induced by overexpression) was transient and, therefore, not detected in donor cells after 4 weeks. Intact neonatal engraftment and multi-lineage output potential of nucleofected embryonic donors is shown.

enforced expression of CXCR4 in pre-HSCs would improve the BM homing/engraftment potential of these cells. We used nucleofection to enforce temporary *Cxcr4* expression in e10.5 embryo cells and confirmed induced CXCR4 levels on embryonic hematopoietic progenitors (Figure 4.1A and Figure 4.1B). The nucleofection protocol can compromise viability of embryonic cells. It is therefore possible for pre-HSCs to lose neonatal-engraftment capacity following nucleofection. However, we confirmed successful neonatal engraftment of cells that were nucleofected to express a control GFP-encoding plasmid (Figure 4.1C). This suggests that the baseline fitness level required for maintaining the engraftment potential of embryonic cells is preserved after nucleofection. Therefore, follow-up experiments will be performed to determine if induced CXCR4 levels can improve pre-HSC homing/engraftment. We will test the *in vitro* transmigration of CXCR4-expressing embryonic progenitors towards a gradient of the CXCR4 ligand CXCL12, as previously described[224,225]. Moreover, we will transplant *Cxcr4*-nucleofected e10.5 and e11.5 embryonic progenitors into adult recipients and assess both short-term BM homing and long-term engraftment of these cells. Identification of signaling molecules important for improved BM homing of pre-HSCs can be translated into enhanced BM engraftment of iHSCs. Non-integrative approaches of gene overexpression offer safe alternatives to integrative viral transduction, which can cause abnormalities such as leukemia in the recipients[226,227]. In recent years, "modified mRNA"-induced expression[228] has been employed with great promise in experiments aimed to modulate engraftability of iHSCs in mouse recipients[71]. Furthermore, several treatment with several molecules (such Estradiol[229,230], Ergosterol[231], and Flonase[232]) have been shown to induce CXCR4 expression in adult HSCs. Accordingly, we will test whether these molecules can induce CXCR4 expression in pre-HSCs.

The Origin Question

A longstanding topic of debate has been the origin of definitive hematopoiesis. As discussed in Chapter 1, primitive blood-forming cells first appear in the extra-embryonic YS prior to the establishment of a heartbeat[80]. Since definitive hematopoiesis appears after the initiation of a heartbeat (and therefore circulation) at e8.5, blood cells can travel between extra- and intra-embryonic tissues, thus complicating a definitive answer to the origin question. To bypass this issue, *Ncx1*$^{-/-}$ that lack blood circulation were used to show that all definitive hematopoietic progenitors were contained within the YS[233] and PL[234]. The appearance of definitive HSCs from YS-derived precursors has been challenged by observations of de novo generation of hematopoietic clusters in the dorsal aorta of the AGM when this tissue was isolated in culture[235,236]. The relationship between embryonic blood-forming waves and their tissue(s) of origin is also unclear[237]. We believe that our pre-HSC identification strategy complemented with genetic tools developed in our lab can address some of these questions. Our Lyve-1^{cre}; Rosa26^{mTmG} and our HoxB6^{creER}; Rosa26^{mTmG} systems allow spatial (Lyve1 model) and spatiotemporal (HoxB6 model) control over fluorescent labeling of precursor cells (and their progeny) that are derived from the YS and extra-embryonic tissues (YS and PL), respectively (personal communication with Yasamine Ghorbanian and Ankita Shukla). Quantification of the labeling of 11a- eKLS pre-HSCs showed higher contribution of extra-embryonic-derived progenitors to the pre-HSC pool, suggesting these cells are at least partially responsible for de novo generation of HSCs (personal communication with Yasamine Ghorbanian and Ankita Shukla). In line with these observations, we also found that the YS contains the highest number of 11a- eKLS cells at e10.5 when we analyzed absolute cell numbers (Chapter 3). So although we do not rule out the involvement of the AGM in definitive hematopoiesis, our data point to YS

and PL as extra-embryonic contributors to adult HSCs. In order to fill the holes in our knowledge about the natural processes leading to HSC generation, it is imperative to define the cellular/molecular/anatomical structure of the tissues that harbor the first definitive hematopoietic populations.

The FL Niche Deserves More Attention

As discussed in Chapter 1, iHSCs resemble an immature and embryonic-like state. Thus, characterizing the *embryonic* niches of hematopoietic cells can provide insight into the stimulating factors/conditions required for the generation of robust iHSCs. The FL is the site of HSC expansion starting at e12 (see Chapter 1). Accordingly, we detected BM-engraftable HSCs in e14.5 FL cells (Chapter 3). Although the FL is not known for its de novo HSC generation capacity, it can certainly support the maturation of pre-HSCs. In line with this notion, we report that in our neonatal transplantation system, the neonatal liver is likely the temporary site of e10.5 and e11.5 pre-HSC maturation until these cells can home to the BM and lodge there permanently (Chapter 3). Thus, we hypothesize that the temporary pre-HSC/HSC niche in the FL can provide the necessary stimulants for increased BM engraftment capacity in pre-HSCs. Furthermore, e14.5 FL HSCs show a more robust BM engraftment potential compared to their adult counterparts[100]. One argument for this observation concerns proliferation potential. Unlike the quiescent status of adult HSCs, FL HSCs are highly proliferative[238]. Yet, higher proliferation does not necessarily translate into higher engraftability. In adults, stimulation of quiescent HSCs to enter cell cycle results in a defect in engraftment potential of these cells[239]. On the other hand in the neonatal liver, resting HSCs have higher engraftment potential compared to actively proliferating HSCs[240]. This is also highlighted in our experiments that investigate the engraftment

potential and cell cycle status of e14.5 FL HSCs (Chapter 3). Furthermore, the higher proliferation of embryonic and neonatal HSCs seems to be a temporal and intrinsic programing in these cells rather than a tissue-dependent phenomenon. This idea is supported by experiments showing higher proliferation of HSCs in the neonatal BM (similar to neonatal liver HSCs) until about 3 weeks of age, at which point HSCs make a sudden shift to a quiescent state[181,240]. Thus, the high proliferation rate associated with FL HSCs does not completely explain the superiority of these cells in BM engraftment.

Higher engraftment potential of FL HSCs, in comparison to adult HSCs, can be attributed to a more robust regenerative (e.g. self-renewal) capacity that FL HSCs possess[241]. It is then plausible to conclude that the FL niche supports pre-HSC maturation by providing a microenvironment that preserves the self-renewal potential of pre-HSCs while allowing induced expansion. In line with this idea, an immortalized cell line from e14.5 FL can maintain adult HSC activity for over a month, a phenomenon not achievable with BM stromal cells[185]. Given the role of the FL microenvironment for pre-HSC maturation, it would be interesting to identify and apply FL-derived stimuli to iHSCs and assess their BM engraftment potential. Hence, it is important to define the cellular and molecular players in the FL niche. A hepatic progenitor population (defined as SCF+ DLK+) that supports adult HSC expansion has been isolated and its secreted factors have been characterized[184]. Whether this niche population supports pre-HSC maturation remains to be determined. Nevertheless, similar approaches to dissect out the FL niche stimuli necessary for pre-HSC maturation is of great interest to efforts aimed to generate BM-engraftable iHSCs. Investigation of the anatomical structure of the FL can also be insightful as unique mechanical forces may be contributing to the HSC-nourishing properties of this niche. For instance, Runx1 expression (major transcription factor for EHT) is induced as a result of the

shear stress of blood flow[242,243]. Also as a comparative analysis, transplantation of iHSCs into neonatal recipients can provide helpful information about the developmental maturity of these cells and possibly reveal involvement of the FL niche to mature iHSCs. Although this question has been investigated in one study[215], the results were not conclusive. As our studies (Chapter 3) and others have defined the behavior of pre-HSCs upon neonatal transplantation, transplantation of iHSCs into neonates can better characterize functional similarities/differences between pre-HSCs and iHSCs.

Closing Statement: We are hopeful that our novel sorting strategy for the isolation of murine adult HSCs and embryonic pre-HSCs would provide a link in a chain of discoveries that lead to improvements in our understanding of hematopoiesis from conception to adulthood. Identifying the factors that regulate hematopoietic development can ultimately translate into therapies such as transplantation of patient-specific iHSCs, which has the potential to affect millions of patients worldwide.

REFERENCES

1 Ramalho-Santos, M. & Willenbring, H. On the origin of the term "stem cell". *Cell stem cell* **1**, 35-38, doi:10.1016/j.stem.2007.05.013 (2007).

2 Mazzarello, P. A unifying concept: the history of cell theory. *Nature cell biology* **1**, E13-15, doi:10.1038/8964 (1999).

3 Eaves, C. J. Hematopoietic stem cells: concepts, definitions, and the new reality. *Blood* **125**, 2605-2613, doi:10.1182/blood-2014-12-570200 (2015).

4 Jacobson, L. O., Simmons, E. L., Marks, E. K. & Eldredge, J. H. Recovery from radiation injury. *Science* **113**, 510-511 (1951).

5 Ford, C. E., Hamerton, J. L., Barnes, D. W. & Loutit, J. F. Cytological identification of radiation-chimaeras. *Nature* **177**, 452-454 (1956).

6 McCulloch, E. A. & Till, J. E. The radiation sensitivity of normal mouse bone marrow cells, determined by quantitative marrow transplantation into irradiated mice. *Radiation research* **13**, 115-125 (1960).

7 Till, J. E. & Mc, C. E. A direct measurement of the radiation sensitivity of normal mouse bone marrow cells. *Radiation research* **14**, 213-222 (1961).

8 Becker, A. J., Mc, C. E. & Till, J. E. Cytological demonstration of the clonal nature of spleen colonies derived from transplanted mouse marrow cells. *Nature* **197**, 452-454 (1963).

9 Wu, A. M., Till, J. E., Siminovitch, L. & McCulloch, E. A. A cytological study of the capacity for differentiation of normal hemopoietic colony-forming cells. *Journal of cellular physiology* **69**, 177-184, doi:10.1002/jcp.1040690208 (1967).

10 Wu, A. M., Till, J. E., Siminovitch, L. & McCulloch, E. A. Cytological evidence for a relationship between normal hemotopoietic colony-forming cells and cells of the lymphoid system. *The Journal of experimental medicine* **127**, 455-464 (1968).

11 Siminovitch, L., McCulloch, E. A. & Till, J. E. The Distribution of Colony-Forming Cells among Spleen Colonies. *Journal of cellular and comparative physiology* **62**, 327-336 (1963).

12 Na Nakorn, T., Traver, D., Weissman, I. L. & Akashi, K. Myeloerythroid-restricted progenitors are sufficient to confer radioprotection and provide the majority of day 8 CFU-S. *The Journal of clinical investigation* **109**, 1579-1585, doi:10.1172/JCI15272 (2002).

13 Spangrude, G. J., Heimfeld, S. & Weissman, I. L. Purification and characterization of mouse hematopoietic stem cells. *Science* **241**, 58-62 (1988).

14 Weissman, I. L. Stem cells: units of development, units of regeneration, and units in evolution. *Cell* **100**, 157-168 (2000).

15 Morrison, S. J., Shah, N. M. & Anderson, D. J. Regulatory mechanisms in stem cell biology. *Cell* **88**, 287-298 (1997).

16 Seita, J. & Weissman, I. L. Hematopoietic stem cell: self-renewal versus differentiation. *Wiley interdisciplinary reviews. Systems biology and medicine* **2**, 640-653, doi:10.1002/wsbm.86 (2010).

17 Rossi, D. J. *et al.* Hematopoietic stem cell quiescence attenuates DNA damage response and permits DNA damage accumulation during aging. *Cell cycle* **6**, 2371-2376, doi:10.4161/cc.6.19.4759 (2007).
18 Ogawa, M. Differentiation and proliferation of hematopoietic stem cells. *Blood* **81**, 2844-2853 (1993).
19 King, K. Y. & Goodell, M. A. Inflammatory modulation of HSCs: viewing the HSC as a foundation for the immune response. *Nature reviews. Immunology* **11**, 685-692, doi:10.1038/nri3062 (2011).
20 Heazlewood, S. Y., Oteiza, A., Cao, H. & Nilsson, S. K. Analyzing hematopoietic stem cell homing, lodgment, and engraftment to better understand the bone marrow niche. *Annals of the New York Academy of Sciences* **1310**, 119-128, doi:10.1111/nyas.12329 (2014).
21 Papayannopoulou, T. & Craddock, C. Homing and trafficking of hemopoietic progenitor cells. *Acta haematologica* **97**, 97-104 (1997).
22 Ley, K., Laudanna, C., Cybulsky, M. I. & Nourshargh, S. Getting to the site of inflammation: the leukocyte adhesion cascade updated. *Nature reviews. Immunology* **7**, 678-689, doi:10.1038/nri2156 (2007).
23 Frenette, P. S., Subbarao, S., Mazo, I. B., von Andrian, U. H. & Wagner, D. D. Endothelial selectins and vascular cell adhesion molecule-1 promote hematopoietic progenitor homing to bone marrow. *Proceedings of the National Academy of Sciences of the United States of America* **95**, 14423-14428 (1998).
24 Vermeulen, M. *et al.* Role of adhesion molecules in the homing and mobilization of murine hematopoietic stem and progenitor cells. *Blood* **92**, 894-900 (1998).
25 Dimitroff, C. J., Lee, J. Y., Fuhlbrigge, R. C. & Sackstein, R. A distinct glycoform of CD44 is an L-selectin ligand on human hematopoietic cells. *Proceedings of the National Academy of Sciences of the United States of America* **97**, 13841-13846, doi:10.1073/pnas.250484797 (2000).
26 Scott, L. M., Priestley, G. V. & Papayannopoulou, T. Deletion of alpha4 integrins from adult hematopoietic cells reveals roles in homeostasis, regeneration, and homing. *Molecular and cellular biology* **23**, 9349-9360 (2003).
27 Avigdor, A. *et al.* CD44 and hyaluronic acid cooperate with SDF-1 in the trafficking of human CD34+ stem/progenitor cells to bone marrow. *Blood* **103**, 2981-2989, doi:10.1182/blood-2003-10-3611 (2004).
28 Zarbock, A., Lowell, C. A. & Ley, K. Spleen tyrosine kinase Syk is necessary for E-selectin-induced alpha(L)beta(2) integrin-mediated rolling on intercellular adhesion molecule-1. *Immunity* **26**, 773-783, doi:10.1016/j.immuni.2007.04.011 (2007).
29 Berlin, C. *et al.* alpha 4 integrins mediate lymphocyte attachment and rolling under physiologic flow. *Cell* **80**, 413-422 (1995).
30 Kerfoot, S. M. & Kubes, P. Overlapping roles of P-selectin and alpha 4 integrin to recruit leukocytes to the central nervous system in experimental autoimmune encephalomyelitis. *Journal of immunology* **169**, 1000-1006 (2002).
31 Vajkoczy, P., Laschinger, M. & Engelhardt, B. Alpha4-integrin-VCAM-1 binding mediates G protein-independent capture of encephalitogenic T cell blasts to CNS white matter microvessels. *The Journal of clinical investigation* **108**, 557-565, doi:10.1172/JCI12440 (2001).

32 Shirvaikar, N., Marquez-Curtis, L. A. & Janowska-Wieczorek, A. Hematopoietic Stem Cell Mobilization and Homing after Transplantation: The Role of MMP-2, MMP-9, and MT1-MMP. *Biochemistry research international* **2012**, 685267, doi:10.1155/2012/685267 (2012).
33 Aiuti, A., Webb, I. J., Bleul, C., Springer, T. & Gutierrez-Ramos, J. C. The chemokine SDF-1 is a chemoattractant for human CD34+ hematopoietic progenitor cells and provides a new mechanism to explain the mobilization of CD34+ progenitors to peripheral blood. *The Journal of experimental medicine* **185**, 111-120 (1997).
34 Sugiyama, T., Kohara, H., Noda, M. & Nagasawa, T. Maintenance of the hematopoietic stem cell pool by CXCL12-CXCR4 chemokine signaling in bone marrow stromal cell niches. *Immunity* **25**, 977-988, doi:10.1016/j.immuni.2006.10.016 (2006).
35 Crane, G. M., Jeffery, E. & Morrison, S. J. Adult haematopoietic stem cell niches. *Nature reviews. Immunology* **17**, 573-590, doi:10.1038/nri.2017.53 (2017).
36 Mendez-Ferrer, S. *et al.* Mesenchymal and haematopoietic stem cells form a unique bone marrow niche. *Nature* **466**, 829-834, doi:10.1038/nature09262 (2010).
37 Pinho, S. *et al.* PDGFRalpha and CD51 mark human nestin+ sphere-forming mesenchymal stem cells capable of hematopoietic progenitor cell expansion. *The Journal of experimental medicine* **210**, 1351-1367, doi:10.1084/jem.20122252 (2013).
38 Kiel, M. J. *et al.* SLAM family receptors distinguish hematopoietic stem and progenitor cells and reveal endothelial niches for stem cells. *Cell* **121**, 1109-1121, doi:10.1016/j.cell.2005.05.026 (2005).
39 Broudy, V. C. Stem cell factor and hematopoiesis. *Blood* **90**, 1345-1364 (1997).
40 Ogawa, M. *et al.* Expression and function of c-kit in hemopoietic progenitor cells. *The Journal of experimental medicine* **174**, 63-71 (1991).
41 Barker, J. E. Early transplantation to a normal microenvironment prevents the development of Steel hematopoietic stem cell defects. *Experimental hematology* **25**, 542-547 (1997).
42 Mosaad, Y. M. Hematopoietic stem cells: an overview. *Transfusion and apheresis science : official journal of the World Apheresis Association : official journal of the European Society for Haemapheresis* **51**, 68-82, doi:10.1016/j.transci.2014.10.016 (2014).
43 Sawyers, C. L., Denny, C. T. & Witte, O. N. Leukemia and the disruption of normal hematopoiesis. *Cell* **64**, 337-350 (1991).
44 Bonnet, D. & Dick, J. E. Human acute myeloid leukemia is organized as a hierarchy that originates from a primitive hematopoietic cell. *Nature medicine* **3**, 730-737 (1997).
45 Miyamoto, T., Weissman, I. L. & Akashi, K. AML1/ETO-expressing nonleukemic stem cells in acute myelogenous leukemia with 8;21 chromosomal translocation. *Proceedings of the National Academy of Sciences of the United States of America* **97**, 7521-7526 (2000).
46 George, A. A. *et al.* Detection of leukemic cells in the CD34(+)CD38(-) bone marrow progenitor population in children with acute lymphoblastic leukemia. *Blood* **97**, 3925-3930 (2001).
47 Mauro, M. J. & Druker, B. J. Chronic myelogenous leukemia. *Current opinion in oncology* **13**, 3-7 (2001).

48 Fischer, A. *et al.* Naturally occurring primary deficiencies of the immune system. *Annual review of immunology* **15**, 93-124, doi:10.1146/annurev.immunol.15.1.93 (1997).
49 Rees, D. C., Williams, T. N. & Gladwin, M. T. Sickle-cell disease. *Lancet* **376**, 2018-2031, doi:10.1016/S0140-6736(10)61029-X (2010).
50 Broadway-Duren, J. B. & Klaassen, H. Anemias. *Critical care nursing clinics of North America* **25**, 411-426, v, doi:10.1016/j.ccell.2013.09.004 (2013).
51 Wang, L., Wang, F. S. & Gershwin, M. E. Human autoimmune diseases: a comprehensive update. *Journal of internal medicine* **278**, 369-395, doi:10.1111/joim.12395 (2015).
52 de la Morena, M. T. & Nelson, R. P., Jr. Recent advances in transplantation for primary immune deficiency diseases: a comprehensive review. *Clinical reviews in allergy & immunology* **46**, 131-144, doi:10.1007/s12016-013-8379-6 (2014).
53 Horn, B. & Cowan, M. J. Unresolved issues in hematopoietic stem cell transplantation for severe combined immunodeficiency: need for safer conditioning and reduced late effects. *The Journal of allergy and clinical immunology* **131**, 1306-1311, doi:10.1016/j.jaci.2013.03.014 (2013).
54 Hatzimichael, E. & Tuthill, M. Hematopoietic stem cell transplantation. *Stem cells and cloning : advances and applications* **3**, 105-117, doi:10.2147/SCCAA.S6815 (2010).
55 Locatelli, F., Lucarelli, B. & Merli, P. Current and future approaches to treat graft failure after allogeneic hematopoietic stem cell transplantation. *Expert opinion on pharmacotherapy* **15**, 23-36, doi:10.1517/14656566.2014.852537 (2014).
56 Gragert, L. *et al.* HLA match likelihoods for hematopoietic stem-cell grafts in the U.S. registry. *The New England journal of medicine* **371**, 339-348, doi:10.1056/NEJMsa1311707 (2014).
57 Ruggeri, L. *et al.* Alloreactive natural killer cells in mismatched hematopoietic stem cell transplantation. *Blood cells, molecules & diseases* **33**, 216-221, doi:10.1016/j.bcmd.2004.08.005 (2004).
58 Barria, E., Mikels, A. & Haas, M. Maintenance and self-renewal of long-term reconstituting hematopoietic stem cells supported by amniotic fluid. *Stem cells and development* **13**, 548-562, doi:10.1089/scd.2004.13.548 (2004).
59 Hagedorn, E. J., Durand, E. M., Fast, E. M. & Zon, L. I. Getting more for your marrow: boosting hematopoietic stem cell numbers with PGE2. *Experimental cell research* **329**, 220-226, doi:10.1016/j.yexcr.2014.07.030 (2014).
60 Takahashi, K. & Yamanaka, S. Induction of pluripotent stem cells from mouse embryonic and adult fibroblast cultures by defined factors. *Cell* **126**, 663-676, doi:10.1016/j.cell.2006.07.024 (2006).
61 Takahashi, K. *et al.* Induction of pluripotent stem cells from adult human fibroblasts by defined factors. *Cell* **131**, 861-872, doi:10.1016/j.cell.2007.11.019 (2007).
62 Aoi, T. *et al.* Generation of pluripotent stem cells from adult mouse liver and stomach cells. *Science* **321**, 699-702, doi:10.1126/science.1154884 (2008).
63 Stadtfeld, M., Brennand, K. & Hochedlinger, K. Reprogramming of pancreatic beta cells into induced pluripotent stem cells. *Current biology : CB* **18**, 890-894, doi:10.1016/j.cub.2008.05.010 (2008).

64 Hanna, J. *et al.* Direct reprogramming of terminally differentiated mature B lymphocytes to pluripotency. *Cell* **133**, 250-264, doi:10.1016/j.cell.2008.03.028 (2008).
65 Giorgetti, A. *et al.* Generation of induced pluripotent stem cells from human cord blood using OCT4 and SOX2. *Cell stem cell* **5**, 353-357, doi:10.1016/j.stem.2009.09.008 (2009).
66 Maherali, N. *et al.* A high-efficiency system for the generation and study of human induced pluripotent stem cells. *Cell stem cell* **3**, 340-345, doi:10.1016/j.stem.2008.08.003 (2008).
67 Zhou, T. *et al.* Generation of human induced pluripotent stem cells from urine samples. *Nature protocols* **7**, 2080-2089, doi:10.1038/nprot.2012.115 (2012).
68 Robinton, D. A. & Daley, G. Q. The promise of induced pluripotent stem cells in research and therapy. *Nature* **481**, 295-305, doi:10.1038/nature10761 (2012).
69 Ebina, W. & Rossi, D. J. Transcription factor-mediated reprogramming toward hematopoietic stem cells. *The EMBO journal* **34**, 694-709, doi:10.15252/embj.201490804 (2015).
70 Riddell, J. *et al.* Reprogramming committed murine blood cells to induced hematopoietic stem cells with defined factors. *Cell* **157**, 549-564, doi:10.1016/j.cell.2014.04.006 (2014).
71 Lee, J. *et al.* mRNA-mediated glycoengineering ameliorates deficient homing of human stem cell-derived hematopoietic progenitors. *J Clin Invest* **127**, 2433-2437, doi:10.1172/JCI92030 (2017).
72 Sugimura, R. *et al.* Haematopoietic stem and progenitor cells from human pluripotent stem cells. *Nature* **545**, 432-438, doi:10.1038/nature22370 (2017).
73 Lis, R. *et al.* Conversion of adult endothelium to immunocompetent haematopoietic stem cells. *Nature* **545**, 439-445, doi:10.1038/nature22326 (2017).
74 Pereira, C. F., Lemischka, I. R. & Moore, K. 'From blood to blood': de-differentiation of hematopoietic progenitors to stem cells. *The EMBO journal* **33**, 1511-1513, doi:10.15252/embj.201488980 (2014).
75 Gritz, E. & Hirschi, K. K. Specification and function of hemogenic endothelium during embryogenesis. *Cellular and molecular life sciences : CMLS* **73**, 1547-1567, doi:10.1007/s00018-016-2134-0 (2016).
76 Sabin, F. R. Preliminary note on the differentiation of angioblasts and the method by which they produce blood-vessels, blood-plasma and red blood-cells as seen in the living chick. 1917. *Journal of hematotherapy & stem cell research* **11**, 5-7, doi:10.1089/152581602753448496 (2002).
77 Jaffredo, T., Gautier, R., Eichmann, A. & Dieterlen-Lievre, F. Intraaortic hemopoietic cells are derived from endothelial cells during ontogeny. *Development* **125**, 4575-4583 (1998).
78 Sugiyama, D. *et al.* Erythropoiesis from acetyl LDL incorporating endothelial cells at the preliver stage. *Blood* **101**, 4733-4738, doi:10.1182/blood-2002-09-2799 (2003).
79 Zovein, A. C. *et al.* Fate tracing reveals the endothelial origin of hematopoietic stem cells. *Cell stem cell* **3**, 625-636, doi:10.1016/j.stem.2008.09.018 (2008).
80 Moore, M. A. & Metcalf, D. Ontogeny of the haemopoietic system: yolk sac origin of in vivo and in vitro colony forming cells in the developing mouse embryo. *Br J Haematol* **18**, 279-296 (1970).

81 Palis, J. Primitive and definitive erythropoiesis in mammals. *Frontiers in physiology* **5**, 3, doi:10.3389/fphys.2014.00003 (2014).
82 Alvarez-Silva, M., Belo-Diabangouaya, P., Salaun, J. & Dieterlen-Lievre, F. Mouse placenta is a major hematopoietic organ. *Development* **130**, 5437-5444, doi:10.1242/dev.00755 (2003).
83 Palis, J., Robertson, S., Kennedy, M., Wall, C. & Keller, G. Development of erythroid and myeloid progenitors in the yolk sac and embryo proper of the mouse. *Development* **126**, 5073-5084 (1999).
84 Palis, J. Hematopoietic stem cell-independent hematopoiesis: emergence of erythroid, megakaryocyte, and myeloid potential in the mammalian embryo. *FEBS letters* **590**, 3965-3974, doi:10.1002/1873-3468.12459 (2016).
85 Davies, L. C. & Taylor, P. R. Tissue-resident macrophages: then and now. *Immunology* **144**, 541-548, doi:10.1111/imm.12451 (2015).
86 Inlay, M. A. *et al.* Identification of multipotent progenitors that emerge prior to hematopoietic stem cells in embryonic development. *Stem Cell Reports* **2**, 457-472, doi:10.1016/j.stemcr.2014.02.001 (2014).
87 Boisset, J. C. *et al.* Progressive maturation toward hematopoietic stem cells in the mouse embryo aorta. *Blood* **125**, 465-469, doi:10.1182/blood-2014-07-588954 (2015).
88 Rybtsov, S., Ivanovs, A., Zhao, S. & Medvinsky, A. Concealed expansion of immature precursors underpins acute burst of adult HSC activity in foetal liver. *Development* **143**, 1284-1289, doi:10.1242/dev.131193 (2016).
89 Bradley, T. R. & Metcalf, D. The growth of mouse bone marrow cells in vitro. *The Australian journal of experimental biology and medical science* **44**, 287-299 (1966).
90 Liu, C. P. & Auerbach, R. In vitro development of murine T cells from prethymic and preliver embryonic yolk sac hematopoietic stem cells. *Development* **113**, 1315-1323 (1991).
91 Godin, I., Dieterlen-Lievre, F. & Cumano, A. Emergence of multipotent hemopoietic cells in the yolk sac and paraaortic splanchnopleura in mouse embryos, beginning at 8.5 days postcoitus. *Proceedings of the National Academy of Sciences of the United States of America* **92**, 773-777 (1995).
92 Medvinsky, A. L., Samoylina, N. L., Muller, A. M. & Dzierzak, E. A. An early pre-liver intraembryonic source of CFU-S in the developing mouse. *Nature* **364**, 64-67, doi:10.1038/364064a0 (1993).
93 Muller, A. M., Medvinsky, A., Strouboulis, J., Grosveld, F. & Dzierzak, E. Development of hematopoietic stem cell activity in the mouse embryo. *Immunity* **1**, 291-301 (1994).
94 Medvinsky, A. & Dzierzak, E. Definitive hematopoiesis is autonomously initiated by the AGM region. *Cell* **86**, 897-906 (1996).
95 de Bruijn, M. F., Speck, N. A., Peeters, M. C. & Dzierzak, E. Definitive hematopoietic stem cells first develop within the major arterial regions of the mouse embryo. *The EMBO journal* **19**, 2465-2474, doi:10.1093/emboj/19.11.2465 (2000).
96 Yoder, M. C. & Hiatt, K. Engraftment of embryonic hematopoietic cells in conditioned newborn recipients. *Blood* **89**, 2176-2183 (1997).

97 Yoder, M. C., Hiatt, K. & Mukherjee, P. In vivo repopulating hematopoietic stem cells are present in the murine yolk sac at day 9.0 postcoitus. *Proceedings of the National Academy of Sciences of the United States of America* **94**, 6776-6780 (1997).
98 Yoder, M. C. *et al.* Characterization of definitive lymphohematopoietic stem cells in the day 9 murine yolk sac. *Immunity* **7**, 335-344 (1997).
99 Taoudi, S. *et al.* Extensive hematopoietic stem cell generation in the AGM region via maturation of VE-cadherin+CD45+ pre-definitive HSCs. *Cell stem cell* **3**, 99-108, doi:10.1016/j.stem.2008.06.004 (2008).
100 Arora, N. *et al.* Effect of developmental stage of HSC and recipient on transplant outcomes. *Developmental cell* **29**, 621-628, doi:10.1016/j.devcel.2014.04.013 (2014).
101 Zhou, F. *et al.* Tracing haematopoietic stem cell formation at single-cell resolution. *Nature* **533**, 487-492, doi:10.1038/nature17997 (2016).
102 Kumaravelu, P. *et al.* Quantitative developmental anatomy of definitive haematopoietic stem cells/long-term repopulating units (HSC/RUs): role of the aorta-gonad-mesonephros (AGM) region and the yolk sac in colonisation of the mouse embryonic liver. *Development* **129**, 4891-4899 (2002).
103 Bertrand, J. Y. *et al.* Characterization of purified intraembryonic hematopoietic stem cells as a tool to define their site of origin. *Proceedings of the National Academy of Sciences of the United States of America* **102**, 134-139, doi:10.1073/pnas.0402270102 (2005).
104 Gekas, C., Dieterlen-Lievre, F., Orkin, S. H. & Mikkola, H. K. The placenta is a niche for hematopoietic stem cells. *Developmental cell* **8**, 365-375, doi:10.1016/j.devcel.2004.12.016 (2005).
105 Beaudin, A. E. *et al.* A Transient Developmental Hematopoietic Stem Cell Gives Rise to Innate-like B and T Cells. *Cell Stem Cell* **19**, 768-783, doi:10.1016/j.stem.2016.08.013 (2016).
106 Uchida, N. & Weissman, I. L. Searching for hematopoietic stem cells: evidence that Thy-1.1lo Lin- Sca-1+ cells are the only stem cells in C57BL/Ka-Thy-1.1 bone marrow. *The Journal of experimental medicine* **175**, 175-184 (1992).
107 Morrison, S. J. & Weissman, I. L. The long-term repopulating subset of hematopoietic stem cells is deterministic and isolatable by phenotype. *Immunity* **1**, 661-673 (1994).
108 Morrison, S. J., Wandycz, A. M., Hemmati, H. D., Wright, D. E. & Weissman, I. L. Identification of a lineage of multipotent hematopoietic progenitors. *Development* **124**, 1929-1939 (1997).
109 Okada, S. *et al.* In vivo and in vitro stem cell function of c-kit- and Sca-1-positive murine hematopoietic cells. *Blood* **80**, 3044-3050 (1992).
110 Ikuta, K. & Weissman, I. L. Evidence that hematopoietic stem cells express mouse c-kit but do not depend on steel factor for their generation. *Proceedings of the National Academy of Sciences of the United States of America* **89**, 1502-1506 (1992).
111 Osawa, M., Hanada, K., Hamada, H. & Nakauchi, H. Long-term lymphohematopoietic reconstitution by a single CD34-low/negative hematopoietic stem cell. *Science* **273**, 242-245 (1996).

112 Balazs, A. B., Fabian, A. J., Esmon, C. T. & Mulligan, R. C. Endothelial protein C receptor (CD201) explicitly identifies hematopoietic stem cells in murine bone marrow. *Blood* **107**, 2317-2321, doi:10.1182/blood-2005-06-2249 (2006).
113 Karlsson, G. *et al.* The tetraspanin CD9 affords high-purity capture of all murine hematopoietic stem cells. *Cell reports* **4**, 642-648, doi:10.1016/j.celrep.2013.07.020 (2013).
114 Christensen, J. L. & Weissman, I. L. Flk-2 is a marker in hematopoietic stem cell differentiation: a simple method to isolate long-term stem cells. *Proceedings of the National Academy of Sciences of the United States of America* **98**, 14541-14546, doi:10.1073/pnas.261562798 (2001).
115 Wiesmann, A. *et al.* Expression of CD27 on murine hematopoietic stem and progenitor cells. *Immunity* **12**, 193-199 (2000).
116 Arai, F. *et al.* Tie2/angiopoietin-1 signaling regulates hematopoietic stem cell quiescence in the bone marrow niche. *Cell* **118**, 149-161, doi:10.1016/j.cell.2004.07.004 (2004).
117 Chen, C. Z. *et al.* Identification of endoglin as a functional marker that defines long-term repopulating hematopoietic stem cells. *Proceedings of the National Academy of Sciences of the United States of America* **99**, 15468-15473, doi:10.1073/pnas.202614899 (2002).
118 Rossi, L., Challen, G. A., Sirin, O., Lin, K. K. & Goodell, M. A. Hematopoietic stem cell characterization and isolation. *Methods in molecular biology* **750**, 47-59, doi:10.1007/978-1-61779-145-1_3 (2011).
119 Uchida, N. *et al.* High doses of purified stem cells cause early hematopoietic recovery in syngeneic and allogeneic hosts. *The Journal of clinical investigation* **101**, 961-966, doi:10.1172/JCI1681 (1998).
120 Simonnet, A. J. *et al.* Phenotypic and functional changes induced in hematopoietic stem/progenitor cells after gamma-ray radiation exposure. *Stem cells* **27**, 1400-1409, doi:10.1002/stem.66 (2009).
121 Baldridge, M. T., King, K. Y. & Goodell, M. A. Inflammatory signals regulate hematopoietic stem cells. *Trends in immunology* **32**, 57-65, doi:10.1016/j.it.2010.12.003 (2011).
122 Vazquez, S. E., Inlay, M. A. & Serwold, T. CD201 and CD27 identify hematopoietic stem and progenitor cells across multiple murine strains independently of Kit and Sca-1. *Experimental hematology* **43**, 578-585, doi:10.1016/j.exphem.2015.04.001 (2015).
123 Zhang, P. *et al.* The lineage-c-Kit+Sca-1+ cell response to Escherichia coli bacteremia in Balb/c mice. *Stem cells* **26**, 1778-1786, doi:10.1634/stemcells.2007-1027 (2008).
124 Pietras, E. M. *et al.* Re-entry into quiescence protects hematopoietic stem cells from the killing effect of chronic exposure to type I interferons. *The Journal of experimental medicine* **211**, 245-262, doi:10.1084/jem.20131043 (2014).
125 Malek, T. R., Danis, K. M. & Codias, E. K. Tumor necrosis factor synergistically acts with IFN-gamma to regulate Ly-6A/E expression in T lymphocytes, thymocytes and bone marrow cells. *Journal of immunology* **142**, 1929-1936 (1989).
126 Sinclair, A., Daly, B. & Dzierzak, E. The Ly-6E.1 (Sca-1) gene requires a 3' chromatin-dependent region for high-level gamma-interferon-induced hematopoietic cell expression. *Blood* **87**, 2750-2761 (1996).

127 Ma, X., Ling, K. W. & Dzierzak, E. Cloning of the Ly-6A (Sca-1) gene locus and identification of a 3' distal fragment responsible for high-level gamma-interferon-induced expression in vitro. *British journal of haematology* **114**, 724-730 (2001).
128 Randall, T. D. & Weissman, I. L. Phenotypic and functional changes induced at the clonal level in hematopoietic stem cells after 5-fluorouracil treatment. *Blood* **89**, 3596-3606 (1997).
129 Spangrude, G. J. & Brooks, D. M. Mouse strain variability in the expression of the hematopoietic stem cell antigen Ly-6A/E by bone marrow cells. *Blood* **82**, 3327-3332 (1993).
130 Lee, P. Y., Wang, J. X., Parisini, E., Dascher, C. C. & Nigrovic, P. A. Ly6 family proteins in neutrophil biology. *Journal of leukocyte biology* **94**, 585-594, doi:10.1189/jlb.0113014 (2013).
131 Rybtsov, S. *et al.* Hierarchical organization and early hematopoietic specification of the developing HSC lineage in the AGM region. *The Journal of experimental medicine* **208**, 1305-1315, doi:10.1084/jem.20102419 (2011).
132 Hadland, B. K. *et al.* A Common Origin for B-1a and B-2 Lymphocytes in Clonal Pre-Hematopoietic Stem Cells. *Stem cell reports* **8**, 1563-1572, doi:10.1016/j.stemcr.2017.04.007 (2017).
133 Kishimoto, T. K. *et al.* The leukocyte integrins. *Advances in immunology* **46**, 149-182 (1989).
134 Humphries, J. D., Byron, A. & Humphries, M. J. Integrin ligands at a glance. *Journal of cell science* **119**, 3901-3903, doi:10.1242/jcs.03098 (2006).
135 Hynes, R. O. The extracellular matrix: not just pretty fibrils. *Science* **326**, 1216-1219, doi:10.1126/science.1176009 (2009).
136 Barczyk, M., Carracedo, S. & Gullberg, D. Integrins. *Cell and tissue research* **339**, 269-280, doi:10.1007/s00441-009-0834-6 (2010).
137 Hynes, R. O. Integrins: bidirectional, allosteric signaling machines. *Cell* **110**, 673-687 (2002).
138 Takada, Y., Ye, X. & Simon, S. The integrins. *Genome biology* **8**, 215, doi:10.1186/gb-2007-8-5-215 (2007).
139 Larson, R. S. & Springer, T. A. Structure and function of leukocyte integrins. *Immunological reviews* **114**, 181-217 (1990).
140 Shimaoka, M. *et al.* Reversibly locking a protein fold in an active conformation with a disulfide bond: integrin alphaL I domains with high affinity and antagonist activity in vivo. *Proceedings of the National Academy of Sciences of the United States of America* **98**, 6009-6014, doi:10.1073/pnas.101130498 (2001).
141 Abram, C. L. & Lowell, C. A. The ins and outs of leukocyte integrin signaling. *Annual review of immunology* **27**, 339-362, doi:10.1146/annurev.immunol.021908.132554 (2009).
142 Hogg, N., Patzak, I. & Willenbrock, F. The insider's guide to leukocyte integrin signalling and function. *Nature reviews. Immunology* **11**, 416-426, doi:10.1038/nri2986 (2011).
143 Salas, A., Shimaoka, M., Phan, U., Kim, M. & Springer, T. A. Transition from rolling to firm adhesion can be mimicked by extension of integrin alphaLbeta2 in an intermediate affinity state. *The Journal of biological chemistry* **281**, 10876-10882, doi:10.1074/jbc.M512472200 (2006).

144 Evans, R., Lellouch, A. C., Svensson, L., McDowall, A. & Hogg, N. The integrin LFA-1 signals through ZAP-70 to regulate expression of high-affinity LFA-1 on T lymphocytes. *Blood* **117**, 3331-3342, doi:10.1182/blood-2010-06-289140 (2011).
145 Binnerts, M. E., van Kooyk, Y., Simmons, D. L. & Figdor, C. G. Distinct binding of T lymphocytes to ICAM-1, -2 or -3 upon activation of LFA-1. *European journal of immunology* **24**, 2155-2160, doi:10.1002/eji.1830240933 (1994).
146 Carrasco, Y. R., Fleire, S. J., Cameron, T., Dustin, M. L. & Batista, F. D. LFA-1/ICAM-1 interaction lowers the threshold of B cell activation by facilitating B cell adhesion and synapse formation. *Immunity* **20**, 589-599 (2004).
147 Shamri, R. *et al.* Lymphocyte arrest requires instantaneous induction of an extended LFA-1 conformation mediated by endothelium-bound chemokines. *Nature immunology* **6**, 497-506, doi:10.1038/ni1194 (2005).
148 Ostermann, G., Weber, K. S., Zernecke, A., Schroder, A. & Weber, C. JAM-1 is a ligand of the beta(2) integrin LFA-1 involved in transendothelial migration of leukocytes. *Nature immunology* **3**, 151-158, doi:10.1038/ni755 (2002).
149 Shimizu, Y. LFA-1: more than just T cell Velcro. *Nature immunology* **4**, 1052-1054, doi:10.1038/ni1103-1052 (2003).
150 Fathman, J. W. *et al.* Upregulation of CD11A on hematopoietic stem cells denotes the loss of long-term reconstitution potential. *Stem cell reports* **3**, 707-715, doi:10.1016/j.stemcr.2014.09.007 (2014).
151 Tan, S. M. The leucocyte beta2 (CD18) integrins: the structure, functional regulation and signalling properties. *Bioscience reports* **32**, 241-269, doi:10.1042/BSR20110101 (2012).
152 Pipitone, N. *et al.* The glucocorticoid inhibition of LFA-1 and CD2 expression by human mononuclear cells is reversed by IL-2, IL-7 and IL-15. *European journal of immunology* **31**, 2135-2142, doi:10.1002/1521-4141(200107)31:7<2135::AID-IMMU2135>3.0.CO;2-S (2001).
153 Lu, Q., Ray, D., Gutsch, D. & Richardson, B. Effect of DNA methylation and chromatin structure on ITGAL expression. *Blood* **99**, 4503-4508 (2002).
154 Schmits, R. *et al.* LFA-1-deficient mice show normal CTL responses to virus but fail to reject immunogenic tumor. *The Journal of experimental medicine* **183**, 1415-1426 (1996).
155 Ghosh, S., Chackerian, A. A., Parker, C. M., Ballantyne, C. M. & Behar, S. M. The LFA-1 adhesion molecule is required for protective immunity during pulmonary Mycobacterium tuberculosis infection. *Journal of immunology* **176**, 4914-4922 (2006).
156 Bose, T. O. *et al.* CD11a regulates effector CD8 T cell differentiation and central memory development in response to infection with Listeria monocytogenes. *Infection and immunity* **81**, 1140-1151, doi:10.1128/IAI.00749-12 (2013).
157 Prince, J. E. *et al.* The differential roles of LFA-1 and Mac-1 in host defense against systemic infection with Streptococcus pneumoniae. *Journal of immunology* **166**, 7362-7369 (2001).
158 Boitano, A. E. *et al.* Aryl hydrocarbon receptor antagonists promote the expansion of human hematopoietic stem cells. *Science* **329**, 1345-1348, doi:10.1126/science.1191536 (2010).

159 Brunstein, C. G. *et al.* Allogeneic hematopoietic cell transplantation for hematologic malignancy: relative risks and benefits of double umbilical cord blood. *Blood* **116**, 4693-4699, doi:10.1182/blood-2010-05-285304 (2010).
160 Chen, J. Y. *et al.* Hoxb5 marks long-term haematopoietic stem cells and reveals a homogenous perivascular niche. *Nature* **530**, 223-227, doi:10.1038/nature16943 (2016).
161 Challen, G. A., Boles, N., Lin, K. K. & Goodell, M. A. Mouse hematopoietic stem cell identification and analysis. *Cytometry. Part A : the journal of the International Society for Analytical Cytology* **75**, 14-24, doi:10.1002/cyto.a.20674 (2009).
162 Kinashi, T. Intracellular signalling controlling integrin activation in lymphocytes. *Nature reviews. Immunology* **5**, 546-559, doi:10.1038/nri1646 (2005).
163 Zhang, Y. & Wang, H. Integrin signalling and function in immune cells. *Immunology* **135**, 268-275, doi:10.1111/j.1365-2567.2011.03549.x (2012).
164 Lum, A. F., Green, C. E., Lee, G. R., Staunton, D. E. & Simon, S. I. Dynamic regulation of LFA-1 activation and neutrophil arrest on intercellular adhesion molecule 1 (ICAM-1) in shear flow. *The Journal of biological chemistry* **277**, 20660-20670, doi:10.1074/jbc.M202223200 (2002).
165 Serwold, T., Ehrlich, L. I. & Weissman, I. L. Reductive isolation from bone marrow and blood implicates common lymphoid progenitors as the major source of thymopoiesis. *Blood* **113**, 807-815, doi:10.1182/blood-2008-08-173682 (2009).
166 Inlay, M. A. *et al.* Ly6d marks the earliest stage of B-cell specification and identifies the branchpoint between B-cell and T-cell development. *Genes & development* **23**, 2376-2381, doi:10.1101/gad.1836009 (2009).
167 Matsumoto, M. & Seya, T. TLR3: interferon induction by double-stranded RNA including poly(I:C). *Advanced drug delivery reviews* **60**, 805-812, doi:10.1016/j.addr.2007.11.005 (2008).
168 Schuettpelz, L. G. & Link, D. C. Regulation of hematopoietic stem cell activity by inflammation. *Frontiers in immunology* **4**, 204, doi:10.3389/fimmu.2013.00204 (2013).
169 Esplin, B. L. *et al.* Chronic exposure to a TLR ligand injures hematopoietic stem cells. *Journal of immunology* **186**, 5367-5375, doi:10.4049/jimmunol.1003438 (2011).
170 Iwasaki, H., Arai, F., Kubota, Y., Dahl, M. & Suda, T. Endothelial protein C receptor-expressing hematopoietic stem cells reside in the perisinusoidal niche in fetal liver. *Blood* **116**, 544-553, doi:10.1182/blood-2009-08-240903 (2010).
171 Gur-Cohen, S. *et al.* PAR1 signaling regulates the retention and recruitment of EPCR-expressing bone marrow hematopoietic stem cells. *Nature medicine* **21**, 1307-1317, doi:10.1038/nm.3960 (2015).
172 Fares, I. *et al.* EPCR expression marks UM171-expanded CD34+ cord blood stem cells. *Blood* **129**, 3344-3351, doi:10.1182/blood-2016-11-750729 (2017).
173 Muzumdar, M. D., Tasic, B., Miyamichi, K., Li, L. & Luo, L. A global double-fluorescent Cre reporter mouse. *Genesis* **45**, 593-605, doi:10.1002/dvg.20335 (2007).
174 Cumano, A. & Godin, I. Ontogeny of the hematopoietic system. *Annu Rev Immunol* **25**, 745-785, doi:10.1146/annurev.immunol.25.022106.141538 (2007).
175 Golub, R. & Cumano, A. Embryonic hematopoiesis. *Blood Cells Mol Dis* **51**, 226-231, doi:10.1016/j.bcmd.2013.08.004 (2013).

176 Lacaud, G. & Kouskoff, V. Hemangioblast, hemogenic endothelium, and primitive versus definitive hematopoiesis. *Exp Hematol* **49**, 19-24, doi:10.1016/j.exphem.2016.12.009 (2017).
177 Verbiest, T. *et al.* NOD Scid Gamma Mice Are Permissive to Allogeneic HSC Transplantation without Prior Conditioning. *Int J Mol Sci* **17**, doi:10.3390/ijms17111850 (2016).
178 Ishikawa, F. Modeling normal and malignant human hematopoiesis in vivo through newborn NSG xenotransplantation. *Int J Hematol* **98**, 634-640, doi:10.1007/s12185-013-1467-9 (2013).
179 Dai, H. *et al.* Donor SIRPalpha polymorphism modulates the innate immune response to allogeneic grafts. *Sci Immunol* **2**, doi:10.1126/sciimmunol.aam6202 (2017).
180 Batsivari, A. *et al.* Understanding Hematopoietic Stem Cell Development through Functional Correlation of Their Proliferative Status with the Intra-aortic Cluster Architecture. *Stem cell reports* **8**, 1549-1562, doi:10.1016/j.stemcr.2017.04.003 (2017).
181 Bowie, M. B. *et al.* Identification of a new intrinsically timed developmental checkpoint that reprograms key hematopoietic stem cell properties. *Proceedings of the National Academy of Sciences of the United States of America* **104**, 5878-5882, doi:10.1073/pnas.0700460104 (2007).
182 Khan, J. A. *et al.* Fetal liver hematopoietic stem cell niches associate with portal vessels. *Science* **351**, 176-180, doi:10.1126/science.aad0084 (2016).
183 Martin, M. A. & Bhatia, M. Analysis of the human fetal liver hematopoietic microenvironment. *Stem cells and development* **14**, 493-504, doi:10.1089/scd.2005.14.493 (2005).
184 Chou, S. & Lodish, H. F. Fetal liver hepatic progenitors are supportive stromal cells for hematopoietic stem cells. *Proceedings of the National Academy of Sciences of the United States of America* **107**, 7799-7804, doi:10.1073/pnas.1003586107 (2010).
185 Moore, K. A., Ema, H. & Lemischka, I. R. In vitro maintenance of highly purified, transplantable hematopoietic stem cells. *Blood* **89**, 4337-4347 (1997).
186 Acar, M. *et al.* Deep imaging of bone marrow shows non-dividing stem cells are mainly perisinusoidal. *Nature* **526**, 126-130, doi:10.1038/nature15250 (2015).
187 Dodt, H. U. *et al.* Ultramicroscopy: three-dimensional visualization of neuronal networks in the whole mouse brain. *Nature methods* **4**, 331-336, doi:10.1038/nmeth1036 (2007).
188 Becker, K., Jahrling, N., Saghafi, S., Weiler, R. & Dodt, H. U. Chemical clearing and dehydration of GFP expressing mouse brains. *PloS one* **7**, e33916, doi:10.1371/journal.pone.0033916 (2012).
189 Hills, D. *et al.* Hoxb4-YFP reporter mouse model: a novel tool for tracking HSC development and studying the role of Hoxb4 in hematopoiesis. *Blood* **117**, 3521-3528, doi:10.1182/blood-2009-12-253989 (2011).
190 Gazit, R. *et al.* Fgd5 identifies hematopoietic stem cells in the murine bone marrow. *The Journal of experimental medicine* **211**, 1315-1331, doi:10.1084/jem.20130428 (2014).

191 Larochelle, A. *et al.* Human and rhesus macaque hematopoietic stem cells cannot be purified based only on SLAM family markers. *Blood* **117**, 1550-1554, doi:10.1182/blood-2009-03-212803 (2011).
192 Berenson, R. J. *et al.* Engraftment after infusion of CD34+ marrow cells in patients with breast cancer or neuroblastoma. *Blood* **77**, 1717-1722 (1991).
193 Andrews, R. G. *et al.* CD34+ marrow cells, devoid of T and B lymphocytes, reconstitute stable lymphopoiesis and myelopoiesis in lethally irradiated allogeneic baboons. *Blood* **80**, 1693-1701 (1992).
194 Calloni, R., Cordero, E. A., Henriques, J. A. & Bonatto, D. Reviewing and updating the major molecular markers for stem cells. *Stem cells and development* **22**, 1455-1476, doi:10.1089/scd.2012.0637 (2013).
195 Terstappen, L. W., Huang, S., Safford, M., Lansdorp, P. M. & Loken, M. R. Sequential generations of hematopoietic colonies derived from single nonlineage-committed CD34+CD38- progenitor cells. *Blood* **77**, 1218-1227 (1991).
196 Ivanovic, Z. Hematopoietic stem cells in research and clinical applications: The "CD34 issue". *World journal of stem cells* **2**, 18-23, doi:10.4252/wjsc.v2.i2.18 (2010).
197 Yin, A. H. *et al.* AC133, a novel marker for human hematopoietic stem and progenitor cells. *Blood* **90**, 5002-5012 (1997).
198 Humeau, L. *et al.* Phenotypic, molecular, and functional characterization of human peripheral blood CD34+/THY1+ cells. *Blood* **87**, 949-955 (1996).
199 Ziegler, B. L. *et al.* KDR receptor: a key marker defining hematopoietic stem cells. *Science* **285**, 1553-1558 (1999).
200 Conze, T. *et al.* CDCP1 is a novel marker for hematopoietic stem cells. *Annals of the New York Academy of Sciences* **996**, 222-226 (2003).
201 Bhatia, M., Wang, J. C., Kapp, U., Bonnet, D. & Dick, J. E. Purification of primitive human hematopoietic cells capable of repopulating immune-deficient mice. *Proceedings of the National Academy of Sciences of the United States of America* **94**, 5320-5325 (1997).
202 Majeti, R., Park, C. Y. & Weissman, I. L. Identification of a hierarchy of multipotent hematopoietic progenitors in human cord blood. *Cell stem cell* **1**, 635-645, doi:10.1016/j.stem.2007.10.001 (2007).
203 Prashad, S. L. *et al.* GPI-80 defines self-renewal ability in hematopoietic stem cells during human development. *Cell stem cell* **16**, 80-87, doi:10.1016/j.stem.2014.10.020 (2015).
204 Zanjani, E. D., Almeida-Porada, G., Livingston, A. G., Porada, C. D. & Ogawa, M. Engraftment and multilineage expression of human bone marrow CD34- cells in vivo. *Annals of the New York Academy of Sciences* **872**, 220-231; discussion 231-222 (1999).
205 Notta, F. *et al.* Isolation of single human hematopoietic stem cells capable of long-term multilineage engraftment. *Science* **333**, 218-221, doi:10.1126/science.1201219 (2011).
206 Ivanovs, A. & Medvinsky, A. In search of human hematopoietic stem cell identity. *Cell stem cell* **16**, 5-6, doi:10.1016/j.stem.2014.12.010 (2015).
207 Fares, I. *et al.* EPCR expression marks UM171-expanded CD34(+) cord blood stem cells. *Blood* **129**, 3344-3351, doi:10.1182/blood-2016-11-750729 (2017).

208 Sugimura, R. Bioengineering Hematopoietic Stem Cell Niche toward Regenerative Medicine. *Advanced drug delivery reviews* **99**, 212-220, doi:10.1016/j.addr.2015.10.010 (2016).
209 Fares, I. *et al.* Cord blood expansion. Pyrimidoindole derivatives are agonists of human hematopoietic stem cell self-renewal. *Science* **345**, 1509-1512, doi:10.1126/science.1256337 (2014).
210 Timeus, F. *et al.* Cell adhesion molecule expression in cord blood CD34+ cells. *Stem cells* **16**, 120-126, doi:10.1002/stem.160120 (1998).
211 Perez, O. D. *et al.* Leukocyte functional antigen 1 lowers T cell activation thresholds and signaling through cytohesin-1 and Jun-activating binding protein 1. *Nature immunology* **4**, 1083-1092, doi:10.1038/ni984 (2003).
212 Li, D., Molldrem, J. J. & Ma, Q. LFA-1 regulates CD8+ T cell activation via T cell receptor-mediated and LFA-1-mediated Erk1/2 signal pathways. *The Journal of biological chemistry* **284**, 21001-21010, doi:10.1074/jbc.M109.002865 (2009).
213 Bose, T. O., Colpitts, S. L., Pham, Q. M., Puddington, L. & Lefrancois, L. CD11a is essential for normal development of hematopoietic intermediates. *Journal of immunology* **193**, 2863-2872, doi:10.4049/jimmunol.1301820 (2014).
214 Harris, E. S., Weyrich, A. S. & Zimmerman, G. A. Lessons from rare maladies: leukocyte adhesion deficiency syndromes. *Current opinion in hematology* **20**, 16-25, doi:10.1097/MOH.0b013e32835a0091 (2013).
215 Lu, Y. F. *et al.* Engineered Murine HSCs Reconstitute Multi-lineage Hematopoiesis and Adaptive Immunity. *Cell reports* **17**, 3178-3192, doi:10.1016/j.celrep.2016.11.077 (2016).
216 Georgopoulos, K. Haematopoietic cell-fate decisions, chromatin regulation and ikaros. *Nature reviews. Immunology* **2**, 162-174, doi:10.1038/nri747 (2002).
217 Khosravi, A. *et al.* Gut microbiota promote hematopoiesis to control bacterial infection. *Cell host & microbe* **15**, 374-381, doi:10.1016/j.chom.2014.02.006 (2014).
218 Josefsdottir, K. S., Baldridge, M. T., Kadmon, C. S. & King, K. Y. Antibiotics impair murine hematopoiesis by depleting the intestinal microbiota. *Blood* **129**, 729-739, doi:10.1182/blood-2016-03-708594 (2017).
219 Rautava, S., Collado, M. C., Salminen, S. & Isolauri, E. Probiotics modulate host-microbe interaction in the placenta and fetal gut: a randomized, double-blind, placebo-controlled trial. *Neonatology* **102**, 178-184, doi:10.1159/000339182 (2012).
220 Funkhouser, L. J. & Bordenstein, S. R. Mom knows best: the universality of maternal microbial transmission. *PLoS biology* **11**, e1001631, doi:10.1371/journal.pbio.1001631 (2013).
221 Nagasawa, T. *et al.* Defects of B-cell lymphopoiesis and bone-marrow myelopoiesis in mice lacking the CXC chemokine PBSF/SDF-1. *Nature* **382**, 635-638, doi:10.1038/382635a0 (1996).
222 Zou, Y. R., Kottmann, A. H., Kuroda, M., Taniuchi, I. & Littman, D. R. Function of the chemokine receptor CXCR4 in haematopoiesis and in cerebellar development. *Nature* **393**, 595-599, doi:10.1038/31269 (1998).
223 Ara, T. *et al.* Long-term hematopoietic stem cells require stromal cell-derived factor-1 for colonizing bone marrow during ontogeny. *Immunity* **19**, 257-267 (2003).

224 Wright, D. E., Bowman, E. P., Wagers, A. J., Butcher, E. C. & Weissman, I. L. Hematopoietic stem cells are uniquely selective in their migratory response to chemokines. *The Journal of experimental medicine* **195**, 1145-1154 (2002).
225 Christensen, J. L., Wright, D. E., Wagers, A. J. & Weissman, I. L. Circulation and chemotaxis of fetal hematopoietic stem cells. *PLoS biology* **2**, E75, doi:10.1371/journal.pbio.0020075 (2004).
226 Zhang, X. B. *et al.* High incidence of leukemia in large animals after stem cell gene therapy with a HOXB4-expressing retroviral vector. *The Journal of clinical investigation* **118**, 1502-1510, doi:10.1172/JCI34371 (2008).
227 Wurm, M. *et al.* Ectopic expression of HOXC6 blocks myeloid differentiation and predisposes to malignant transformation. *Experimental hematology* **42**, 114-125 e114, doi:10.1016/j.exphem.2013.10.004 (2014).
228 Warren, L. *et al.* Highly efficient reprogramming to pluripotency and directed differentiation of human cells with synthetic modified mRNA. *Cell stem cell* **7**, 618-630, doi:10.1016/j.stem.2010.08.012 (2010).
229 Boudot, A. *et al.* Differential estrogen-regulation of CXCL12 chemokine receptors, CXCR4 and CXCR7, contributes to the growth effect of estrogens in breast cancer cells. *PloS one* **6**, e20898, doi:10.1371/journal.pone.0020898 (2011).
230 Wang, X., Mamillapalli, R., Mutlu, L., Du, H. & Taylor, H. S. Chemoattraction of bone marrow-derived stem cells towards human endometrial stromal cells is mediated by estradiol regulated CXCL12 and CXCR4 expression. *Stem cell research* **15**, 14-22, doi:10.1016/j.scr.2015.04.004 (2015).
231 Astuti, Y. *et al.* A Functional Bioluminescent Zebrafish Screen for Enhancing Hematopoietic Cell Homing. *Stem cell reports* **8**, 177-190, doi:10.1016/j.stemcr.2016.12.004 (2017).
232 Guo, B., Huang, X., Cooper, S. & Broxmeyer, H. E. Glucocorticoid hormone-induced chromatin remodeling enhances human hematopoietic stem cell homing and engraftment. *Nature medicine* **23**, 424-428, doi:10.1038/nm.4298 (2017).
233 Lux, C. T. *et al.* All primitive and definitive hematopoietic progenitor cells emerging before E10 in the mouse embryo are products of the yolk sac. *Blood* **111**, 3435-3438, doi:10.1182/blood-2007-08-107086 (2008).
234 Rhodes, K. E. *et al.* The emergence of hematopoietic stem cells is initiated in the placental vasculature in the absence of circulation. *Cell stem cell* **2**, 252-263, doi:10.1016/j.stem.2008.01.001 (2008).
235 Cumano, A., Dieterlen-Lievre, F. & Godin, I. Lymphoid potential, probed before circulation in mouse, is restricted to caudal intraembryonic splanchnopleura. *Cell* **86**, 907-916 (1996).
236 Boisset, J. C. *et al.* In vivo imaging of haematopoietic cells emerging from the mouse aortic endothelium. *Nature* **464**, 116-120, doi:10.1038/nature08764 (2010).
237 Lee, L. K. *et al.* LYVE1 Marks the Divergence of Yolk Sac Definitive Hemogenic Endothelium from the Primitive Erythroid Lineage. *Cell reports* **17**, 2286-2298, doi:10.1016/j.celrep.2016.10.080 (2016).
238 Morrison, S. J., Hemmati, H. D., Wandycz, A. M. & Weissman, I. L. The purification and characterization of fetal liver hematopoietic stem cells. *Proceedings of the National Academy of Sciences of the United States of America* **92**, 10302-10306 (1995).

239 Habibian, H. K. *et al.* The fluctuating phenotype of the lymphohematopoietic stem cell with cell cycle transit. *The Journal of experimental medicine* **188**, 393-398 (1998).
240 Bowie, M. B. *et al.* Hematopoietic stem cells proliferate until after birth and show a reversible phase-specific engraftment defect. *The Journal of clinical investigation* **116**, 2808-2816, doi:10.1172/JCI28310 (2006).
241 Pawliuk, R., Eaves, C. & Humphries, R. K. Evidence of both ontogeny and transplant dose-regulated expansion of hematopoietic stem cells in vivo. *Blood* **88**, 2852-2858 (1996).
242 North, T. E. *et al.* Hematopoietic stem cell development is dependent on blood flow. *Cell* **137**, 736-748, doi:10.1016/j.cell.2009.04.023 (2009).
243 Adamo, L. *et al.* Biomechanical forces promote embryonic haematopoiesis. *Nature* **459**, 1131-1135, doi:10.1038/nature08073 (2009).